

1989

Study of surface texture using Fourier transform methods.

Satya. Kurada
University of Windsor

Follow this and additional works at: <http://scholar.uwindsor.ca/etd>

Recommended Citation

Kurada, Satya., "Study of surface texture using Fourier transform methods." (1989). *Electronic Theses and Dissertations*. Paper 3654.

This online database contains the full-text of PhD dissertations and Masters' theses of University of Windsor students from 1954 forward. These documents are made available for personal study and research purposes only, in accordance with the Canadian Copyright Act and the Creative Commons license—CC BY-NC-ND (Attribution, Non-Commercial, No Derivative Works). Under this license, works must always be attributed to the copyright holder (original author), cannot be used for any commercial purposes, and may not be altered. Any other use would require the permission of the copyright holder. Students may inquire about withdrawing their dissertation and/or thesis from this database. For additional inquiries, please contact the repository administrator via email (scholarship@uwindsor.ca) or by telephone at 519-253-3000ext. 3208.



National Library
of Canada

Bibliothèque nationale
du Canada

Canadian Theses Service · Service des thèses canadiennes

Ottawa, Canada
K1A 0N4

NOTICE

The quality of this microform is heavily dependent upon the quality of the original thesis submitted for microfilming. Every effort has been made to ensure the highest quality of reproduction possible.

If pages are missing, contact the university which granted the degree.

Some pages may have indistinct print especially if the original pages were typed with a poor typewriter ribbon or if the university sent us an inferior photocopy.

Reproduction in full or in part of this microform is governed by the Canadian Copyright Act, R.S.C. 1970, c. C-30, and subsequent amendments.

AVIS

La qualité de cette microforme dépend grandement de la qualité de la thèse soumise au microfilmage. Nous avons tout fait pour assurer une qualité supérieure de reproduction.

S'il manque des pages, veuillez communiquer avec l'université qui a conféré le grade.

La qualité d'impression de certaines pages peut laisser à désirer, surtout si les pages originales ont été dactylographiées à l'aide d'un ruban usé ou si l'université nous a fait parvenir une photocopie de qualité inférieure.

La reproduction, même partielle, de cette microforme est soumise à la Loi canadienne sur le droit d'auteur, SRC 1970, c. C-30, et ses amendements subséquents.

STUDY OF SURFACE TEXTURE USING FOURIER TRANSFORM
METHODS

by

© Satya Kurada

A Thesis
Submitted to
the Faculty of Graduate Studies and Research
Through
the Department of Mechanical Engineering
in Partial Fulfillment of the Requirements for
the Degree of Master of Applied Science at
the University of Windsor

Windsor, Ontario, Canada

1988



National Library
of Canada

Bibliothèque nationale
du Canada

Canadian Theses Service Service des thèses canadiennes

Ottawa, Canada
K1A 0N4

The author has granted an irrevocable non-exclusive licence allowing the National Library of Canada to reproduce, loan, distribute or sell copies of his/her thesis by any means and in any form or format, making this thesis available to interested persons.

The author retains ownership of the copyright in his/her thesis. Neither the thesis nor substantial extracts from it may be printed or otherwise reproduced without his/her permission.

L'auteur a accordé une licence irrévocable et non exclusive permettant à la Bibliothèque nationale du Canada de reproduire, prêter, distribuer ou vendre des copies de sa thèse de quelque manière et sous quelque forme que ce soit pour mettre des exemplaires de cette thèse à la disposition des personnes intéressées.

L'auteur conserve la propriété du droit d'auteur qui protège sa thèse. Ni la thèse ni des extraits substantiels de celle-ci ne doivent être imprimés ou autrement reproduits sans son autorisation.

ISBN 0-315-50514-1

Canada

© Satya Kurada 1988

ABSTRACT

A machine vision system based on the optical Fourier transform technique is developed to analyze the surface texture of different machined surfaces. The system consists of a He-Ne laser for light source, a microscope optical system for producing the Fourier transform and a CCD camera for capturing the Fourier pattern. The analog signal from the camera is then transferred to an IBM PC-AT through a digitizer board for further analysis.

The objectives of this investigation are classified into three parts. The first part of the study involves the computation of frequency spectra by optical Fourier transform techniques for different types of surfaces.

The second part of the study compares the frequency spectra obtained by the optical system and those from the profilometer. A number of parameters are derived to facilitate the comparison. The agreement between the two methods is found to be good at lower roughness range but the distinction became clearly obvious as the roughness increases. The comparison is performed on five different materials and five different

machining processes.

The final part of the study involves the process of characterizing the roughness of different types of samples by the parameters derived from the optical Fourier spectrum. It is found that the normalized spectrum RMS and peak have a good correlation with the average surface roughness R_a obtained by the profilometer. Correlation curves for five different materials are obtained. Results obtained by the optical method also indicate that the measurement precision of the optical method is better than that of the stylus.

In an industrial environment the machined parts are usually covered with a film of oil. The effect of an oil coating on the correlation curves is investigated in this study. It is observed that the sensitivity of the method does not decrease appreciably.

The two dimensional optical Fourier transform is also used to analyze the effect of surface defects, e.g. stylus scratches on the surface roughness. The scratches can be easily revealed by visual inspection of the Fourier pattern or by analyzing the frequency spectrum.

Dedicated with
love and respect
to
Aswini & Prasad

ACKNOWLEDGMENTS

I am deeply indebted to Dr. V.M. Huynh for his support and guidance throughout the course of my degree. I express my sincere thanks to Dr. W. North, Dr. J. Soltis and Dr. N. Wilson for their expertise and encouragement. I am also thankful to Mr. R. Tatersall and Mr. W. Beck for their invaluable assistance.

I would like to thank Mr. Thomas Lau, Mr. Francis Luk and Mr. Srinivas Mantripragada for their technical assistance. I am especially grateful to Mr. Philip Aylesworth and Mrs. Susan Aylesworth whose guidance has been a perennial source of inspiration for me in my personal life throughout my degree at Windsor. I express my sincerest thanks and gratitude to my parents for their help, love and patience.

Acknowledgment is made to the Natural Science and Engineering Research Council of Canada (NSERC grant no. A5286) for providing the financial support for this study.

CONTENTS

	<u>Page</u>
ABSTRACT	iii
ACKNOWLEDGMENTS	v
TABLE OF CONTENTS	vii
LIST OF ILLUSTRATIONS	ix
LIST OF TABLES	xiii
LIST OF ABBREVIATIONS	xiv
I. INTRODUCTION	1
1.1 Components of surface texture	2
1.2 Surface roughness measurement-techniques ..	5
1.2.1 Contact measurement	5
1.2.2 Non-contact measurement	9
II. THEORETICAL BACKGROUND	18
2.1 Fourier transforms	18
2.1.1 One dimensional transforms	18
2.1.2 Two dimensional transforms	22
2.2 Fourier analysis applied to optics	26
2.2.1 Fraunhofer diffraction	27
2.3 Application of Fourier transforms	31
2.4 Objectives of the present research	33
III. EXPERIMENTAL APPARATUS & PROCEDURE	35
3.1 Optical method	35
3.1.1 Description of the apparatus	35
Experimental procedure.....	39
3.2 Mechanical method	43
3.2.1 Description of apparatus	43
3.2.2 Experimental Procedure	44
3.3 Roughness specimens	47
3.4 Calculation Procedure	47

	<u>Page</u>
IV. RESULTS AND DISCUSSION	51
4.1 Fourier analysis of surface roughness	51
4.2 Calibration of the apparatus	52
4.3 Fourier spectrum of ground surfaces- of different materials	56
4.4 Fourier spectrum of surfaces obtained by different machining processes	68
4.5 Characterization of surface roughness from the optical method	75
4.5.1 Experimental uncertainty	88
4.5.2 Measurement precision	88
4.6 Measurement of surface roughness along the direction of lay	91
4.7 Measurement in oil	97
4.8 Identification of scratches	97
 V. CONCLUSIONS	 103
 VI. RECOMMENDATIONS	 107
 LIST OF REFERENCES	 109

Appendices

A	Equipment Description	111
B	Computer program listing	116
C	Chemical Composition and Mechanical Properties of Test Samples	132
D	Data for grinding samples	135
E	Data for Samples from Different Machining Processes	145
F	Uncertainty Analysis	148
	Vita Auctoris	150

LIST OF FIGURES

<u>Figure</u>		<u>Page</u>
1.1	A schematic diagram of the components of surface texture	4
1.2	A schematic diagram of surface roughness measurement techniques	6
1.3	A photograph showing the scratches made by the stylus profilometer	7
1.4	Experimental set-up used in laser speckle method	12
1.5	A schematic diagram showing a simple experimental set-up used in interferometric method	13
1.6	Principle of Schmalz microscope	15
2.1	Illustration shows how any real wave form can be produced by adding sine waves together	19
2.2	a) Time domain signal of a sine wave	23
	b) Frequency spectrum	23
2.3	a) Time domain signal of a triangular wave	24
	b) Frequency spectrum	24
2.4	a) Time domain signal of a square wave ..	25
	b) Frequency spectrum	25
2.5	Narrow slits of various lengths and their optical Fourier transforms	28
2.6	A schematic diagram showing the Fraunhofer diffraction	29
3.1	A block diagram of the experimental set-up for the optical method	36
3.2	A photograph showing the experimental set-up for the optical method	38

3.3	a) Frequency spectrum of the standard calibration sample for maximum output of the polarizer	40
	b) Frequency spectrum for minimum output of the polarizer	40
3.4	A flow diagram for the experimental procedure	41
3.5	Arrangement of the light source and camera with respect to the specimen	42
3.6	A block diagram of the experimental set-up used in the mechanical method	45
3.7	A photograph showing the experimental set-up used in the mechanical method	46
4.1	Typical characteristics of the calibrated sample (Ra=3.0um)	53
4.2	Typical characteristics of the calibrated sample (Ra=0.5um)	54
4.3	Typical characteristics of tool steel sample (Ra=0.07um)	57
4.4	Typical characteristics of stainless steel sample (Ra=0.05um)	59
4.5	Typical characteristics of aluminum sample (Ra=0.22um)	60
4.6	Typical characteristics of brass sample (Ra=0.07um)	61
4.7	Typical characteristics of magnesium sample	62
4.8	Correlation between the normalized spectrum RMS(optical) and normalized spectrum RMS(stylus) for tool steel samples	66
4.9	Correlation between the normalized spectrum peak(optical) and normalized spectrum peak(stylus) for tool steel samples	67

4.10	Typical characteristics of flat lapping sample (Ra=0.05um)	69
4.11	Typical characteristics of horizontal milling sample (Ra=0.4um)	70
4.12	Typical characteristics of vertical milling sample (Ra=0.4um) *.....	72
4.13	Typical characteristics of a reaming sample (Ra=0.4um)	73
4.14	Typical characteristics of a turning sample (Ra=0.4um)	74
4.15	Correlation between normalized spectrum RMS(optical) and normalized spectrum RMS(stylus) for flat lapping samples ...	77
4.16	Correlation between the normalized spectrum peak(optical) and normalized spectrum peak(stylus) for flat lapping samples	78
4.17	Correlation between spectrum RMS(optical) and surface roughness Ra for tool steel samples	80
4.18	Correlation between spectrum peak(optical) and surface roughness Ra for tool steel samples	81
4.19	Correlation between spectrum RMS(optical) and surface roughness Ra for ground surfaces of five different materials ...	83
4.20	Correlation between spectrum peak(optical) and surface roughness Ra for ground surfaces of five different materials ...	84
4.21	Correlation between spectrum RMS(optical) and surface roughness Ra for four different machining processes	86
4.22	Correlation between spectrum peak(optical) and surface roughness Ra for four different machining processes	87
4.23	Correlation between spectrum RMS(optical)	

	along lay and surface roughness Ra for tool steel samples	92
4.24	Correlation between spectrum peak (optical) along lay and surface roughness Ra for tool steel samples	93
4.25	Correlation between the spectrum RMS (optical) along lay and spectrum RMS (optical) perpendicular to lay for surface ground tool steel samples	95
4.26	Correlation between the spectrum peak (optical) along lay and spectrum peak (optical) perpendicular to lay for ground tool steel samples	96
4.27	Correlation between the spectrum RMS (optical) and surface roughness Ra for oiled and oil-free ground surface copper samples	98
4.28	Correlation between the spectrum peak (optical) and surface roughness Ra for oiled and oil-free ground surface copper samples	99
4.29	a) The photograph of the standard calibrated sample with scratches	101
	b) The Fourier pattern	101
4.30	a) The frequency spectrum along lay for the standard calibration sample without scratches	102
	b) The frequency spectrum for the same surface without scratches	102

LIST OF TABLES

<u>Table</u>		<u>Page</u>
3.1	a) Samples from different machining processes used in the work, their roughness range, and No. of samples ..	48
	b) Surface ground samples of different materials used in the work with their roughness range	48
4.1	Comparison of frequency spectra at harmonic frequencies	55
4.2	Frequency spectra obtained by the optical and mechanical methods for surface ground tool steel samples	64
4.3	Comparison of the frequency spectra obtained by the two methods for samples of different machining processes	76
4.4	Correlation equations for different materials	82
4.5	Measurement precision of stylus method for surface ground copper sample	89
4.6	Measurement precision of optical method for surface ground copper sample	90
4.7	Correlation equations for tool steel samples relating roughness parameters in both the machining directions	97

LIST OF ABBREVIATIONS

- A_0, A_1 = Amplitudes of feed components
- A_i = Amplitude components of frequency spectrum
- $A(k)$ = Fourier cosine transform
- $B(k)$ = Fourier sine transform
- C.V = Coefficient of variation
- $(C.V)_m$ = Coeff. of variation obtained from mechanical method
- $(C.V)_o$ = Coeff. of variation obtained from optical method
- F = spatial frequency in cycles/mm
- f = focal length of the transform lens
- f_i = frequency in cycles/mm
- f_m = Mean frequency in cycles/mm
- f_s = spatial frequency, of the feed components
- k = Spatial frequency component
- k_x = Angular spatial frequency along x-axis
- k_y = Angular spatial frequency along y-axis
- L = Assessment length
- M = Magnification of the system
- N = Number of points
- R_a = Average surface roughness (μm)
- $(\text{Peak})_o$ = Peak value obtained from the optical frequency spectrum
- RMS = Root mean square of the frequency spectrum
- $(\text{RMS})_o$ = Root mean square of the optical frequency spectrum

STD = Standard deviation of frequency
t = time
w = angular spatial frequency
x = traveling distance
y = ordinate on the profile curve
z = spatial distance in μm
 λ = Wavelength of laser (0.632 μm)



CHAPTER I

INTRODUCTION

Measurement of surface texture has become an important part of quality control over the past few years as the manufacturing industries are more concerned about their product quality and reliability. Accurate characterization of surface texture plays a vital role in the design and production of mechanical parts since it influences corrosion resistance, probability of crack formation, lubrication performance, uniformity in painting and plating operations and other important properties of the surface.

Surface texture specifications are crucial for performance of industrial surfaces. Measurement of surface texture has traditionally been required in metal working, automotive and aircraft industries to improve product quality. A critical need for information about surface texture is now being realized by the electronics, plastics and chemical industries. Advances in surface texture characterization has helped the development in applications such as:

- a) Automobile components
- b) Computer Memory disks
- c) Miniaturized printed circuits
- d) Plastic cylinders for Copy machines

e) Rubber tires

The measurement of surface finish is of significant economic importance, since the cost of production increases non-linearly with the improvement in surface finish. For instance, if a surface is manufactured to a better finish than necessary it would result in wastage of enormous sums of money and at the same time if a surface is manufactured such that it does not fulfill the specifications the whole production series has to be rejected [1].

1.1 Components of surface texture [2,3] :

According to ANSI(B46.1-1978), surface texture is the repetitive or random deviations from the nominal surface which form the three dimensional topography of the surface (See Figure 1.1).

Surface texture includes roughness, waviness, lay and flaws.

a) Roughness: Roughness consists of the finer irregularities of the surface texture, usually including those irregularities resulting from the inherent action of the production process. These are considered to include traverse feed marks and other irregularities within the sampling length.

The most commonly used parameter to characterize roughness is the Ra. It is the arithmetic mean of the profile departures, y, from the mean line.

Mathematically

$$Ra = 1/L \int_0^L |y(x)| dx$$

Where y(x) is the ordinate of profile curve

L is the assessment length,

and x is the travelling distance

b) Waviness: Waviness is the more widely spaced component of surface texture. Unless otherwise noted, waviness is to include all irregularities whose spacing is greater than the roughness sampling length and less than the waviness sampling length. Waviness may result from such factors as machine or work deflections, vibrations, chatter, etc. The profile of a real surface may be considered as roughness superimposed on a wavy surface.

c) Lay: Lay is the direction of the predominant surface pattern, ordinarily determined by the production method used.

d) Flaws: Flaws are unintentional irregularities which occur at one place or at relatively infrequent or widely varying intervals on the surface. Flaws include such defects as cracks, scratches, dents, pores, blowholes,

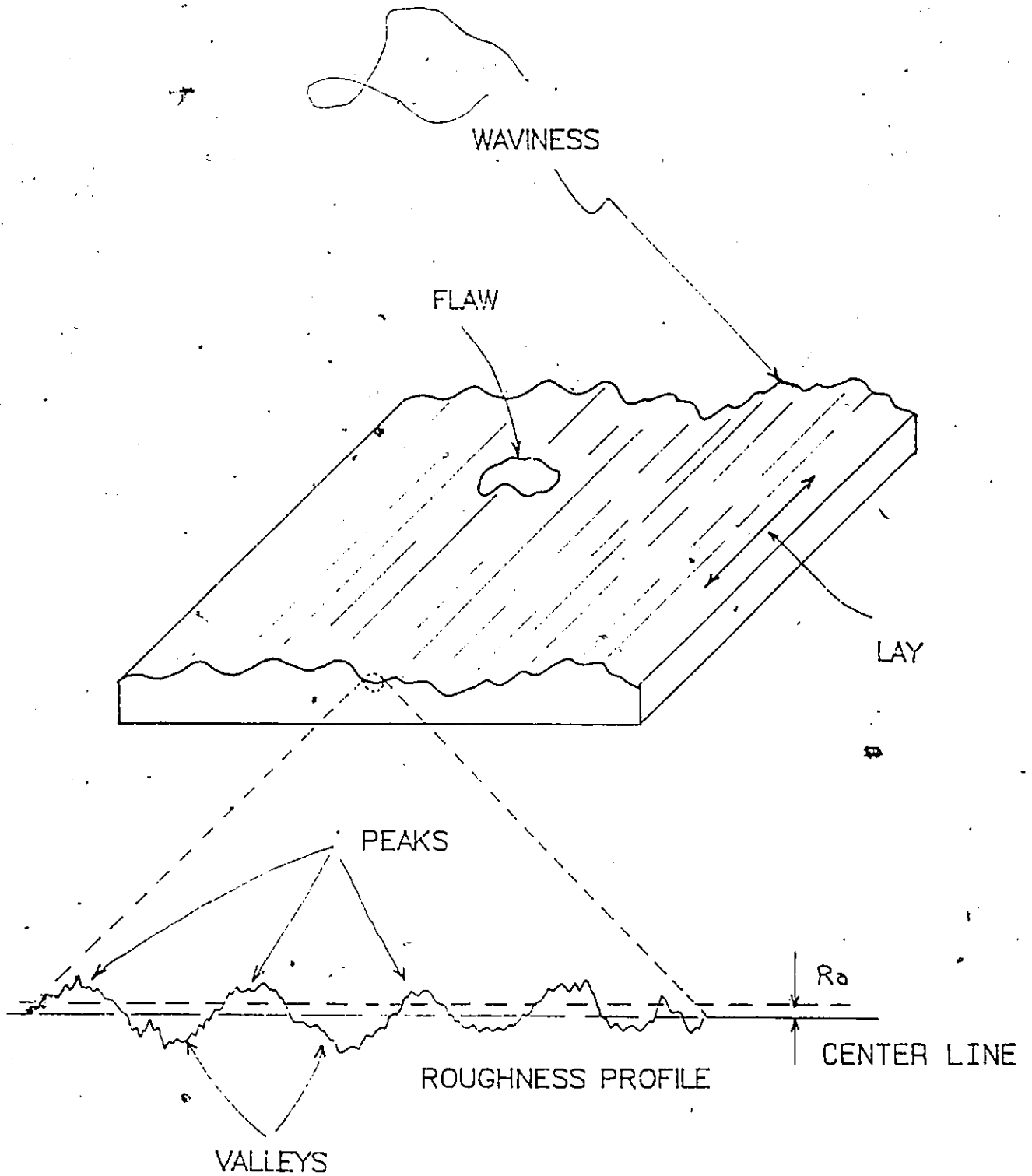


Figure 1.1 A schematic diagram of the components of surface texture

etc.

1.2 Surface Roughness Measurement Techniques:

The modern technological requirements on accurate characterization of surface roughness have resulted in different techniques that can be implemented in the production industry. These techniques can be classified into two categories (See Figure 1.2) :

1.2.1 Contact Measurement [2,4] : The traditional industrial measuring method is the stylus profilometer. The profilometer consists of a diamond tipped stylus which can traverse across the surface profile. The vertical movements of the stylus are transmitted to a coil inside the tracer body. The coil moves in the field of a permanent magnet and this produces a small fluctuating voltage whose magnitude is directly proportional to the height of the surface profile.

The traverse of the stylus can be done either manually or mechanically. The manual operation gives a rough estimate. The use of a mechanical power drive results in constant speed of travel of the stylus and thus produces more consistent readings.

The profilometer is the most widely accepted instrument for surface roughness measurement in the industrial clean room because all the national and

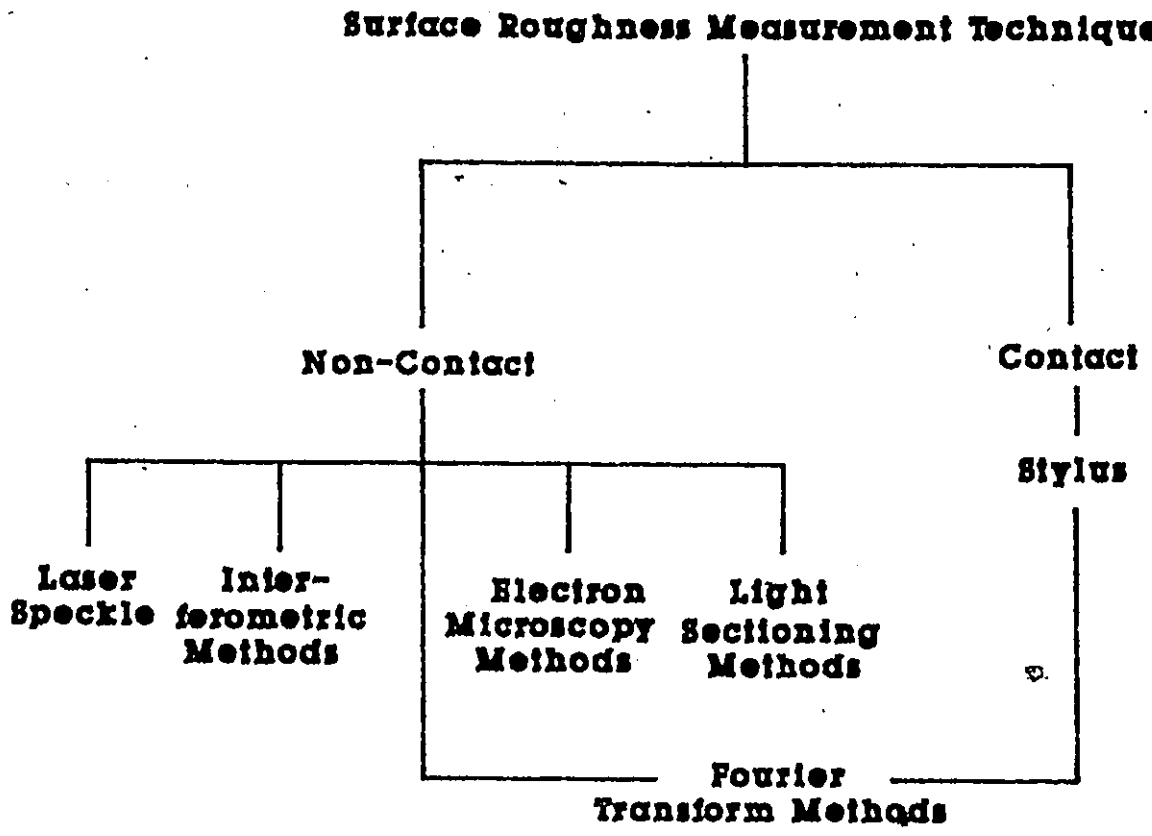


Figure 1.2 A schematic diagram of surface roughness measurement techniques

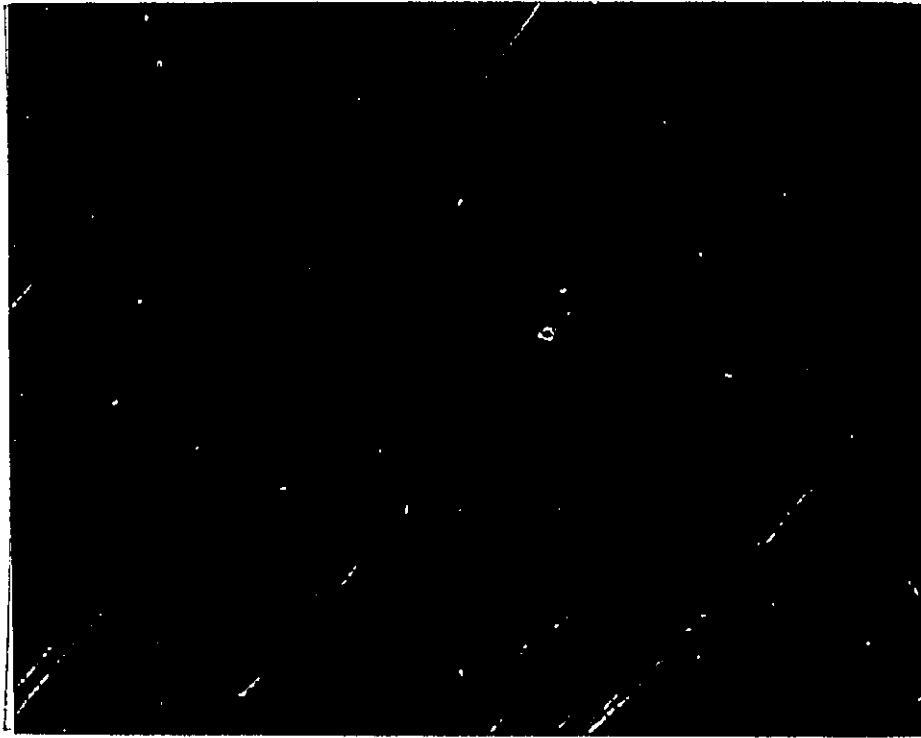


Figure 1.3 Photograph showing the scratches
made by the Stylus profilometer

international standards are defined in terms of the measurements made by the profilometer. In spite of the above mentioned advantage, the use of stylus profilometer is not desirable for on-line production because of the following disadvantages:

a) Surface Scratches : The stylus profilometer requires direct physical contact with the work surface whose roughness has to be measured. This results in scratches on the work surface because of the excessive pressure exerted by the stylus on the surface. This problem is more evident on soft surfaces. Figure 1.3 shows a photograph taken by a Scanning Electron Microscope to reveal the scratches.

b) Repeatability of the Instrument : Another shortcoming of the stylus profilometer is the lack of repeatability of measurement. This is due to the fact that the stylus has to traverse across the surface profile to produce an Ra reading and it can never move over exactly the same spot to establish any repeatability.

c) On-line Compatibility : The compatibility of the stylus profilometer for production line measurements is questionable. In many processes where the measurement of surface roughness is of great importance, only a few samples of the total production can be measured because of the requirement that the samples have to be

removed from the production line for roughness measurement.

d) What is really required is the Ra value obtained from the entire part surface which requires an infinite number of profile measurements.

e) The stylus profilometer will not produce accurate measurements on a soft surface.

f) Fragile probe.

1.2.2 Non-Contact Measurement : Due to the above mentioned disadvantages with the stylus profilometer a need for new techniques was realized. The optical techniques were developed as an alternative. The main advantage of using an optical method is that it inspects an area of a surface rather than a line , resulting in a better surface averaged reading. The optical methods can be easily implemented for on-line applications because of the following advantages:

1. They do not require any direct contact with the work surface.

2. No probe to wear out.

3. Rugged.

The optical techniques can be classified into five

different types based on their usage. A brief description of these methods is presented in the following sections:

a) Laser Speckle [5,6,7] : Since the advent of lasers the speckling phenomenon produced by coherent laser light has received considerable attention. The basic method for investigating surface roughness properties of objects by using speckle patterns consists of two steps:

i) a coherent super-position of the light beam transmitted through (or reflected from) the rough surface of an object with the original beam to produce a speckle pattern at the image plane.

ii) measurements of the average contrast of the resultant image speckle intensity variations.

These two steps are taken by employing an optical imaging system that produces the speckle patterns at the image plane of the object. A laser speckle roughness meter has been constructed using the above mentioned steps. The actual arrangement of the instrument is shown schematically in Figure 1.4. Coherent light from a He-Ne laser is reflected by a mirror M_1 to illuminate the rough surface of an object placed on a sample holder, which is slowly traversed across the illuminating beam by an X-Y scanning stage. The optical imaging system consists of an objective lens L_0 of 4X, a rotatable disk D having

various sized diaphragms, a beam switching mirror M_2 , and an observer's viewing lens L_e . An image of small area A_1 of the surface is formed at the plane A_3 where the speckle pattern is observed as an intensity variation due to the movement of the object on the X-Y scanning stage. A photomultiplier, in conjunction with a small pinhole P_s fixed at the center of the image plane A_3 , is used to detect the intensity variation of the speckle pattern. The photomultiplier output is fed into the signal analyzing system for calculating the average contrast V of speckle intensity variation. The average contrast V was plotted against RMS roughness for different samples.

This method suffers from the limitation that it does not provide any detailed information about the functional aspects of surface texture.

b) Interferometric Methods [2,8] : The interferometric methods are widely used in analysis of surface finish. In these methods the interference fringes are used for measuring the surface irregularities. The optical principle is shown in Figure 1.5. A beam of parallel monochromatic light is projected on to the specimen through a beam splitter and an optical flat. A portion of this is reflected from the optical flat and the rest is transmitted through to the specimen. The reflection from the specimen and that from the optical flat is recombined

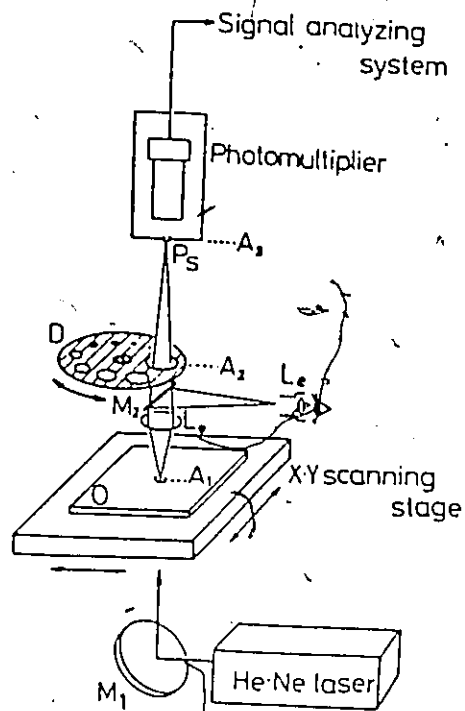


Figure 1.4 Experimental set-up used in Laser speckle (transmission) method [5]

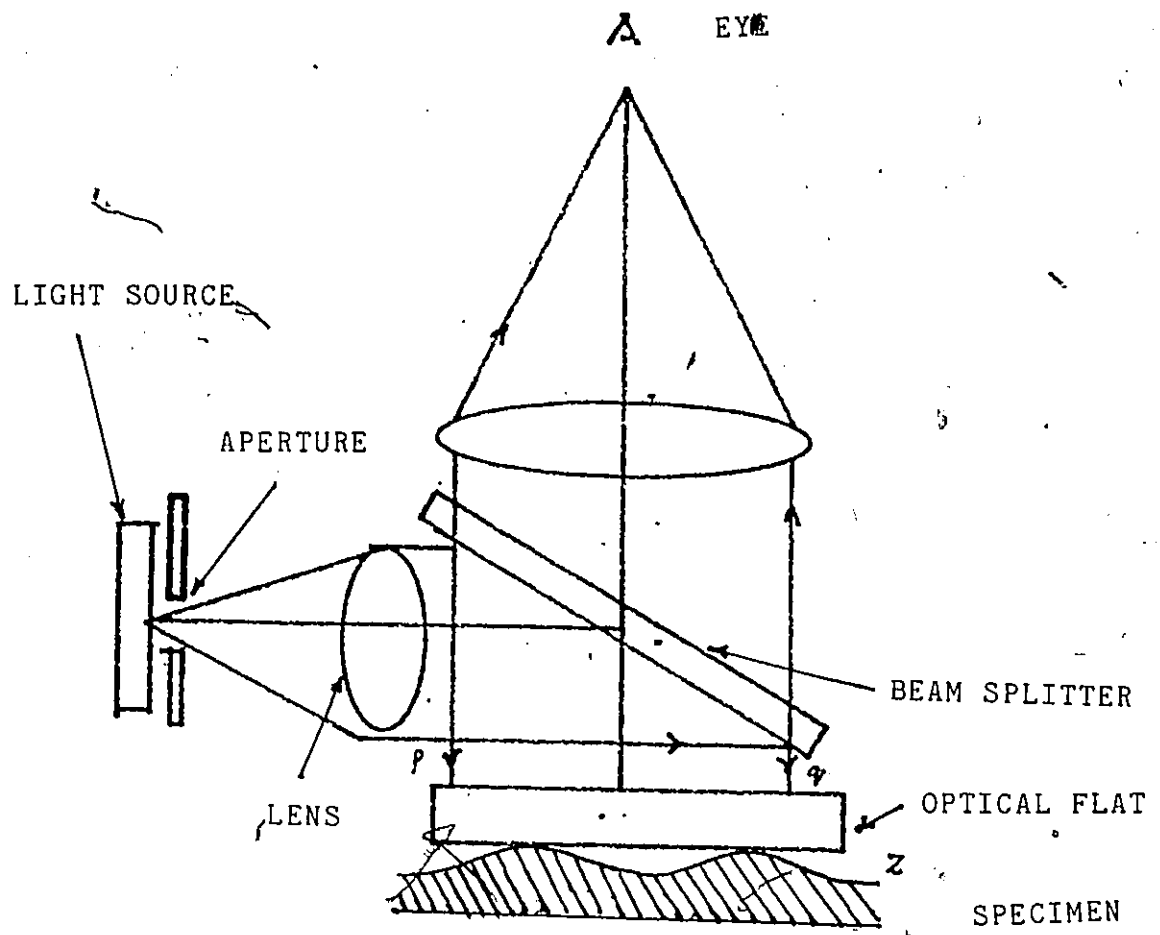


Figure 1.5 A schematic diagram showing the simple experimental set-up used in interferometric methods [8].

and passed through the beam splitter and is focused for viewing. Because of the path length difference between the two beams, there is a series of critical planes for which the path difference is an odd or even multiple of half wavelengths. The former leads to minimum and the latter to maximum brightness of the re-combined beams (fringe pattern). If the specimen Z is not flat in relation to the optical flat, it will cause a distortion in the fringe pattern.

The fringes are separated by a distance of multiple of half the wavelength of illumination. This spacing provides a means for measuring surface waviness.

c) Light Sectioning Methods [2] : The basic principle of this method is to use an oblique thin sheet of light to project at 45° to the surface normal and view the reflected specular beam. This procedure was developed by Schmaltz in 1931. The Schmaltz instrument uses two objective lenses at 45 degrees to the surface, (see Figure 1.6). One lens is for focusing a thin sheet of light and the other for observing the profile. The method is generally limited to 400X maximum magnification.

d) Electron Microscopy [2,9] : Electron microscopy is a sophisticated approach to reveal qualitative information about topography of a surface. Two electron microscopes can be used for this purpose: Transmission Electron

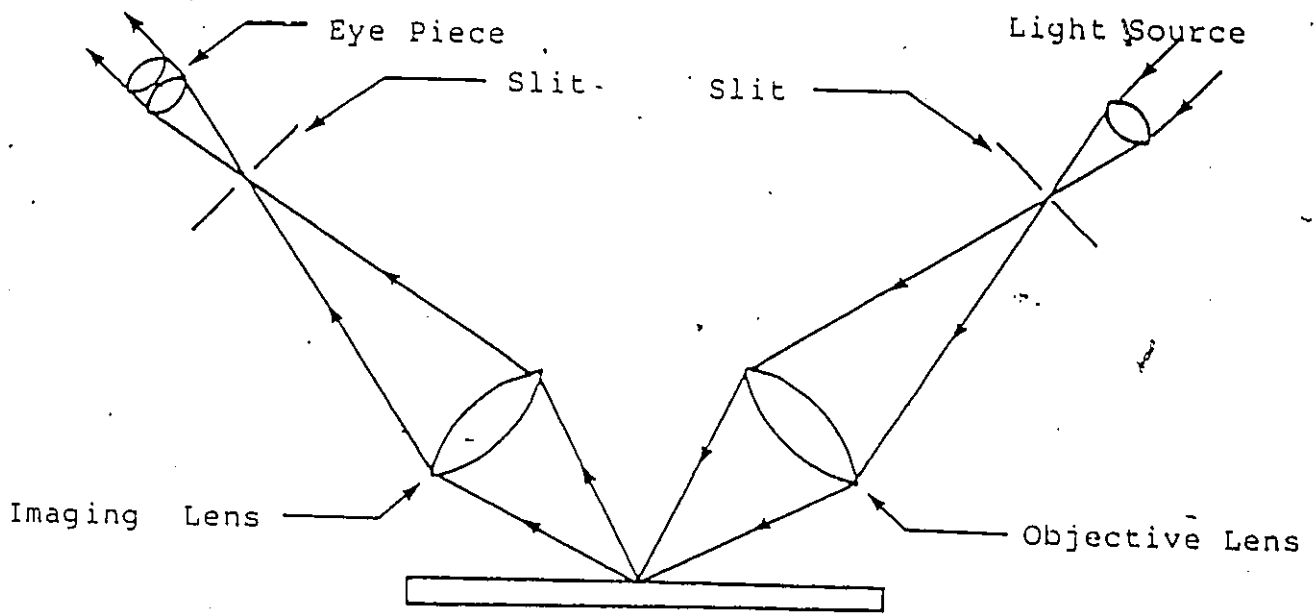
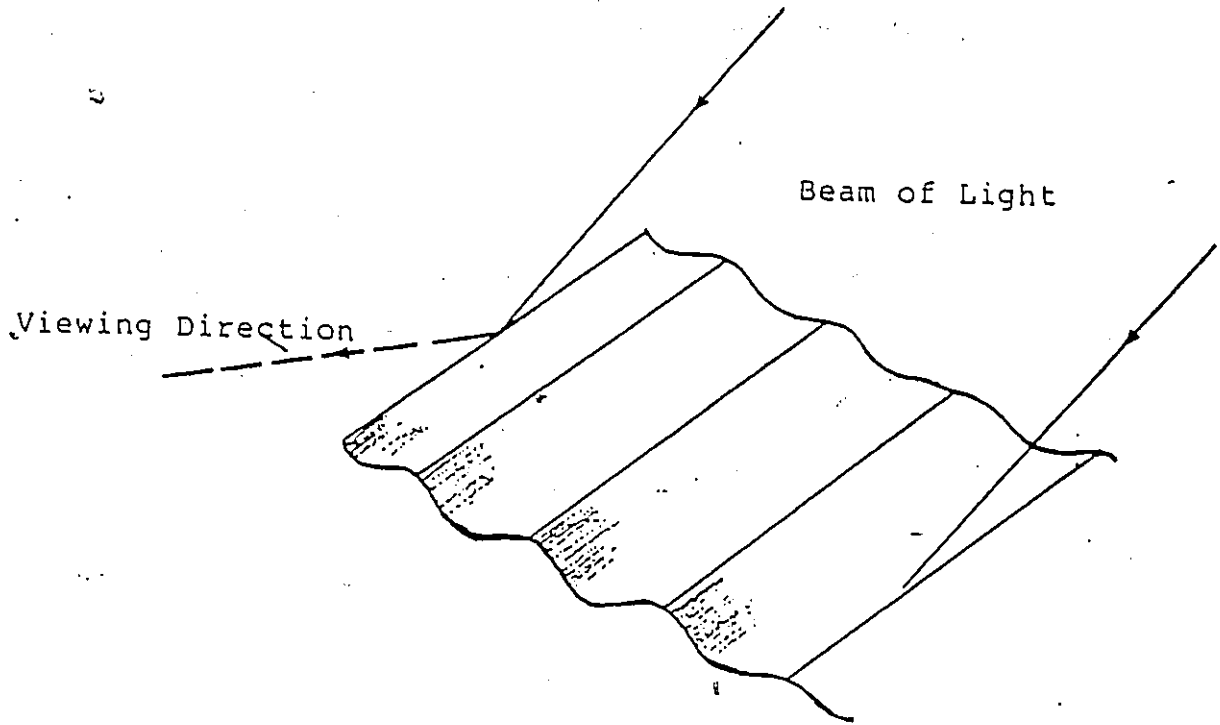


Figure 1.6 Principle of Schmalz Microscope

Microscope (TEM) and Scanning Electron Microscope (SEM).

The TEM uses transmitted electrons to form an image of the surface of interest. The low penetrating power of electrons requires that the specimen and the entire electron path be in a high vacuum region with absolute pressures of 10^{-5} mm of Hg or less; specimens must be prepared to have a thickness of 100nm or less.

The SEM employs a beam of electrons focused to as small a spot as possible on the specimen surface. The image of the specimen surface is produced by modulating the intensity of a spot on a CRT with a signal derived from the signal radiations. The requirements for a high vacuum discussed for TEM, also holds true for SEM. However since the SEM uses reflected or emitted radiations, there are no restrictive requirements on specimen thickness.

The electron microscope is not feasible for regular production line usage because of the high costs and the complex procedure used to derive information about the surface texture.

e) Fourier Transform Methods : Fourier transform methods have been extensively used for inspection of surfaces. This technique involves the transformation of the signal from one domain to another, for example from

spatial domain to frequency domain, so that information can be easily interpreted. This transformation can be obtained either mathematically or optically (contact or non-contact). In the contact method a FFT algorithm is used to transform the signal from the time domain to frequency domain. In the non-contact method the diffraction phenomena forms the basis for optically computing the Fourier transform.

Among the five methods discussed above, Fourier analysis seems to be the best candidate for gathering information about different kinds of surfaces [10], and furthermore is ideal for revealing the characteristics of a surface.

CHAPTER II

THEORETICAL BACKGROUND

In this chapter the first section provides a brief introduction to the theory of Fourier transforms. The next section describes the Fourier analysis as applied to optics. The third section gives a brief review of various research work conducted using Fourier transforms. The section ends with a description of the objectives of the present study.

2.1 Fourier Transforms : It was shown by Baron Jean Baptiste Fourier that any periodic wave form that exists in the real world can be generated by adding up sine waves of different frequencies and amplitudes. Figure 2.1 shows a simple wave form composed of two sine waves. By selecting the amplitudes, frequencies and phases of these sine waves correctly, any wave form identical to the desired signal can be generated [11].

2.1.1 One Dimensional Transforms : One dimensional function f of some space variable (x) could be expressed as a linear combination of an infinite number of harmonic contributions [12] :

$$f(x) = \frac{1}{2\pi} \left[\int_0^{\infty} A(k) \cos kx \, dk + \int_0^{\infty} B(k) \sin kx \, dk \right] \text{ --- (2.1)}$$

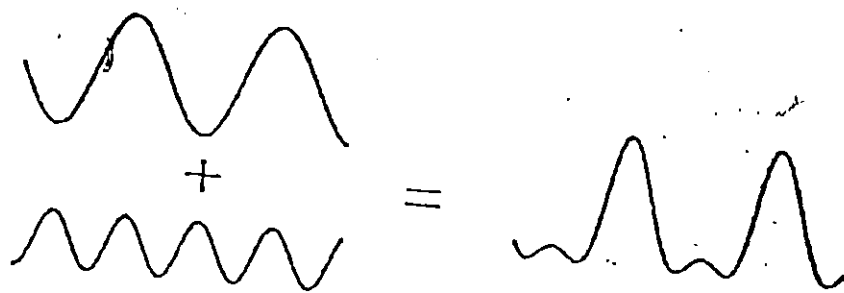


Figure 2.1 Illustration shows how any real wave form can be produced by adding sine waves together.

57

The weighting factors $A(k), B(k)$ which determine the significance of the contribution of various spatial frequency components (k), are the Fourier cosine and sine transforms of $f(x)$ given by

$$A(k) = \int_{-\infty}^{+\infty} f(x') \cos kx' dx' \quad \text{-----} \quad (2.2)$$

$$B(k) = \int_{-\infty}^{+\infty} f(x') \sin kx' dx'$$

respectively. Here the quantity x' is a dummy variable over which the integration is performed so that neither $A(k)$ nor $B(k)$ are explicit functions of x' . By substituting Eqn (2.2) into Eqn (2.1) one can obtain sine and cosine transforms consolidated into a single complex exponential expression

$$f(x) = \frac{1}{\pi} \int_0^{\infty} \cos kx \int_{-\infty}^{+\infty} f(x') \cos kx' dx' dk + \frac{1}{\pi} \int_0^{\infty} \sin kx \int_{-\infty}^{+\infty} f(x') \sin kx' dx' dk. \quad \text{-----} \quad (2.3)$$

But since $\cos k(x'-x) = \cos kx \cos kx' + \sin kx \sin kx'$ this can be rewritten as

$$f(x) = \frac{1}{\pi} \int_0^{\infty} \left[\int_{-\infty}^{+\infty} f(x') \cos k(x'-x) dx' \right] dk \quad \text{----} \quad (2.4)$$

The quantity in the square brackets is an even function of k and therefore changing the limits on the outer integral leads to

$$f(x) = \frac{1}{2\pi} \int_{-\infty}^{+\infty} \left[\int_{-\infty}^{+\infty} f(x') \cos k(x'-x) dx' \right] dk \quad \text{---- (2.5)}$$

Using Euler's theorem the above expression is simplified into the complex form of the Fourier integral.

$$f(x) = \frac{1}{2\pi} \int_{-\infty}^{+\infty} \left[\int_{-\infty}^{+\infty} f(x') e^{ikx'} dx' \right] e^{-ikx} dk \quad \text{--- (2.6)}$$

Thus we can write

$$f(x) = \frac{1}{2\pi} \int_{-\infty}^{+\infty} F(k) e^{-ikx} dk, \quad \text{----- (2.7)}$$

Provided that

$$F(k) = \int_{-\infty}^{+\infty} f(x) e^{ikx} dx, \quad \text{----- (2.8)}$$

having set $x'=x$ for Eqn (2.8). The function $F(k)$ is said to be the Fourier transform of $f(x)$, which is symbolically denoted by

$$F(k) = \mathcal{F}\{f(x)\} \quad \text{----- (2.9)}$$

Just as $F(k)$ is the transform of $f(x)$, $f(x)$ itself is said to be the inverse Fourier transform of $F(k)$, or symbolically

$$f(x) = \mathcal{F}^{-1}\{F(k)\} \quad \text{----- (2.10)}$$

and $f(x)$ and $F(k)$ are frequently referred to as a Fourier transform pair. If f were a function of time

rather than space, x has to be replaced by t and then k , the angular spatial frequency, by w , the angular temporal frequency, in order to get the appropriate transform pair in the time domain, that is

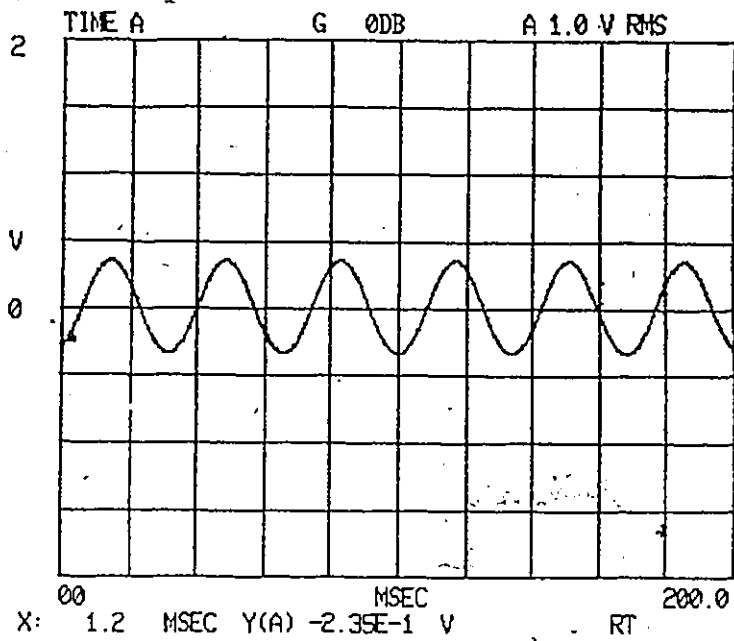
$$f(t) = \frac{1}{2\pi} \int_{-\infty}^{+\infty} F(w)e^{-iwt} dw \quad \text{----- (2.11)}$$

and

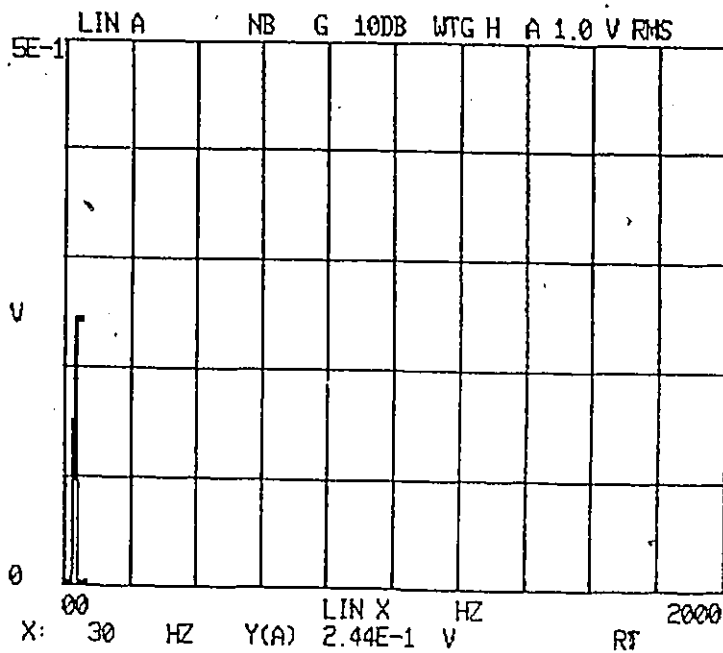
$$F(w) = \int_{-\infty}^{+\infty} f(t)e^{iwt} dt \quad \text{----- (2.12)}$$

The time domain signals and transforms of some typical functions are shown in Figures 2.2, 2.3 & 2.4. As can be seen from Figure 2.2(a), the signal is a pure sine wave which contains only one wavelength and is therefore transformed to a spectrum with one single peak (Fig. 2.2b). Figure 2.3(a) shows the pure triangular signal. It is obvious that the spectrum contains some additional discrete components, see Fig. 2.3b. From this it is inferred that the triangular profile does not contain only one wavelength but a combination of number of components. The square wave in Figure 2.4(a) is made up of an infinite number of sine waves, all harmonically related, where the lowest frequency is the frequency of the square wave.

2.1.2 Two Dimensional transforms : The discussion so far has been limited to one-dimensional functions. The

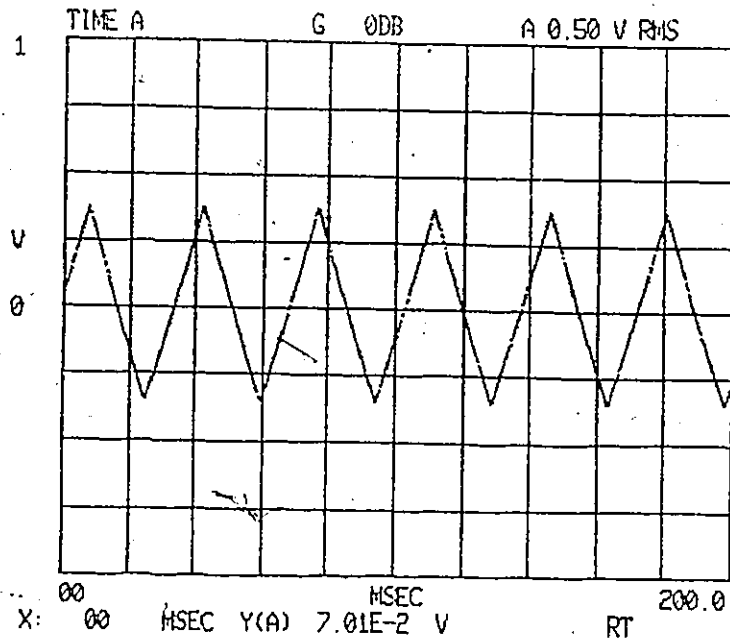


(a)

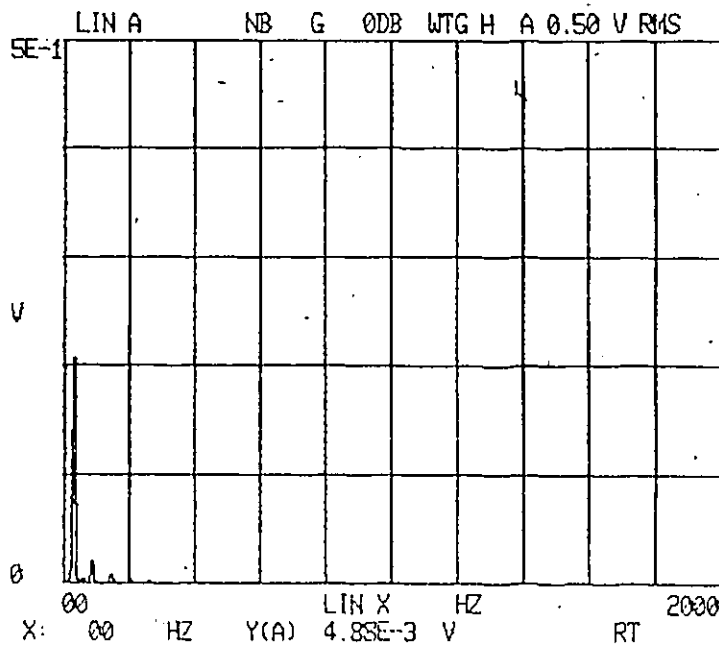


(b)

Figure 2.2 (a) Time domain signal of a sine wave and its
(b) Frequency spectrum

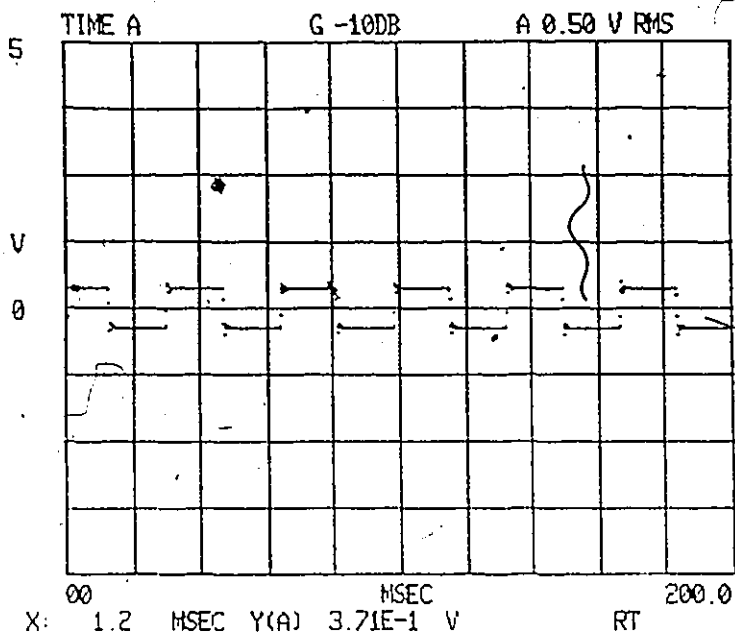


(a)

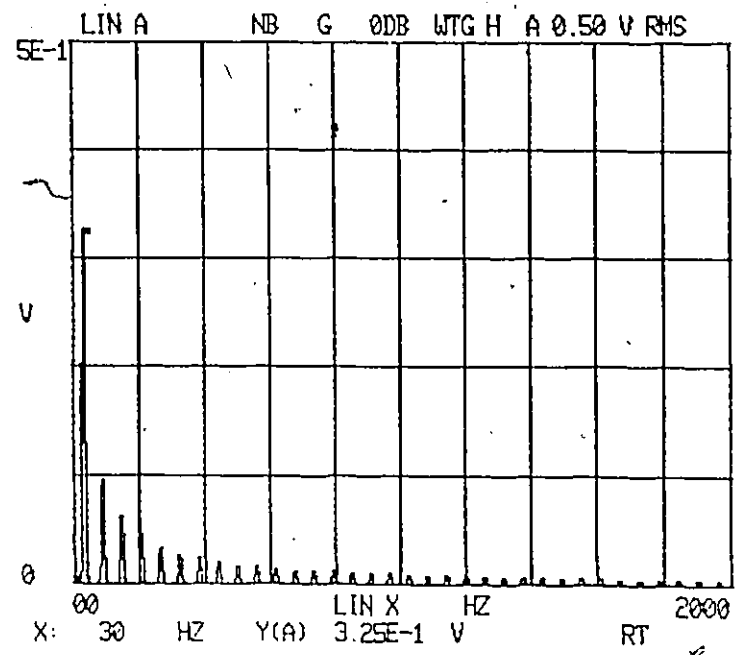


(b)

Figure 2.3 (a) Time domain signal of a triangular wave and its
 (b) Frequency spectrum



(a)



(b)

Figure 2.4 (a) Time domain signal of a Square wave and its
 (b) Frequency spectrum

Fourier transform pair can readily be generalized to two dimensions i.e.

$$f(x,y) = \frac{1}{(2\pi)^2} \iint_{-\infty}^{+\infty} F(k_x, k_y) e^{-i(k_x x + k_y y)} dk_x dk_y \quad \text{----- (2.13)}$$

where

$$F(k_x, k_y) = \iint_{-\infty}^{+\infty} f(x,y) e^{i(k_x x + k_y y)} dx dy \quad \text{-- (2.14)}$$

The quantities k_x and k_y are the angular spatial frequencies along the two axes. .

2.2 Fourier Analysis Applied To Optics : Light is a form of electromagnetic waves. If a wave is propagated in a free space, it travels at constant velocity. If the wave is partially blocked by a sharp edge or an aperture, the direction of travel will be altered as if it is bent. This apparent bending of the path is called diffraction [13].

There are two main classes of diffraction which are classified corresponding to the different approximations used in the evaluation of diffraction integral: far field & near field. The first one uses the field distribution far from the object (at infinity) is called the Fraunhofer diffraction pattern and is the Fourier transform of the object. The second uses the field distribution near the object is called the Fresnel

diffraction pattern [13].

The Fraunhofer pattern can be observed by placing a screen at a far distance from the object (as an approximation to infinity). Another way the Fraunhofer pattern can be formed by using an additional lens to focus the pattern at the focal plane.

An object of low spatial frequency, that is, an object that has large details, and wide separation between details will give a Fourier transform of small elements that are close together. An object of high spatial frequency will give maxima that are wide apart (see Figure 2.5)

2.2.1 Fraunhofer Diffraction :

Huygens' proposed that each point on a wave front acts as a source of new waves which propagate in all directions. At a given time, the new waves advance a certain distance, and the envelope of all these secondary wavelets yields the new wave front.

Consider a point Q in the aperture in a coordinate system (x,y) . see Figure 2.6. The amplitude of light wave at Q is $A(x,y)$. P is a point on the image plane having an amplitude $A'(x',y')$. The screen or image plane is located at a long distance from the aperture, so that $r=QP$ is

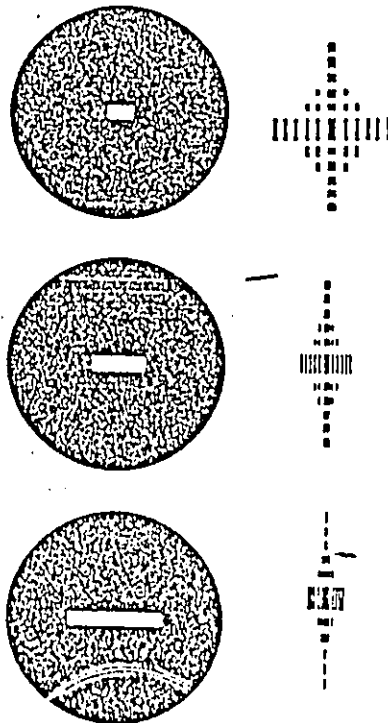


Figure 2.5 Narrow slits of various lengths (left) and their optical Fourier transforms (right).

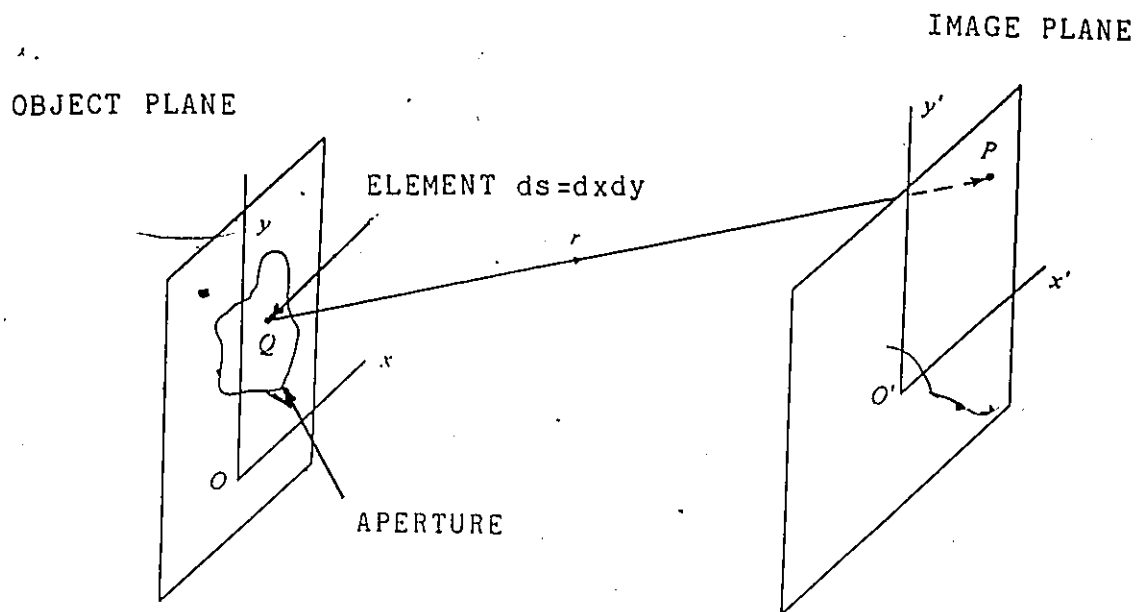


Figure 2.6 A Schematic diagram showing the Fraunhofer diffraction [13]

large compared to the dimensions of the opening. Because of the large value of r , we can assume that every point (x,y) in the aperture is approximately equidistant from the point (x',y') on the screen, where the complex amplitude can be described by an exponential term. Multiplying $A(x,y)$ by the area $dS=dx dy$ of an elementary section on the aperture and by a phase factor to obtain the expression

$$dA'(x',y') = CA(x,y)e^{ikr} dx dy \quad \text{-----} \quad (2.15)$$

where the constant C incorporates any necessary dimensional or scale factors. In accordance with Huygens' principle, the total amplitude on the screen is the sum of all individual contributions from the aperture, so that

$$A'(x',y') = C \int A(x,y)e^{ikr} dS \quad \text{-----} \quad (2.16)$$

The diffraction integral can also be written as

$$A'(x',y') = C \iint A(x,y)e^{-ikr} dx dy \quad \text{-----} \quad (2.17)$$

without changing the resulting intensity. For a rectangular opening, for example,

$$A'(x',y') = C \int \int A(x,y)e^{-ik(x+y)} dx dy \quad \text{-----} \quad (2.18)$$

Eqn (2.17) will have the form of Eqn (2.13) if $k_x=k_y=k$ and $C=1$. Since the constant does not have the

value unity, it should be mentioned that the intensity of the Fraunhofer diffraction pattern is proportional (but not identical) to the Fourier transform of the aperture function. In summary, the Fraunhofer diffraction phenomena provides an optical method for determining the Fourier transform of a function [13].

2.3 Applications of Fourier transforms :

The idea of using optical Fourier transform technique to characterize surface roughness is recently introduced by B. J. Pernick [14]. He has demonstrated that the characteristic patterns or signature shapes generated in the Fourier plane (optical Fourier transform) of laser illuminated samples are related to surface roughness for machined metal surfaces. He acquired the optical Fourier transform for different machined surfaces by placing the machined samples behind a square aperture and illuminating the samples by a laser light. A transform lens and a cylindrical lens were used to collect the reflected and scattered light through the aperture. A Gaussian curve was fitted to the resulting Fourier spectrum and a Gaussian width was obtained to quantify roughness. In this method, a very small bandwidth of the spectrum was selected for analysis and the results were obtained for a small set of samples.

E. G. Thwaite [15] investigated the conditions which allow the reliable measurement of the power spectrum of rough surfaces by optical Fourier transformation. He observed that it was possible to obtain the power spectrum by optical Fourier transform when the ratio of amplitude to illumination wavelength is below 0.2. The investigation was mainly limited to periodic surfaces. The range of samples examined by the above mentioned method was extended to a limited samples for grinding, lapping and laminated plastic [16].

A prototype optical spectrum analyzer was proposed by E. G. Thwaite [17] for obtaining the power spectrum of surfaces by utilizing the optical Fourier transform technique. It was observed that there are some differences between the stylus method and the optical but the optical method is judged to be good enough for practical purpose.

E. G. Thwaite (18) has investigated the idea of generating a optical Fourier transform by using infrared illumination (wavelength = $3.39\mu\text{m}$). It was observed that by extension of the wavelength into near infrared one can obtain results comparable to those measured at visual wavelengths for some specimens.

2.4 Objective of the research

The main objective of this research work is to

obtain the frequency spectrum from the optical Fourier transform technique and then to derive the surface texture parameters from the spectra.

Although a successful attempt has been made to obtain the frequency spectra by the optical Fourier technique by Pernick [14] and Thwaite [15], the main drawback of their work has been that the results were based on a small set of periodic samples. Moreover, no effort has been made by any worker to use the two dimensional properties of the optical Fourier technique.

This research work , therefore, pursues the following objectives:

a) To obtain the two dimensional optical Fourier transform for different types of machined surfaces.

b) To compare the frequency spectrum obtained by the optical method and the mechanical method for samples of different machining processes and different materials.

c) To derive surface texture parameters from the optical method for samples of different materials and machining processes.

d) To determine if there is any correlation between the roughness in the lay direction and perpendicular to the lay direction.

e) To determine how a thin film of oil work surface effects the correlation curves.

f) To quantify the surface scratches produced by the stylus profilometer from the two dimensional optical Fourier spectrum obtained by the optical method.

CHAPTER III

EXPERIMENTAL APPARATUS AND PROCEDURE

In this research work, optical Fourier transform is used to study the surface texture of different types of surfaces and also to derive texture parameters to characterize a given surface. This chapter describes the apparatus and procedure used for obtaining an optical Fourier transform. To confirm the results obtained by the optical method, stylus profilometer is used to obtain the surface profile for the derivation of the frequency spectrum. The apparatus and procedure used in the stylus method is also described in this chapter.

3.1 Optical Method:

In the optical method the diffraction phenomena which provides a method for optically computing the Fourier transforms constitutes the basis for this study. The apparatus and the procedure adopted in this work will be described in detail in the following sections.

3.1.1 Description of the Apparatus:

A block diagram of the apparatus used in the experiment is shown in Figure 3.1. The experimental set-up consists of a 2 mw He-Ne laser used in conjunction with a half silver mirror to illuminate the specimen. The

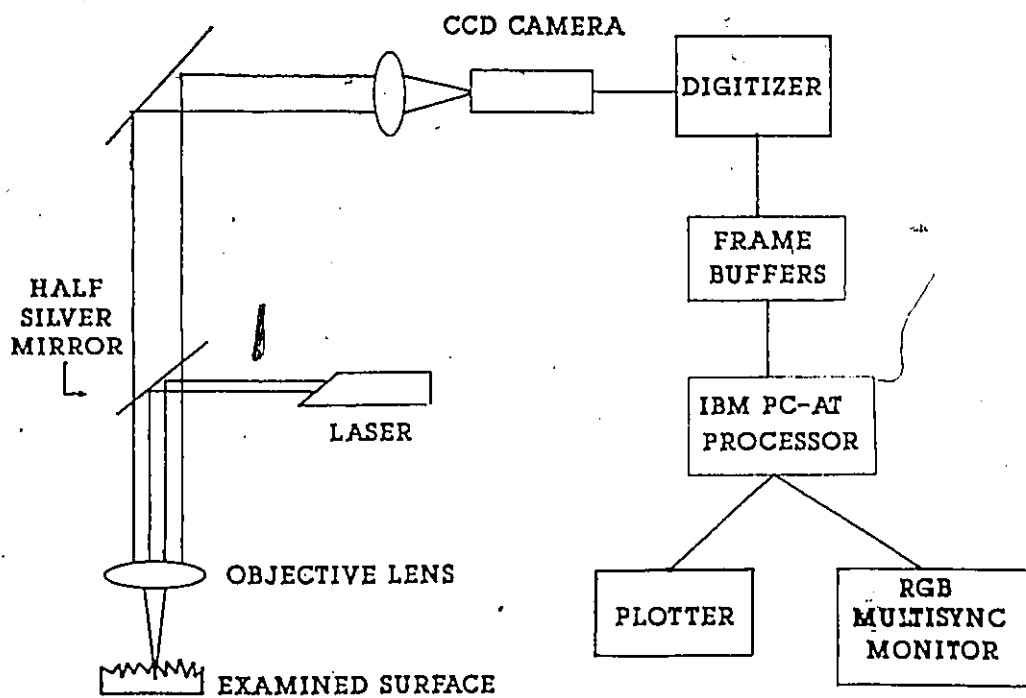


Figure 3.1 A block diagram of the experimental set-up for the optical method.

specimen is located in the front focal plane (object plane) of the objective lens which forms an image at infinity. A second lens in conjunction with another half silver mirror is used to focus this image at its back focal plane (Fourier plane). A solid state RCA CCD camera (TC 2800) located in the Fourier plane is used to capture the optical Fourier transform pattern. A photograph of the arrangement is shown in Figure 3.2. The analog signal from the camera is then transferred to a frame grabber board. The board digitizes the analog signal to an image of 512 x 512 pixels with 256 levels of grey. The digitized image is stored in one of four frame buffers available on the frame grabber board. The frame grabber board uses an IBM PC-AT bus and takes 1/30 sec to capture and digitize an image. The operations performed on the image can be displayed on a video monitor. A plotter and a printer are connected to the microcomputer to produce a hard copy output. Details of the hardware are given in Appendix A.

A spatial filter (50u) is used with the laser beam to eliminate any spatial noise and provide a clean fundamental laser mode. The light from the laser light source was passed through a polarizing filter before reaching the sample. The purpose of the polarizer is to control the intensity of the pattern. For smooth surfaces the Fourier pattern appears saturated, and to reduce the

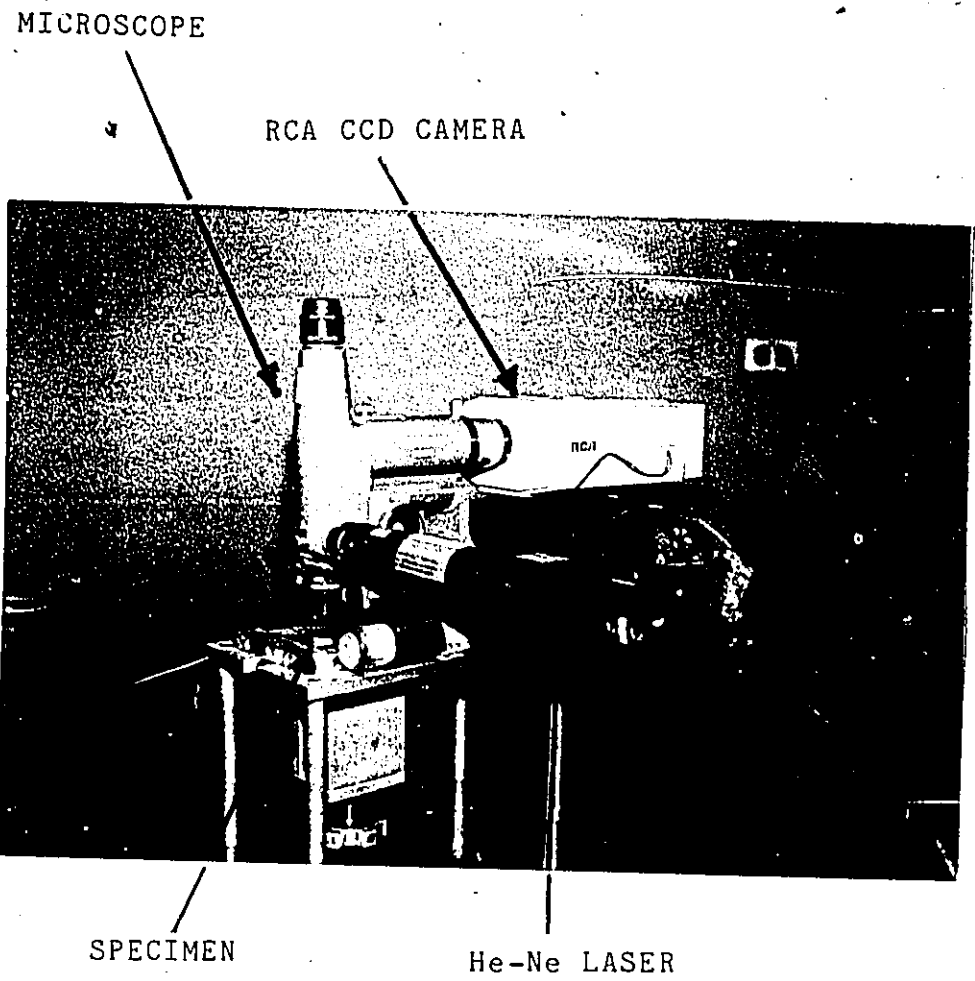
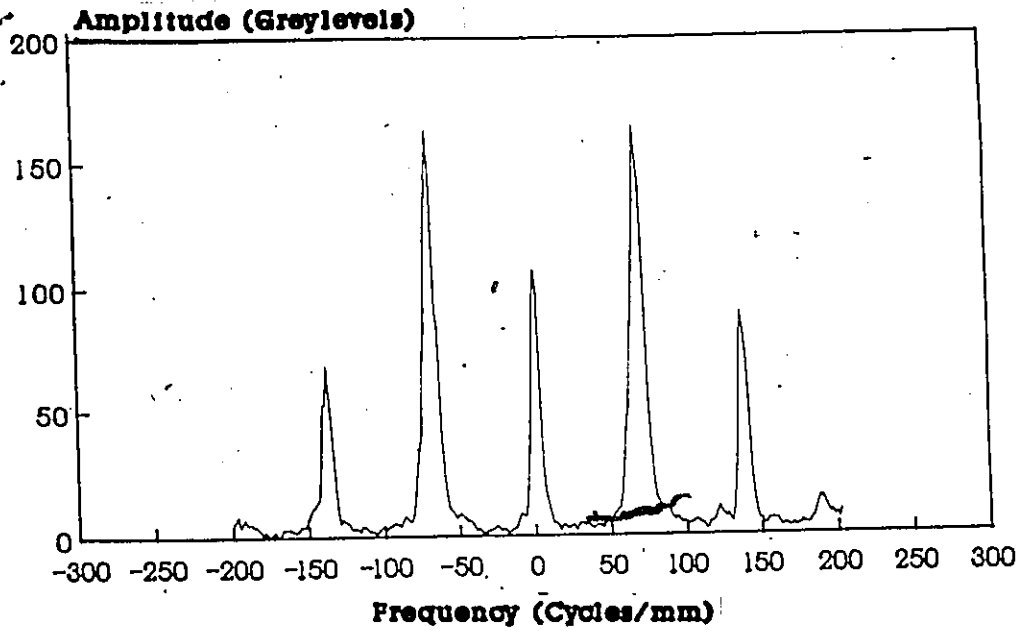


Figure 3.2 A photograph showing the experimental set-up for the optical method

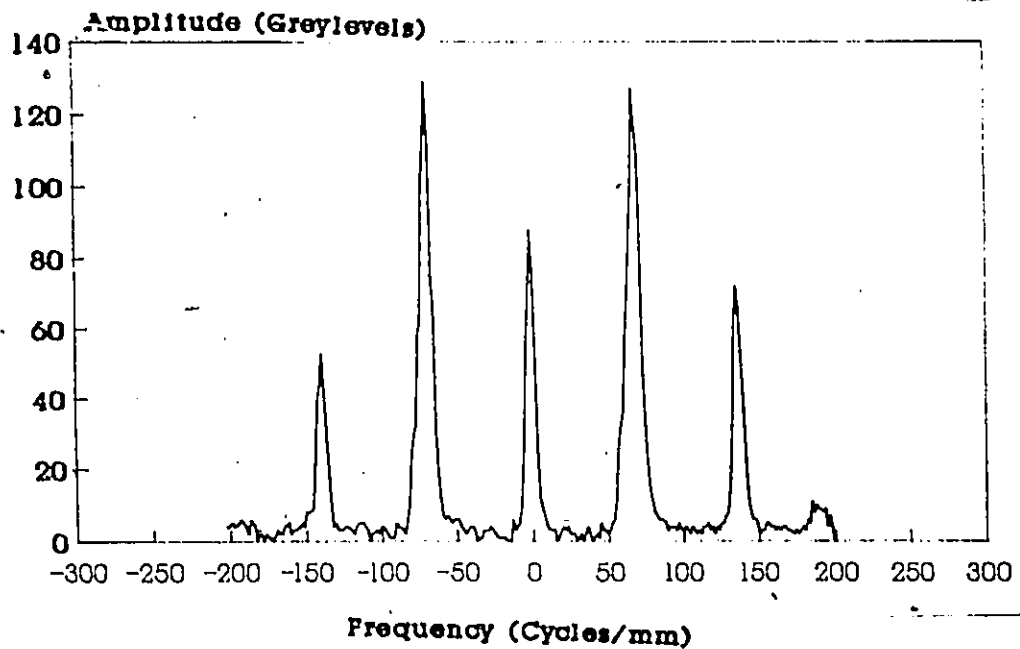
intensity the polarizing filter was rotated to a given position obtain the minimum output of the frequency spectra. Figure 3.3 (a) & (b) show the frequency spectra of the standard calibration sample ($R_a = 0.5\mu\text{m}$) for maximum and minimum output of the polarizer.

3.1.2 Experimental Procedure

The experimental procedure for obtaining a frequency spectra for different types of surfaces using optical method is described as follows. A flow diagram for the experimental procedure is given in Figure 3.4. The specimen is positioned in such a way that the lay direction is parallel to the z-axis (see Figure 3.5) which is perpendicular to the plane of illumination (x,y). Thus the laser is located such that the plane waves are parallel to the lay direction. The second step involves focusing the image onto the image plane of the camera by adjusting the distance between the objective lens and the surface. The image is then captured by the camera in a plane parallel to y-z and digitized by the digitizer board. A picture of the pattern as seen on the monitor is shown in Figure 3.5, where y,z correspond to the vertical and horizontal directions respectively. To generate a spatial record, a cross-section is selected along the center-line of the pattern (parallel to z-axis) and the grey level for a point z is determined by



(a)



(b)

Figure 3.3 (a) Frequency spectrum of the standard calibration sample ($R_a=0.5\mu\text{m}$) for maximum output.
 (b) Frequency spectrum for minimum output of the polarizer.

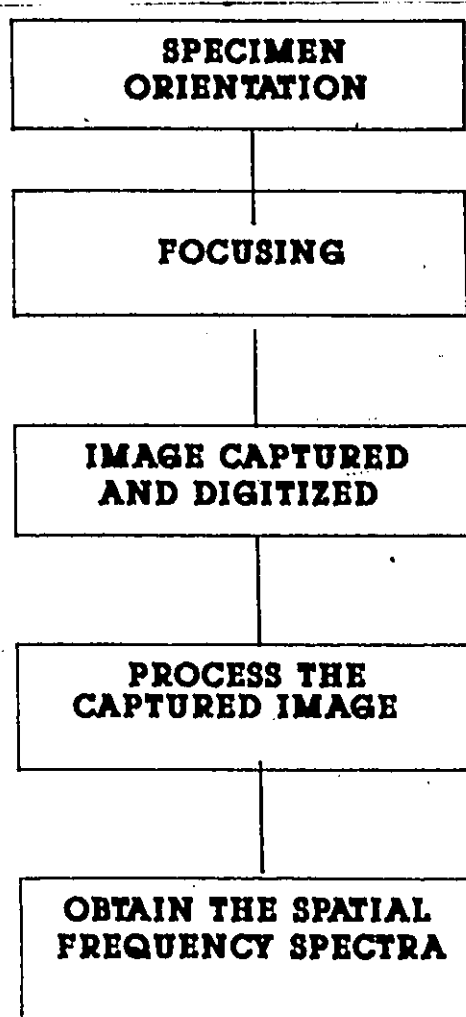


Figure 3.4 A flow diagram for the experimental procedure.

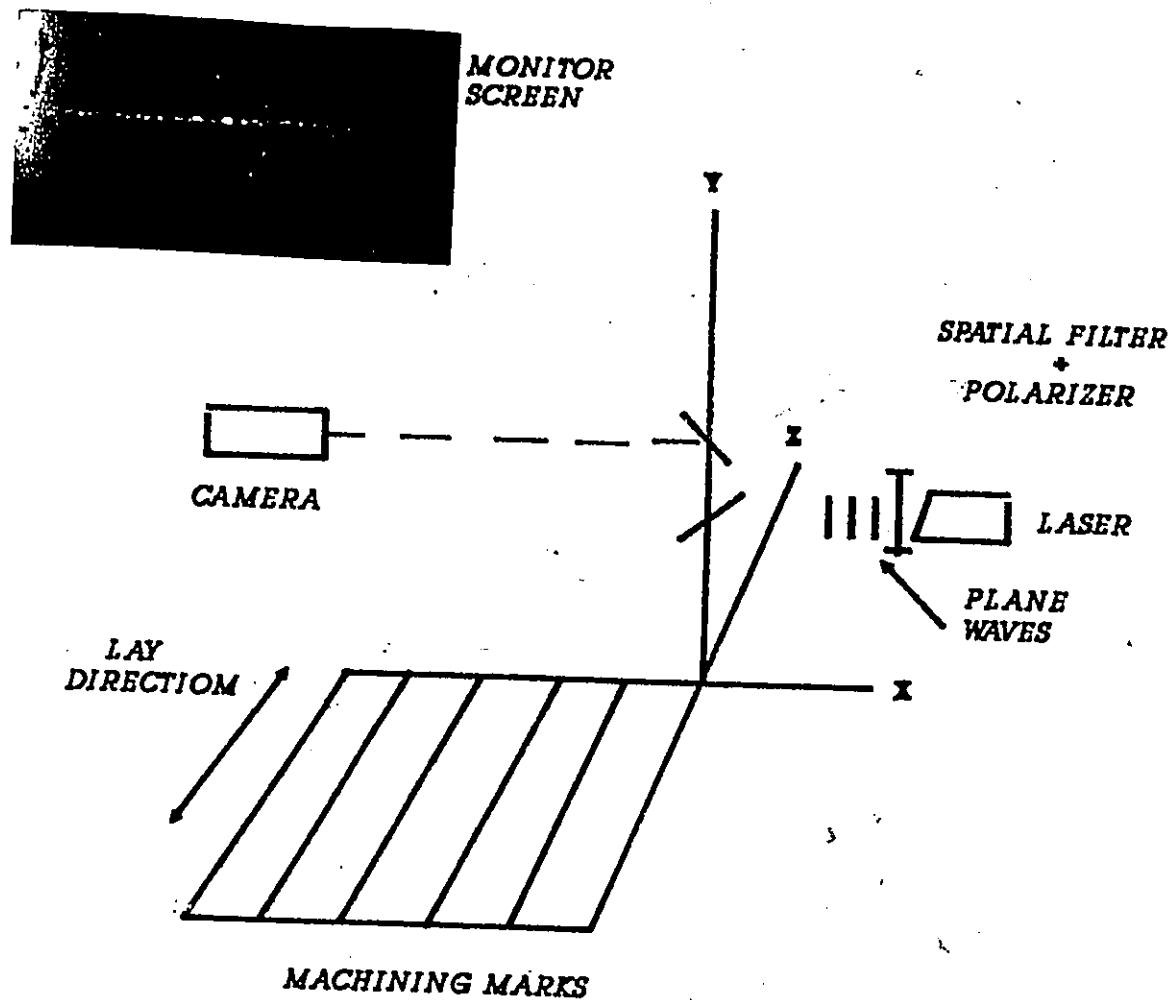


Figure 3.5 Arrangement of the light source and camera with respect to the specimen

averaging an equal number of pixels directly above or below the point. The next step is to obtain the spatial frequency values from the spatial record. The spatial frequency of a component located at a spatial distance z is given by a simple relationship

$$F = (z * M) / (\lambda * f) \text{ ----- (3.1)}$$

where F is the spatial frequency in cycles/mm,

M is the magnification of the system,

f is the focal length of the transform lens,

λ is the illumination wavelength ($0.632\mu\text{m}$)

and z is the spatial distance in μm

This equation is used to transform the spatial distance of the pattern to a spatial frequency value. Software for obtaining frequency spectrum was written in Fortran 77 and is given in Appendix. B

3.2 Mechanical Method:

In the mechanical method the Fourier transform is applied to the surface profile measured by a stylus instrument. The apparatus and the procedure adopted in this method is described in the following sections.

3.2.1 Description of Apparatus:

The experimental set-up shown in Figure 3.6 consists of a Mitutoyo Surftest III profilometer whose stylus traverses the surface of interest. The detailed information about the profilometer is provided in the operation manual [4]. The signal from the profilometer which is in the time domain is transformed into the frequency domain by an SD375 Dynamic analyzer which uses an FFT algorithm. The frequency spectrum output and other data from the FFT analyzer is stored in a HP computer for further analysis or printed on a thermal printer. The photograph of the experimental set-up is shown in Figure 3.7. The specifications for the SD 375 dynamic analyzer are given in Appendix A.

3.2.2 Experimental Procedure:

The experimental procedure used in the stylus method is described in this section. Specimens were cleaned with a soft paper to keep them free from dirt. The specimen is positioned in such a way that the direction of stylus travel is perpendicular to the lay. The cut-off value was selected to be 0.8mm and the damper was ON. The diamond stylus traveled 8mm at the speed of 2mm/sec. To reduce the noise in the signal, three stylus traverses are made and averaged for a given specimen. This time domain signal was fed into the dynamic

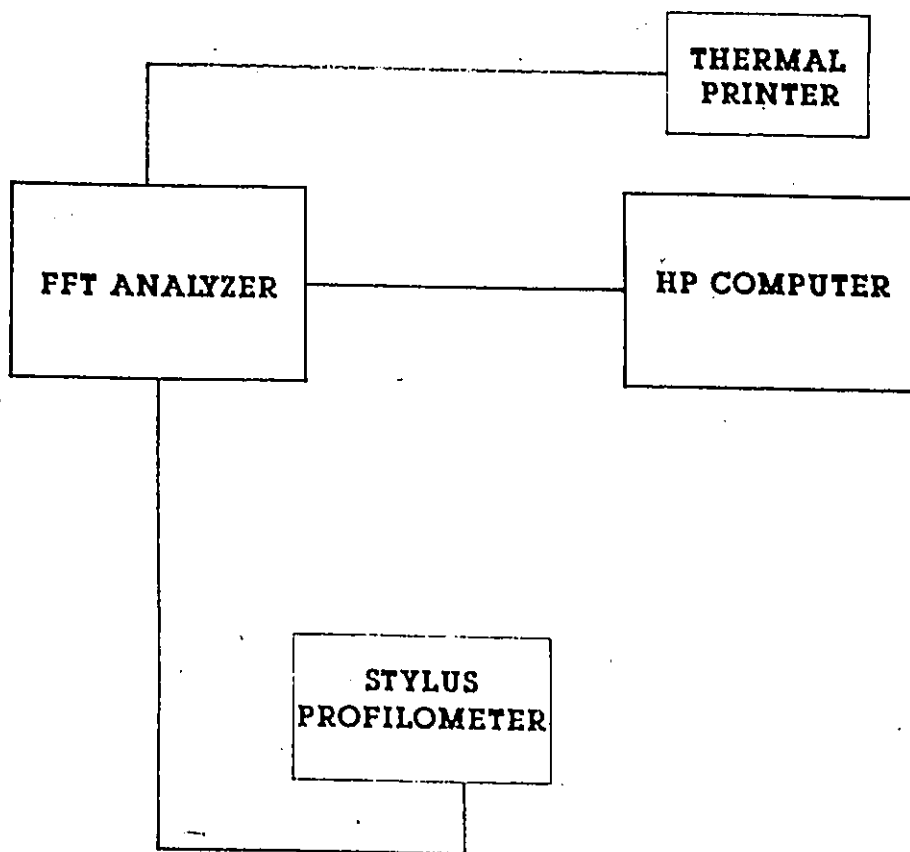
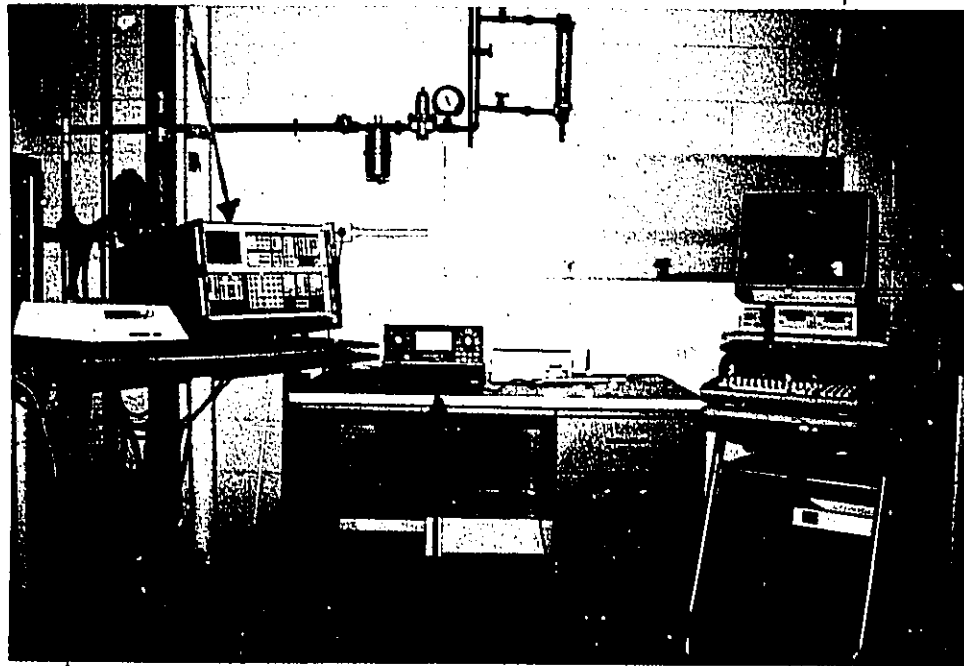


Figure 3.6 A block diagram of the experimental set-up used in the mechanical method.

FFT ANALYZER

HP COMPUTER



THERMAL PRINTER STYLUS PROFILOMETER

Figure 3.7 A photograph showing the experimental set-up used in the mechanical method

analyzer, where the signal is converted into frequency domain by an FFT algorithm. The frequency (Hz) scale as obtained is converted into spatial frequency (cycles/mm) scale by using the stylus traverse speed information.

3.3 Roughness Specimens:

Two types of machined samples were used in this work: Rubert gauge & grinding samples. The Rubert gauge is a set of surface roughness standards, manufactured by Rubert & Co. Ltd., England, having samples from different manufacturing processes. Table 3.1a lists all the different types of samples and their roughness range from the Rubert block. Table 3.1b provides details about the ground samples of different types of materials, namely, aluminum, brass, copper, tool steel and magnesium, which were used in the work. The samples were machined using different grades of grinding wheels and feed rates to produce various degrees of roughness. The mechanical and chemical properties of these materials are shown in Appendix C.

3.4 Calculation Procedure(Parameters):

This section describes the quantitative parameters which characterize the frequency spectra obtained by the two methods. A spatial frequency bandwidth of 0 to 200 cycles/mm with a sampling frequency

Table 3.1 (a) Samples from different machining processes used in this work, their roughness range and No. of samples.

Process	Roughness Range	No of samples
Flat Lapping	0.05-0.2 μ m	3
Grinding	0.05-0.81 μ m	5
Horizontal Milling	0.4-0.81 μ m	2
Vertical Milling	0.4-0.81 μ m	2
Reaming	0.4-1.6 μ m	3
Turning	0.4-1.6 μ m	3

Table 3.1 (b) Surface ground samples of different materials used in this work with their roughness range

Material	Roughness Range	No of samples
Aluminum	0.07-0.83 μ m	8
Brass	0.07-1.3 μ m	8
Copper	0.07-0.85 μ m	8
Stainless Steel	0.05-0.81 μ m	5
Tool Steel	0.076-0.8 μ m	8
Magnesium	0.15-0.23 μ m	2

1.487 cycles/mm was used for calculating all the parameters. A brief description of all these parameters is given below.

a) Mean Frequency : This is a weighted estimate of the mean frequency in cycles/mm of the frequency spectrum. This is one of the parameters used for comparing the two spectra. Mean frequency is given by

$$f_m = [(\sum A_i f_i) / (\sum A_i)] \text{ ----- (3.2)}$$

where:

A_i is amplitude components of frequency spectrum

f_i is the frequency in cycles/mm

b) Standard Deviation of frequency: The standard deviation of the mean frequency is a measure of the variation from the mean frequency in cycles/mm.

$$\text{STD} = [\sum A_i (f_i - f_m)^2 / N]^{0.5} \text{ -----(3.3)}$$

where:

N is the number of points

c) Coefficient of Variation of mean frequency : Coefficient of variation is the ratio of standard deviation to mean frequency.

$$\text{C.V} = (\text{STD}/\text{Mean}) \text{ -----(3.4)}$$

d) Spectrum RMS : This gives an estimate of the RMS

energy level of the defined spatial frequency bandwidth. This parameter was used to represent surface roughness in this study. The RMS is defined as

$$\text{RMS} = [(\sum A_i^2)/N]^{0.5} \text{ ---- (3.4)}$$

e) Spectrum Peak : Another parameter used to characterize roughness was the spectrum peak which is the greatest intensity value within a particular spatial frequency range. This parameter is of significance in monitoring tool wear and geometrical defects.

The spectrum RMS and peak values were normalized with respect to the standard calibration sample with roughness Ra of 0.5 μ m.

f) Percent Deviation : The percent deviation is calculated from the values of coefficient of variation of frequency from the two spectra. This gives an estimate of the deviation between the two spectra.

$$\text{Percent Deviation} = [((C.V)_m - (C.V)_o) / (C.V)_m] \text{ ---- (3.5)}$$

where:

(C.V)_o is the coefficient of variation obtained from the optical method.

(C.V)_m is the coefficient of variation obtained from the mechanical method.

CHAPTER IV

RESULTS AND DISCUSSION

The optical Fourier transform technique was used to compute the frequency spectra for different types of machined surfaces. The results obtained by the optical method were compared with those obtained by the stylus profilometer. The parameters derived from the frequency spectra were used to characterize surface texture. The two dimensional properties of the Fourier spectrum were also used to reveal information about surface defects on the part.

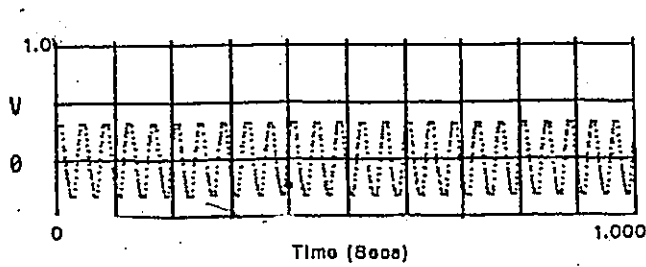
4.1 Fourier Analysis of surface roughness:

For a machined surface, the roughness profile is a combination of periodic and random roughness. The discrete peaks in a spectrum indicate periodic roughness which is caused by the machining operation. These discrete peaks can be the feed components which occur at spatial frequencies of nf_s , where n is any integer and f_s is spatial frequency of first order feed component (19). The random roughness is the roughness level between these discrete peaks. This is a result of the irregularities in the manufacturing process.

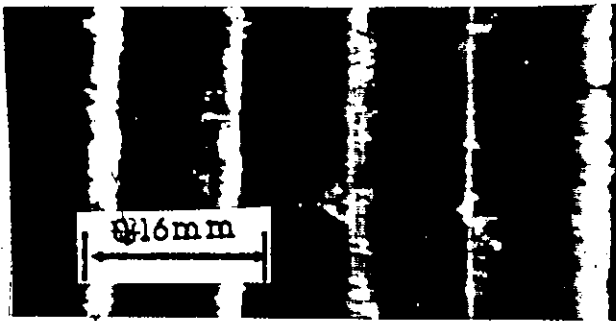
4.2 Calibration of the apparatus:

Two standard surfaces with accurately machined grooves ($R_a=0.5\mu\text{m}$ & $R_a=3.0\mu\text{m}$) were used to calibrate the instrument. Figure 4.1 shows the results of measurement for the $3.0\mu\text{m}$ sample. Figure 4.1 (a) shows the time domain signal obtained from the stylus profilometer. As can be seen, the profile is of triangular shape. Figure 4.1(b) shows the photograph of the surface seen under a microscope with dark field illumination. From the photograph it was observed that the surface is periodic in nature. Figure 4.1 (c) shows the optical Fourier transform pattern as seen on the monitor. Figure 4.1 (d) shows the frequency spectrum derived from the time domain signal. The plot of the frequency spectrum obtained from the optical Fourier transform (note the origin of the graph) is shown in Figure 4.1 (e). The frequency spectrum contains discrete peaks which confirms the observation that the surface is periodic. Figure 4.2 shows the results of the measurement for the $0.5\mu\text{m}$ sample. As observed from the optical pattern and the frequency spectra, this surface is also periodic in nature with discrete peaks.

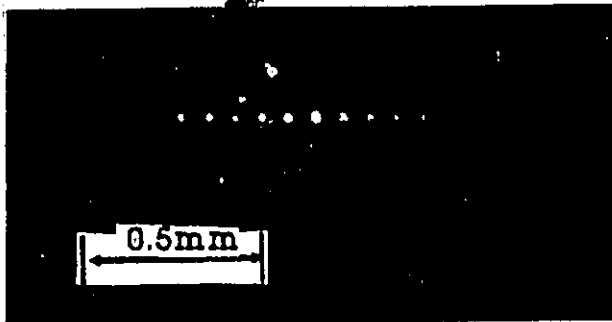
Table 4.1 shows the comparison of the frequency spectra obtained by the two methods. From the results it was observed that the f_s values obtained by the optical



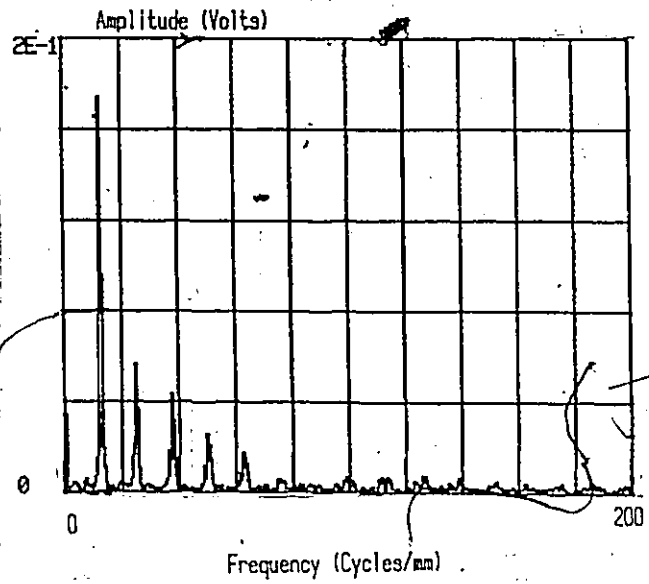
(a)



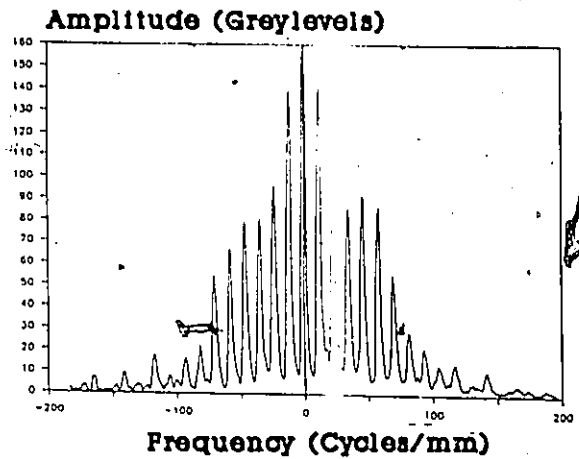
(b)



(c)



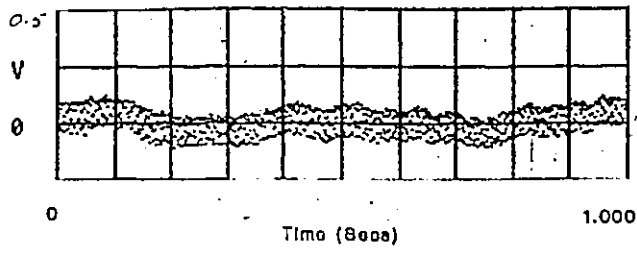
(d)



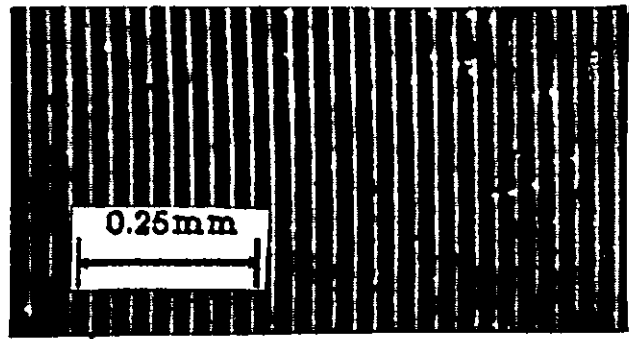
(e)

Figure 4.1 Typical characteristics of standard calibrated sample ($R_a=3.0\mu\text{m}$)

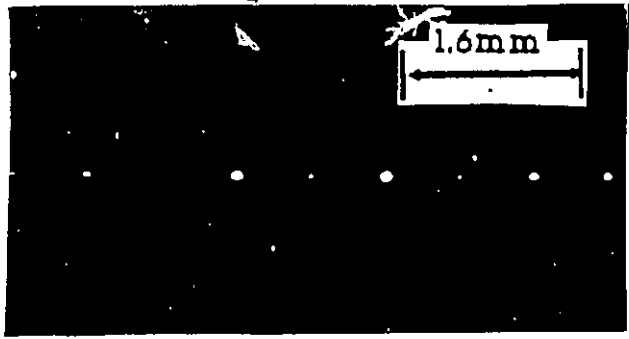
- (a) Time domain signal
- (b) Photograph of the original surface
- (c) Photograph of the Fourier pattern
- (d) Frequency spectrum obtained from stylus
- (e) Frequency spectrum obtained from the optical method



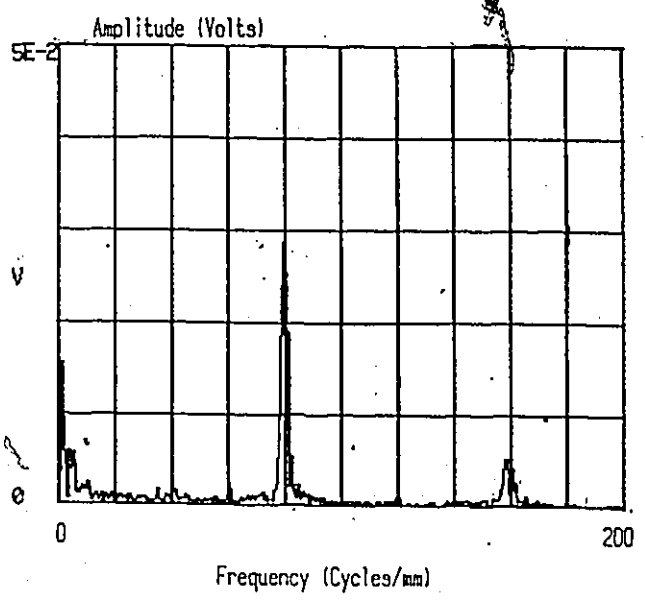
(a)



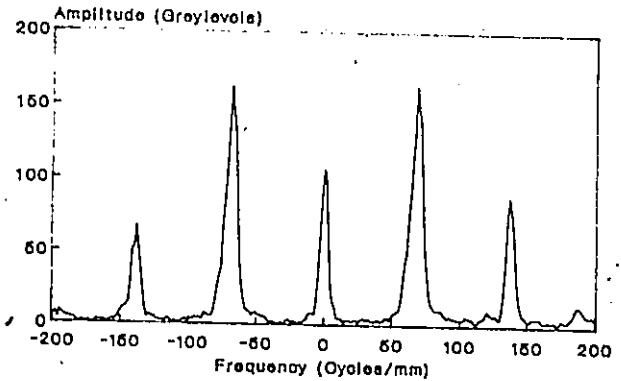
(b)



(c)



(d)



(e)

Figure 4.2 Typical characteristics of standard calibrated sample ($R_a=0.5\mu\text{m}$)
 (a) Time domain signal
 (b) Photograph of the original surface
 (c) Photograph of the Fourier pattern
 (d) Frequency spectrum obtained from stylus
 (e) Frequency spectrum obtained from the optical method

Table 4.1 Comparison of Frequency Spectra

	Optical		Mechanical	
	Frequency (cycles/mm) f_s	Amplitude Ratio	Frequency (cycles/mm) f_s	Amplitude Ratio
Sample 1 ($R_a=0.5\mu\text{m}$)	72	1.6	76	1.8
	144	0.5	154	0.2
Sample 2 ($R_a=3.0\mu\text{m}$)	11	0.9	13	0.3
	22	0.6	26	0.4
	33	0.7	39	0.75

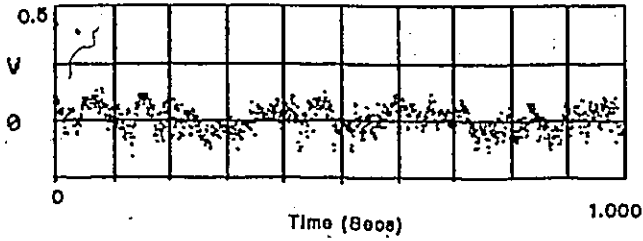
method compare well with those obtained by the mechanical method for both the samples. The amplitude ratio (A_1/A_0 , $A_2/A_1, \dots$) values, where A_0, A_1, \dots correspond to the amplitude values for each individual peak, obtained by the optical method also are comparable with those obtained by the mechanical method.

4.3 Fourier spectrum of ground surfaces of different materials (Two-Dimensional):

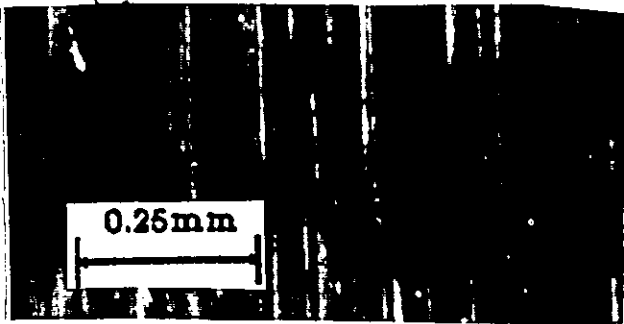
Grinding samples of six different types of materials, namely, tool steel, stainless steel, aluminum, copper, brass, and magnesium were used in this work. Only typical results are shown here, the rest are provided in the Appendix D.

a) Description of surface texture from optical Fourier transform:

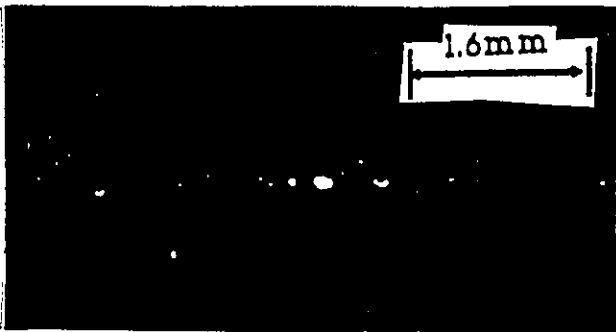
The results of measurement for a typical tool steel surface are shown in Figure 4.3. The surface consists of grooves which appear random in depth. Figure 4.3 (c) shows the optical Fourier pattern. The central spot in the pattern corresponds to zero spatial frequency. Also the Fourier pattern indicates that the surface has more information in one direction (perpendicular to lay) when compared to the other, thus the pattern is one-dimensional. This is a typical



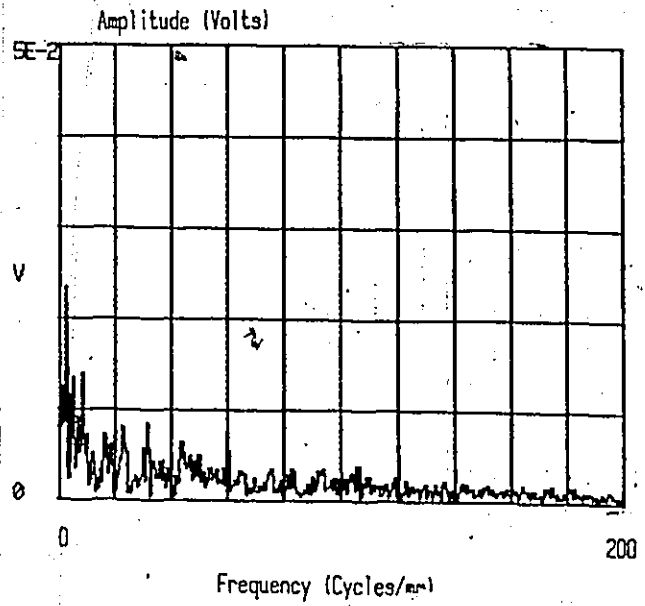
(a)



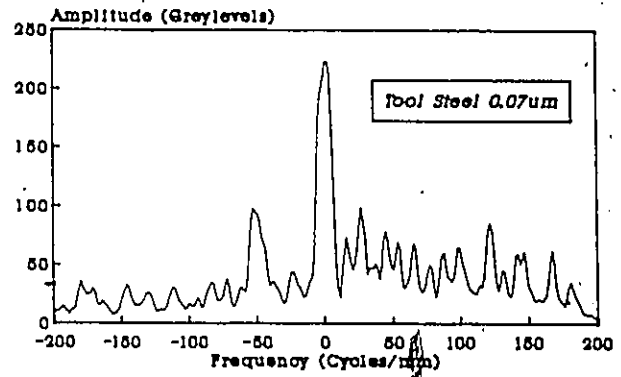
(b)



(c)



(d)



(e)

Figure 4.3 Typical characteristics of tool steel sample ($R_a=0.07\mu\text{m}$) (Ground).

- (a) Time domain signal
- (b) Photograph of the original surface
- (c) Photograph of the Fourier pattern
- (d) Frequency spectrum obtained from stylus
- (e) Frequency spectrum obtained from the optical method

characteristic of most of the ground samples. The frequency spectra obtained by both methods contain a few small discrete peaks indicating the presence of some degree of periodicity in the surface. The texture overall, in general is closer to a random surface.

Typical characteristics of a stainless steel sample are shown in Figure 4.4. The frequency spectra consists of a few discrete peaks similar to that obtained for the tool steel sample.

Figure 4.5 shows the characteristics of a typical aluminum surface. The optical Fourier spectrum shows discrete peaks at higher frequencies where as the spectra obtained by the stylus method does not show any frequency components at higher frequency. This might be attributed to the fact that the stylus is limited in its capability to quantify information at high frequencies because of the relatively large size of the stylus tip and the high velocity of traverse.

The typical characteristics of a brass sample are shown in Figure 4.6. The frequency spectra obtained by the optical method contains a few discrete peaks but the spectra obtained by the mechanical method does not show any noticeable discrete peaks.

Figure 4.7 shows the characteristics of a

National Library
of Canada

Canadian Theses Service

Bibliothèque nationale
du Canada

Service des thèses canadiennes

NOTICE

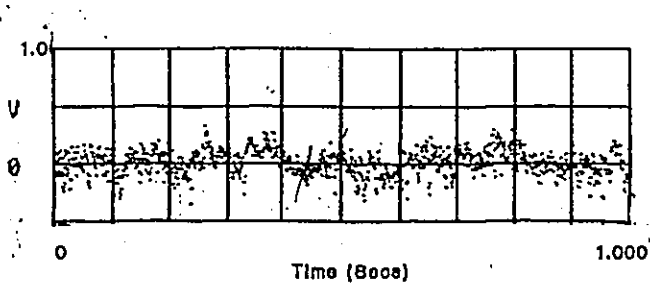
AVIS

THE QUALITY OF THIS MICROFICHE
IS HEAVILY DEPENDENT UPON THE
QUALITY OF THE THESIS SUBMITTED
FOR MICROFILMING.

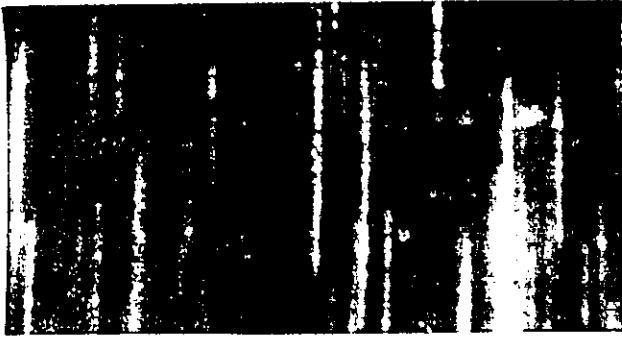
UNFORTUNATELY THE COLOURED
ILLUSTRATIONS OF THIS THESIS
CAN ONLY YIELD DIFFERENT TONES
OF GREY.

LA QUALITE DE CETTE MICROFICHE
DEPEND GRANDEMENT DE LA QUALITE DE LA
THESE SOUMISE AU MICROFILMAGE.

MALHEUREUSEMENT, LES DIFFERENTES
ILLUSTRATIONS EN COULEURS DE CETTE
THESE NE PEUVENT DONNER QUE DES
TEINTES DE GRIS.



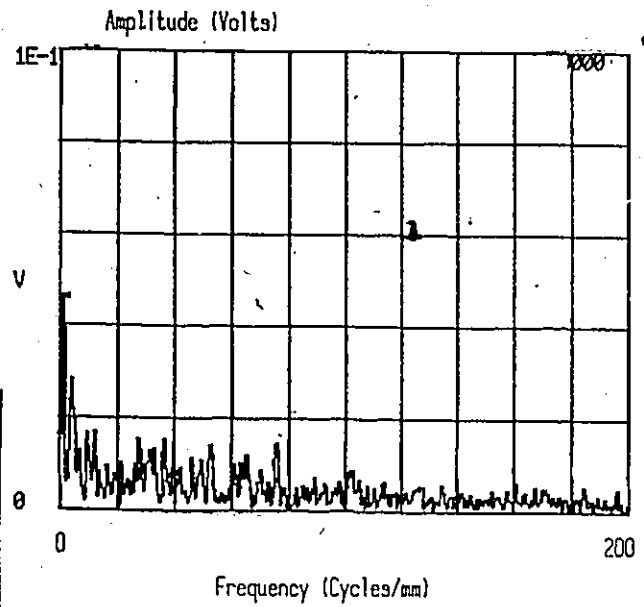
(a)



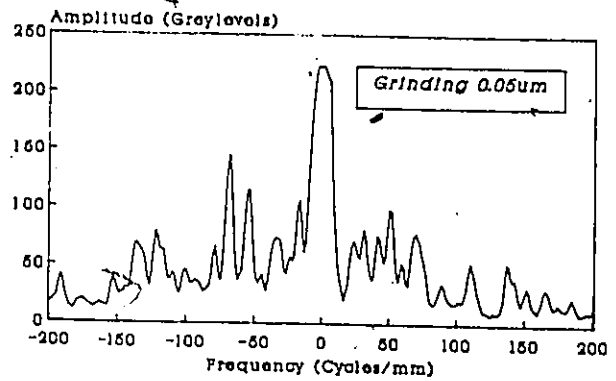
(b)



(c)



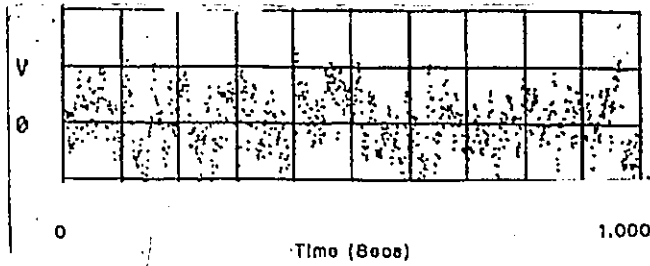
(d)



(e)

Figure 4.4 Typical characteristics of stainless steel sample ($R_a=0.05\mu\text{m}$), (Ground).

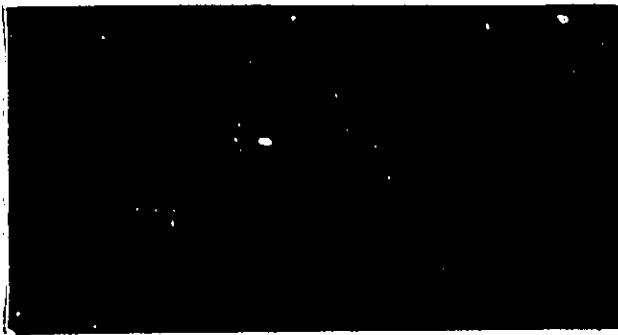
- (a) Time domain signal
- (b) Photograph of the original surface
- (c) Photograph of the Fourier pattern
- (d) Frequency spectrum obtained from stylus
- (e) Frequency spectrum obtained from the optical method



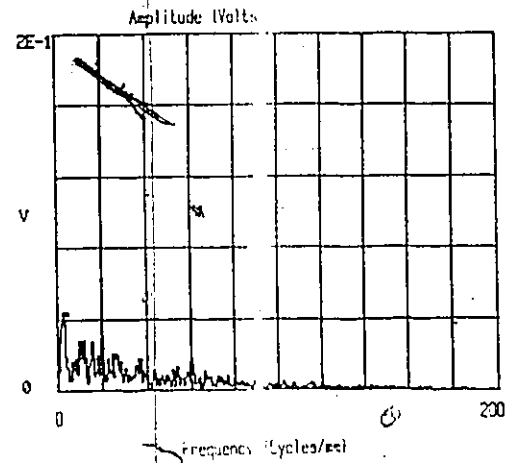
(a)



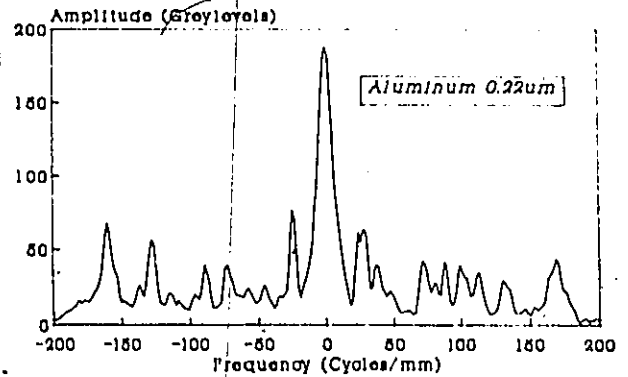
(b)



(c)



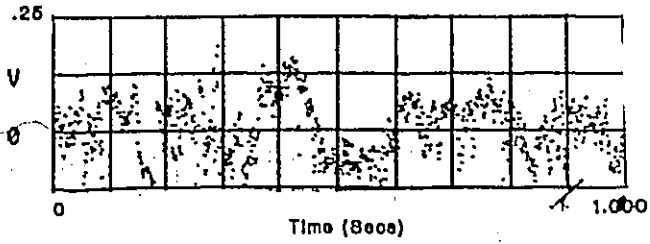
(d)



(e)

Figure 4.5 Typical characteristics of aluminum sample ($R_a=0.22\mu\text{m}$)(Ground).

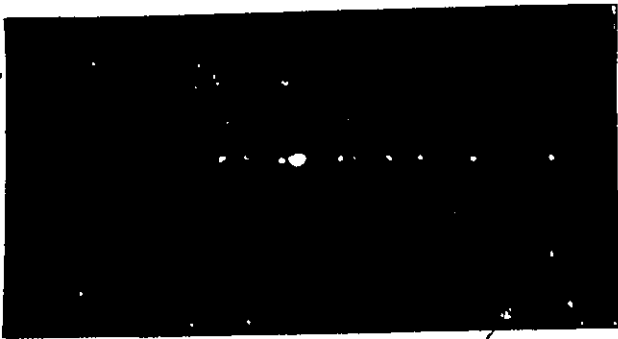
- (a) Time domain signal
- (b) Photograph of the original surface
- (c) Photograph of the Fourier pattern
- (d) Frequency spectrum obtained from stylus
- (e) Frequency spectrum obtained from the optical method



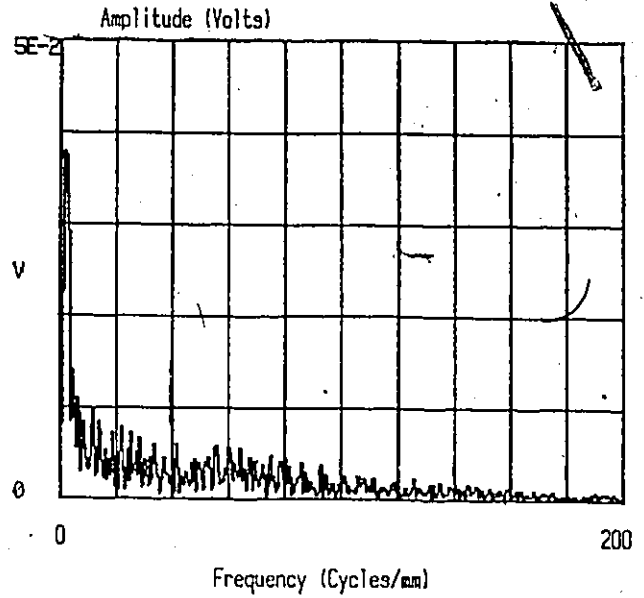
(a)



(b)



(c)



(d)

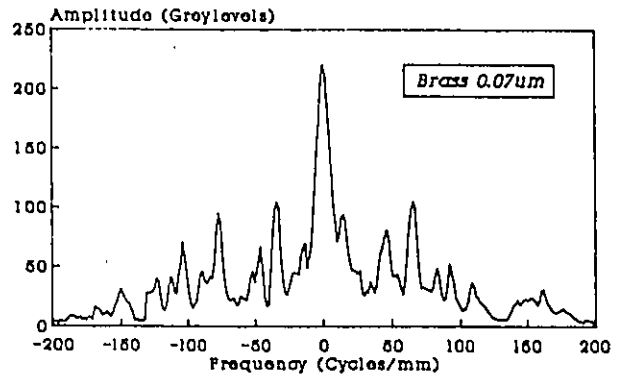
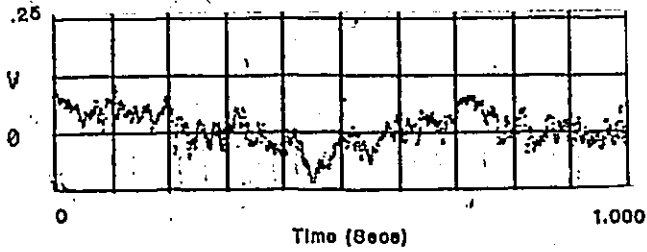
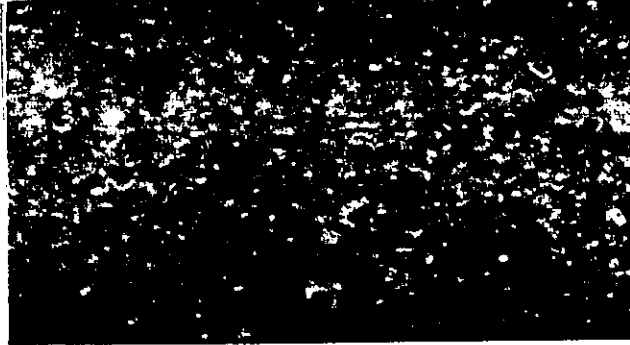


Figure 4.6 Typical characteristics of brass sample ($R_a=0.07\mu\text{m}$) (Ground).
 (a) Time domain signal
 (b) Photograph of the original surface
 (c) Photograph of the Fourier pattern
 (d) Frequency spectrum obtained from stylus
 (e) Frequency spectrum obtained from the optical method



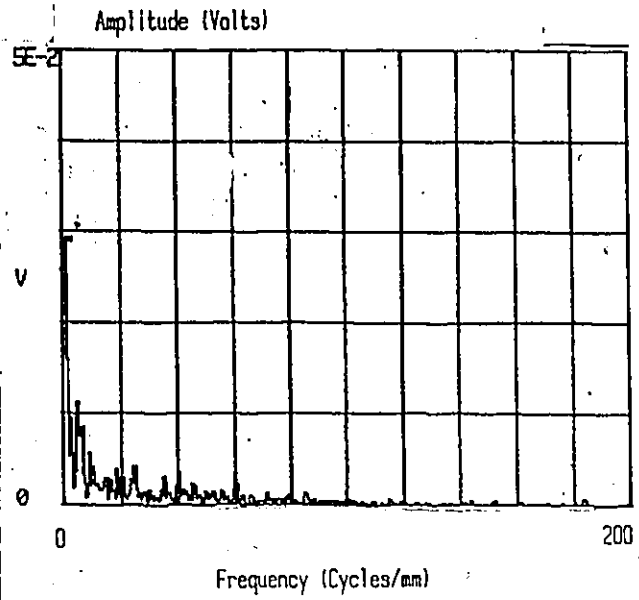
(a)



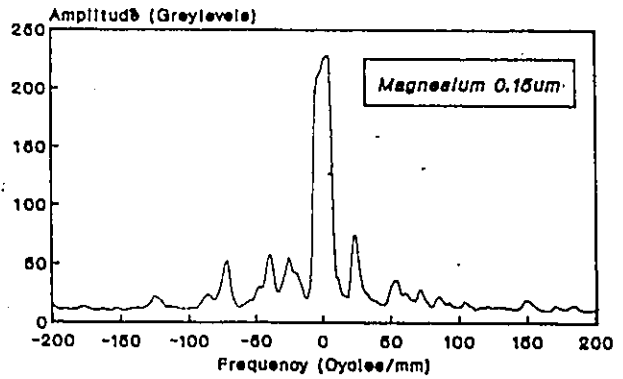
(b)



(c)



(d)



(e)

Figure 4.7 Typical characteristics of magnesium sample ($R_a=0.15\mu\text{m}$)
 (a) Time domain signal
 (b) Photograph of the original surface
 (c) Photograph of the Fourier pattern
 (d) Frequency spectrum obtained from stylus
 (e) Frequency spectrum obtained from the optical method

magnesium sample. As can be seen from Figure 4.7 (b) the surface does not show any predominant lay direction. This might be due to the following reasons, namely, polishing technique being employed and the samples were oxidized. As a result, the optical Fourier pattern is two dimensional and tends to be isotropic.

b) Correlation between optical Fourier transform and mechanical technique:

To compare the two frequency spectra, the rigorous approach is to consider the ratio of amplitudes. If the ratios do not deviate greatly from a constant then the spectra are similar. Since the two frequency spectra obtained in this work were of similar shape, the distribution was defined by its mean and standard deviation of frequency for comparison. For further simplification, a parameter derived from the coefficient of variation was used to indicate the deviation between the two spectra.

Table 4.2 shows the results for the eight surface ground tool steel samples used in the study. Mean frequency is an estimate of the weighted mean of the frequency spectra. Standard deviation is a measure of variation from the mean frequency. The percent deviation between the two spectra was calculated by using the coefficient of variation values obtained from both

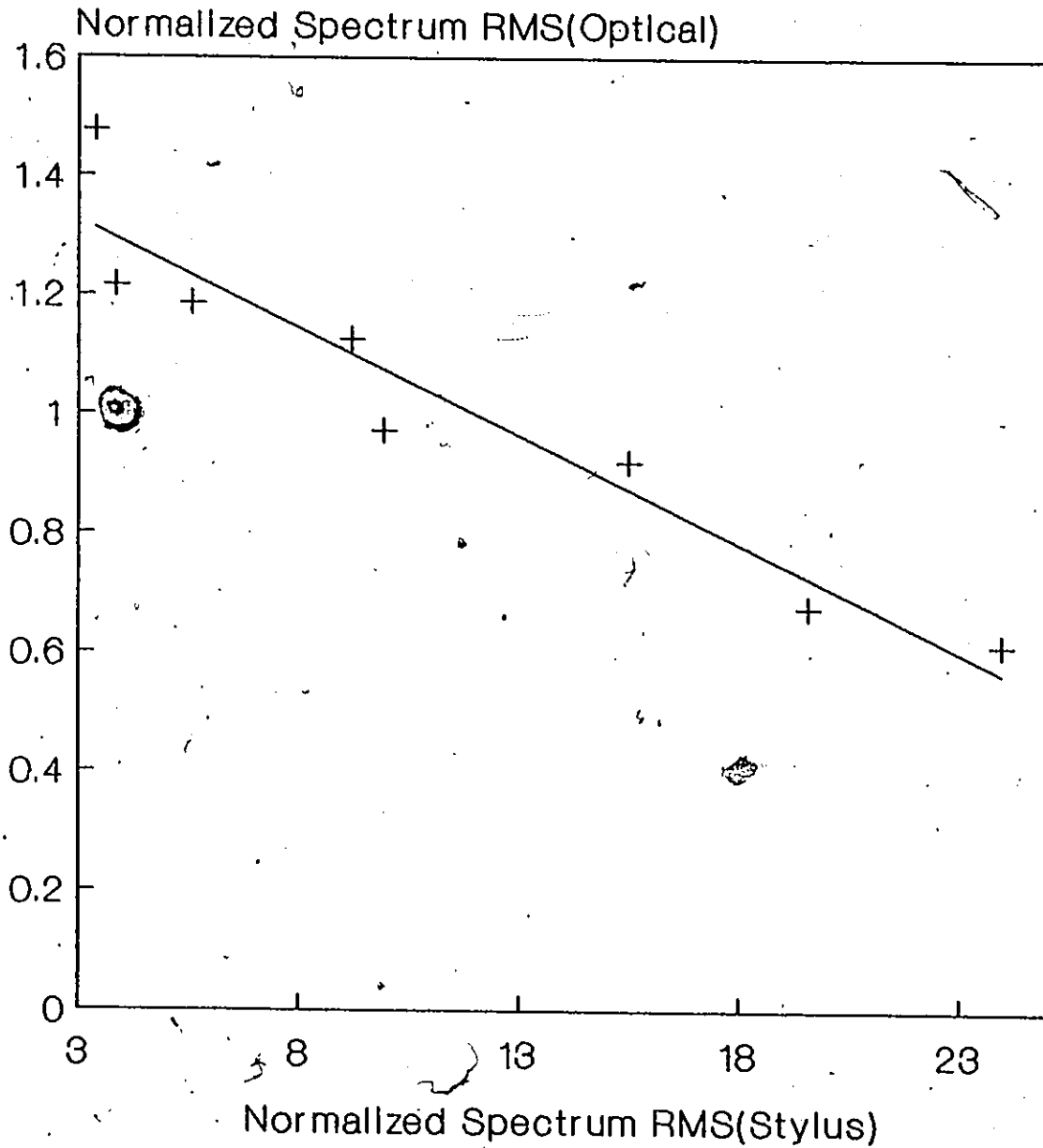
Table 4.2 Frequency spectra obtained by the optical & mechanical methods for surface ground Tool Steel samples.

Ra (μm)	Mechanical method		Optical method		Percent deviation %
	Mean (cycles/mm)	STD (cycles/mm)	Mean (cycles/mm)	STD (cycles/mm)	
0.07	63.09	54.51	67.79	57.08	2.43
0.15	69.13	53.93	67.29	54.23	-3.2
0.17	63.61	53.46	66.80	54.84	2.26
0.23	65.98	51.79	78.11	56.78	7.2
0.3	56.10	50.62	76.03	61.96	9.64
0.5	52.86	47.72	77.52	62.09	11.2
0.62	56.02	48.29	76.44	58.4	11.36
0.8	44.83	41.88	72.20	55.02	18.41

methods. It was observed that for smoother surfaces the mean frequency obtained by the two methods are almost identical, but as the surface becomes rougher there is a wider discrepancy between the values obtained by the two methods. The deviation between the two methods at higher roughness may be attributed to the fact that the profilometer is not quite accurate in resolving amplitudes at spatial-frequencies higher than 70 cycles/mm. This limitation is due to the size of the stylus tip and the velocity of traverse.

The RMS and peak values are obtained from the frequency spectrum for the samples. The spectrum RMS gives an estimate of the RMS energy level of the frequency spectra and the spectrum peak examines the amplitude value at a particular spatial frequency. The spectrum RMS and peak values were normalized with respect to the corresponding values of a standard calibration sample which has an Ra value equal to 0.5 μ m. Figure 4.8 shows the correlation between the RMS values obtained by the two methods for tool steel samples. An inverse linear relationship exists between the values obtained by the two methods. This result is due to the decrease in intensity of scattering pattern with increase in roughness. A least square fit equation is also shown in Figure 4.8. The correlation between the peak values obtained by the two methods is shown in Figure 4.9, and a

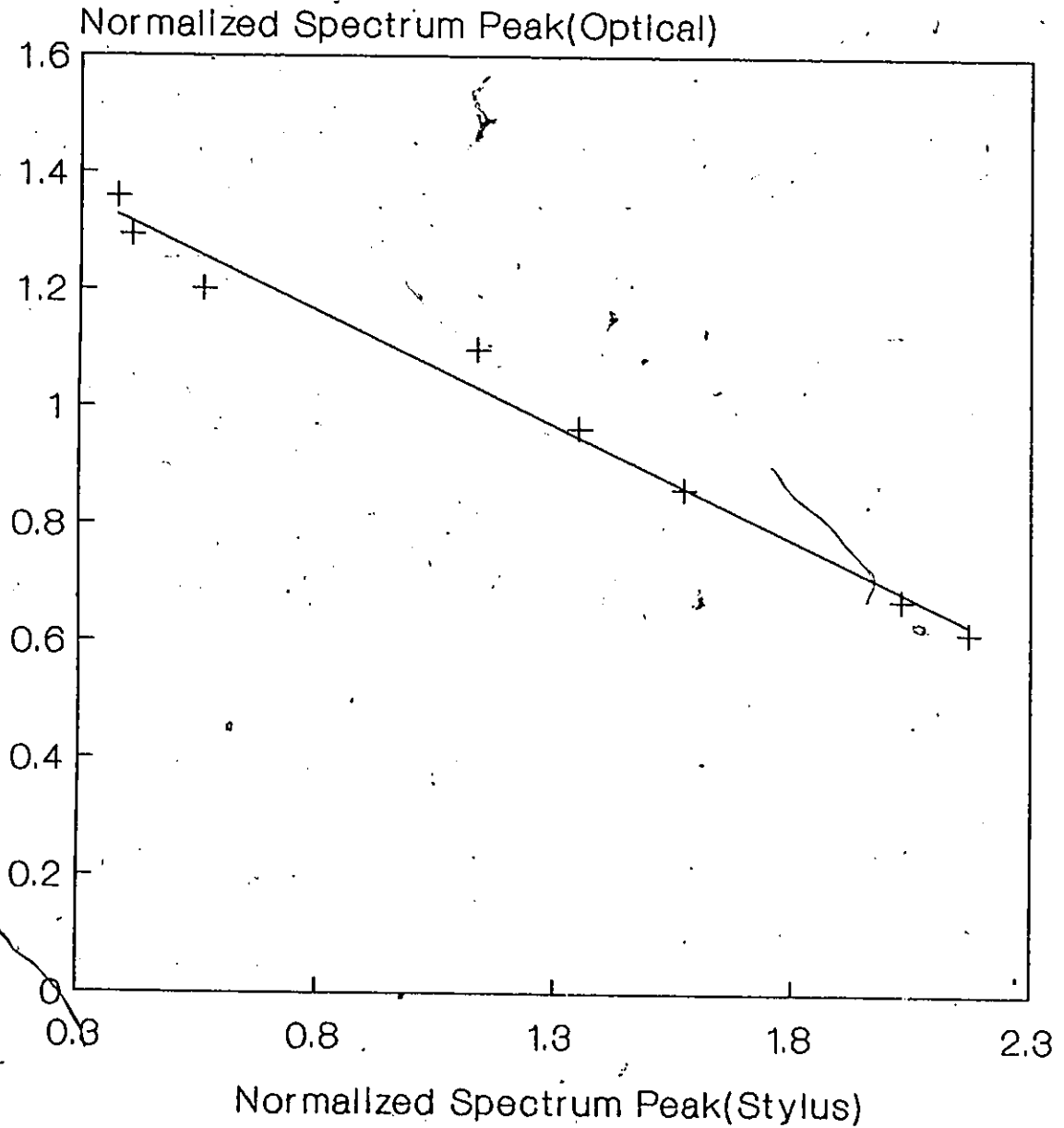
Spectrum RMS - Optical Vs Stylus



Fitted curve:
 $(RMS)_o = 1.433 - 0.433(RMS)_m$

Figure 4.8. Correlation between the normalized spectrum RMS(optical) and normalized spectrum RMS(stylus) for tool steel samples..

Spectrum peak - Optical Vs Stylus



Fitted curve:

$$(\text{Peak})_o = 1.475 - 0.390(\text{Peak})_m$$

Figure 4.9 Correlation between the normalized spectrum Peak(optical) and normalized spectrum Peak(stylus) for tool steel samples.

similar trend was found. Thus the optical RMS and peak values can be used as an alternative for characterization of surface texture.

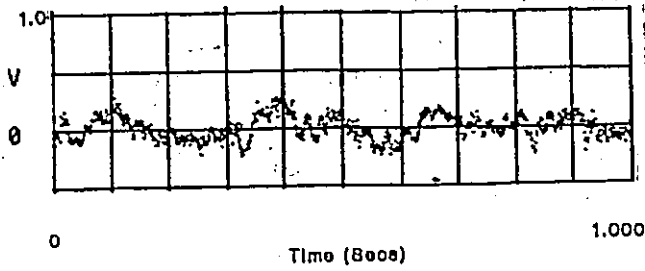
4.4 Fourier spectrum of surfaces obtained by different machining processes:

Samples from six different ~~machining~~ processes, namely, grinding, flat lapping, horizontal milling, vertical milling, reaming and turning were used in this work to examine the texture produced by these processes.

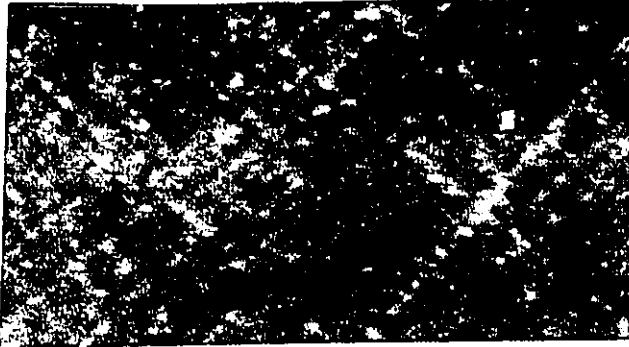
a) Description of surface texture from optical Fourier transform:

The characteristics of a typical flat lapping sample are shown in Figure 4.10. The machining marks extend in two directions perpendicular to each other as seen from Figure 4.10 (b). The illumination direction is parallel to one direction of the machining marks. The optical Fourier spectrum was obtained for both directions as shown in Figure 4.10 (e). The roughness in the two directions is close to a random surface even though there are some small discrete peaks in the spectrum.

The characteristics of a typical horizontal milled surface are shown in Figure 4.11. The surface profile is irregular and the feed marks are difficult to recognize as can be seen from Figure 4.11 (b). The feed



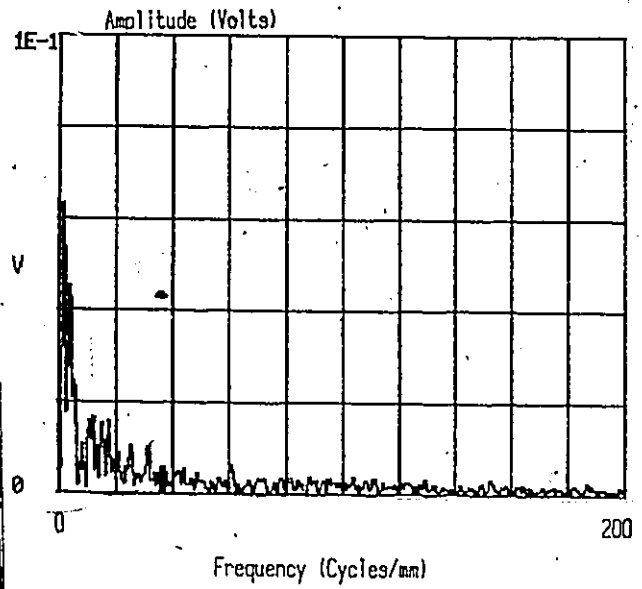
(a)



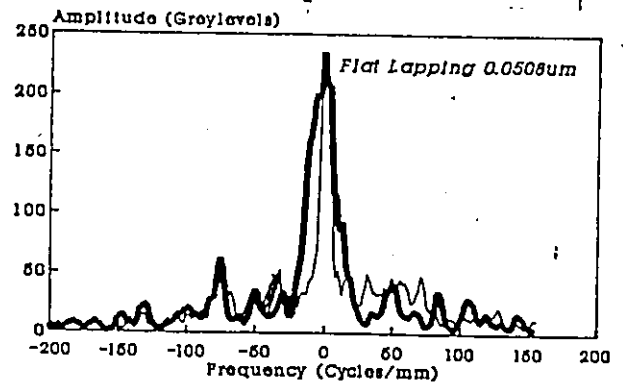
(b)



(c)

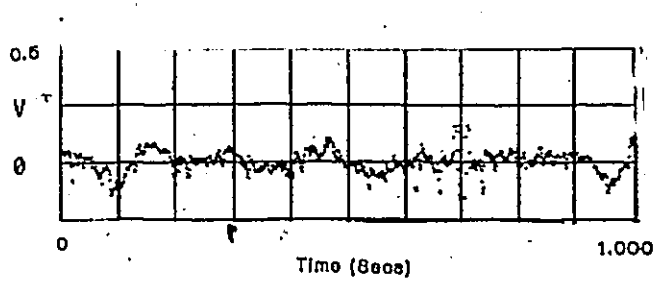


(d)

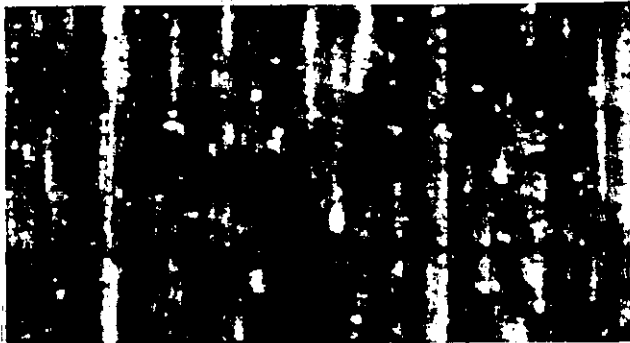


(e)

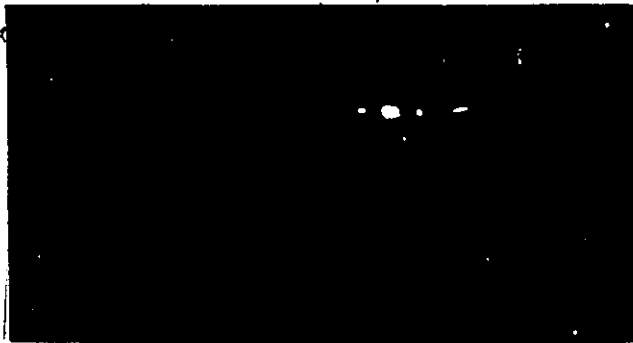
Figure 4.10 Typical characteristics of flat lapping sample ($R_a=0.05\mu\text{m}$)
 (a) Time domain signal
 (b) Photograph of the original surface
 (c) Photograph of the Fourier pattern
 (d) Frequency spectrum obtained from stylus
 (e) Frequency spectra obtained from the optical method in both directions of machining marks.



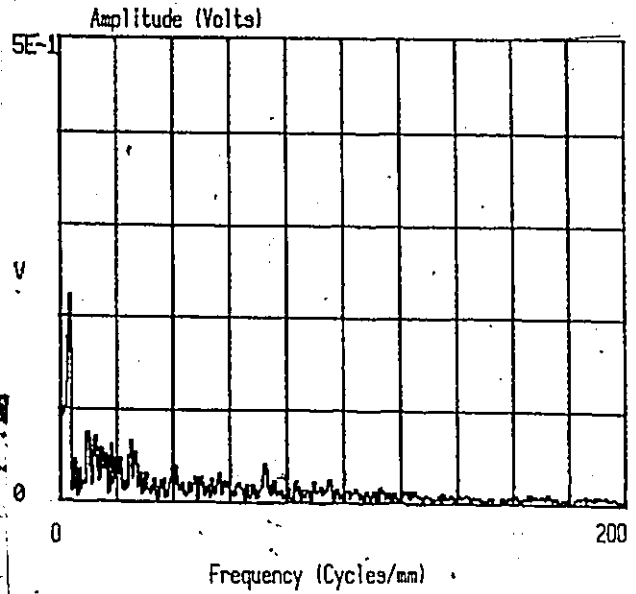
(a)



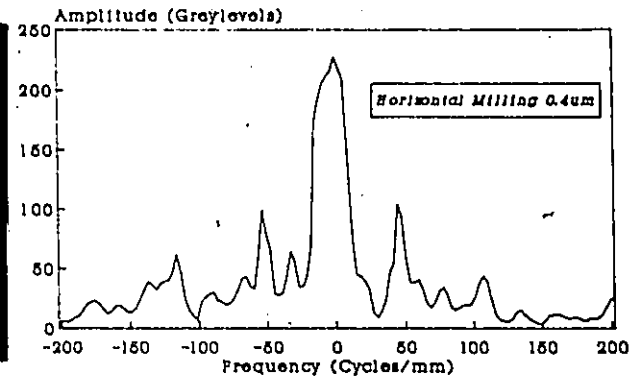
(b)



(c)



(d)



(e)

Figure 4.11 Typical characteristics of horizontal milling sample ($R_a=0.4\mu\text{m}$)

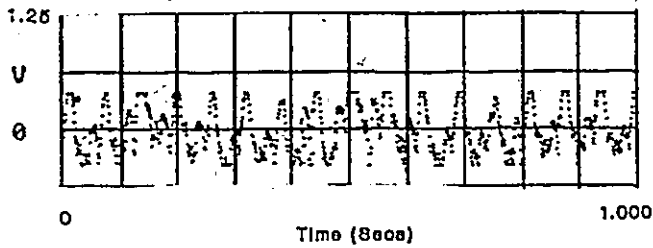
- (a) Time domain signal
- (b) Photograph of the original surface
- (c) Photograph of the Fourier pattern
- (d) Frequency spectrum obtained from stylus
- (e) Frequency spectrum obtained from the optical method

marks are clearly visible as discrete peaks in the frequency spectrum obtained by the two methods (Figures 4.11 (d) & (e)). The distribution of amplitudes are similar but the optical result has greater concentration near zero. This may produce greater RMS value and thus represents a lower roughness.

The characteristics of a vertical milling sample are shown in Figure 4.12. The spectrum consists of a typical pattern of discrete peaks of large amplitudes. This indicates that the surface is of periodic nature. It was also observed from the optical method that the first order feed component appears at a spatial frequency of 20 cycles/mm which compares favorably with that obtained by the mechanical method (18 cycles/mm). There is some spectrum distribution in the other direction (vertical) which shows some modulation in lay direction.

The characteristics of a typical reamed surface are shown in Figure 4.13. The periodicity of the surface can be seen from the photograph of the original surface and is verified by the frequency spectrum obtained by the two methods. The basic frequency of the sample obtained from the optical spectrum is approximately 20 cycles/mm and is within 1% of the result obtained by the stylus method.

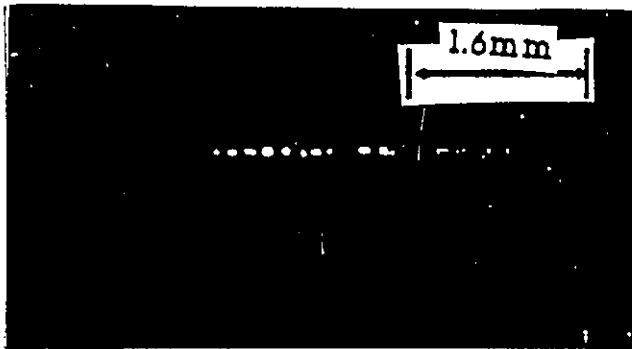
The characteristics of a typical turned surface are



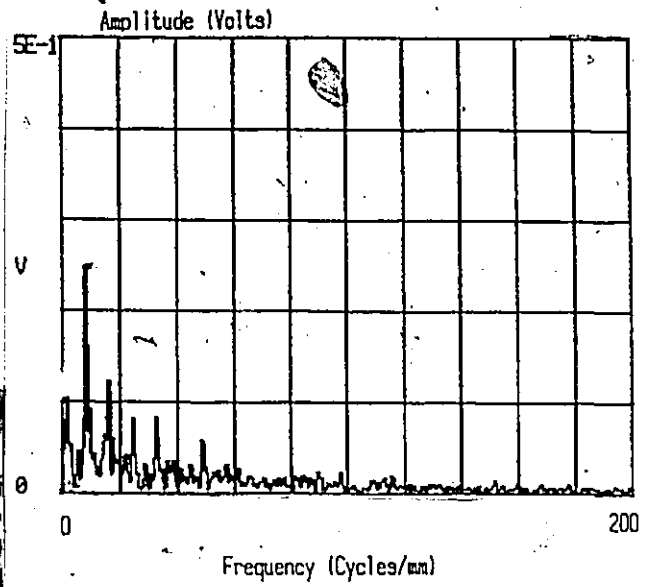
(a)



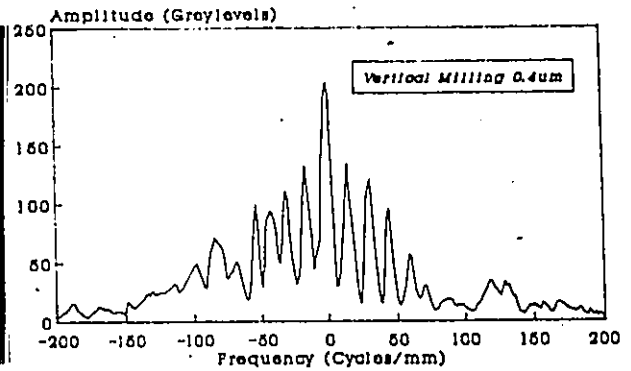
(b)



(c)



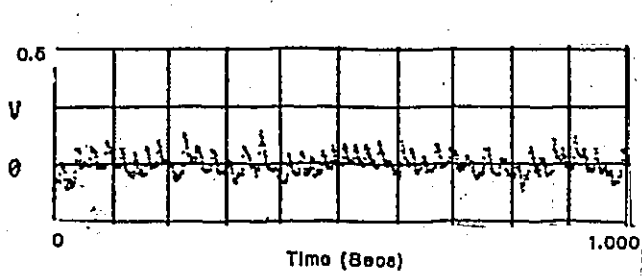
(d)



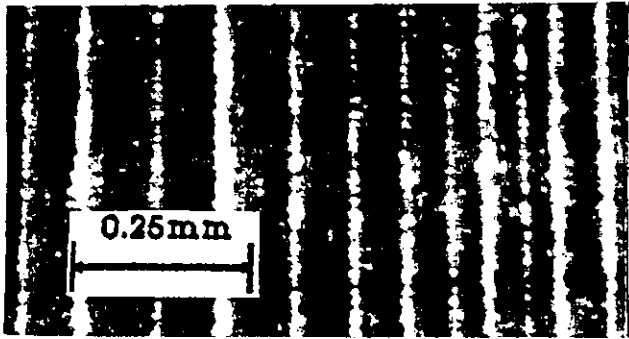
(e)

Figure 4.12 Typical characteristics of vertical milling sample ($R_a=0.4\mu\text{m}$)

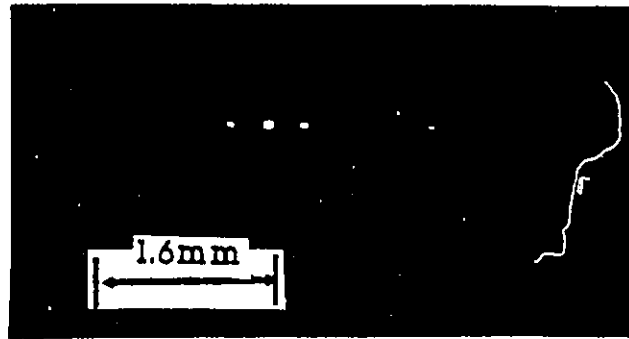
- (a) Time domain signal
- (b) Photograph of the original surface
- (c) Photograph of the Fourier pattern
- (d) Frequency spectrum obtained from stylus
- (e) Frequency spectrum obtained from the optical method



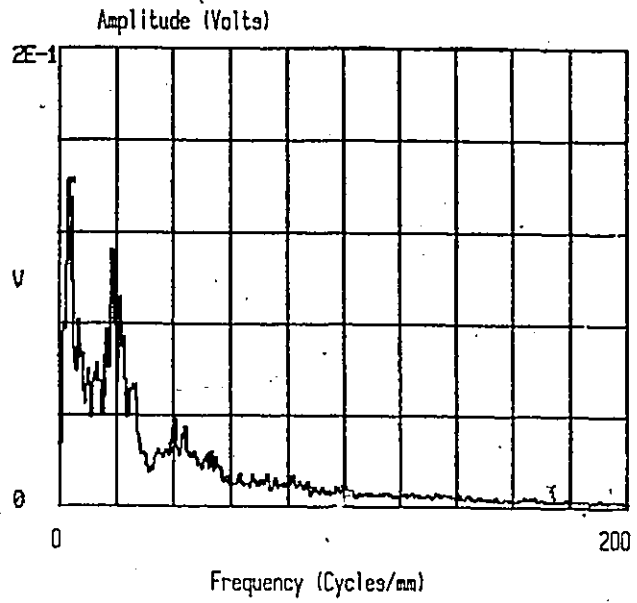
(a)



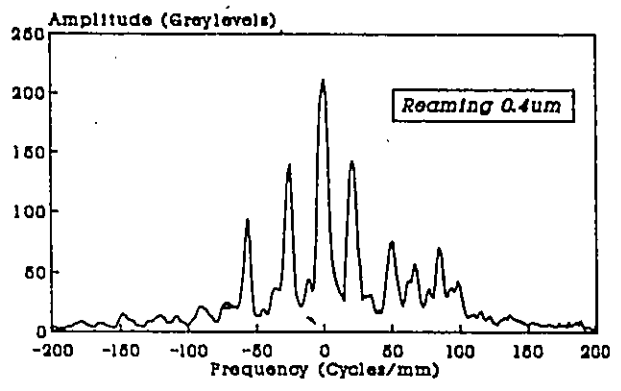
(b)



(c)

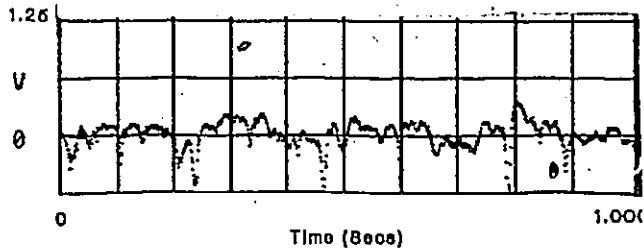


(d)

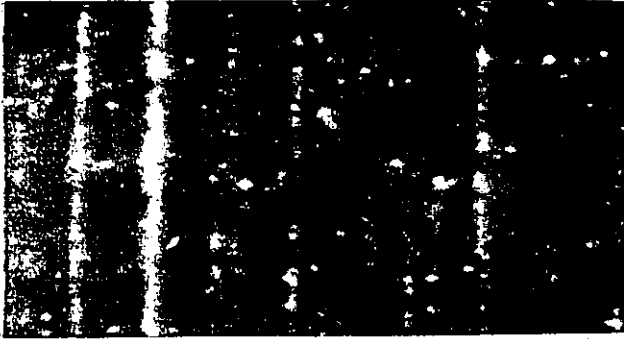


(e)

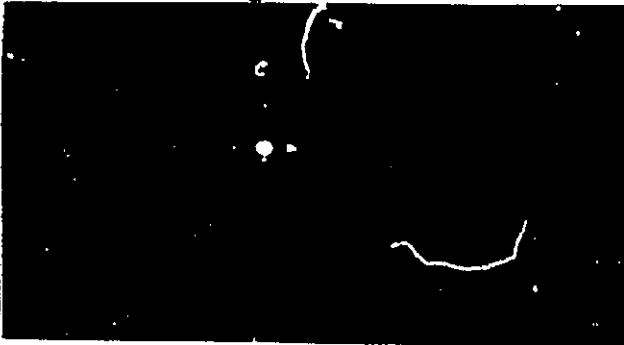
Figure 4.13 Typical characteristics of reaming sample ($R_a=0.4\mu m$)
 (a) Time domain signal
 (b) Photograph of the original surface
 (c) Photograph of the Fourier pattern
 (d) Frequency spectrum obtained from stylus
 (e) Frequency spectrum obtained from the optical method



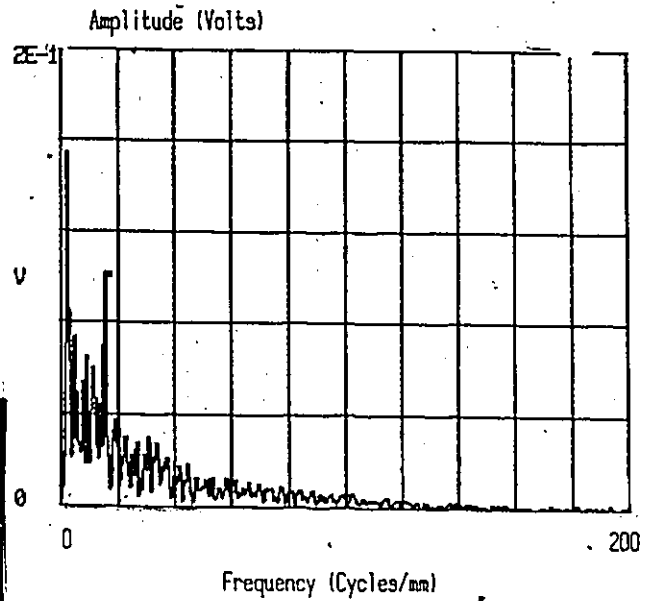
(a)



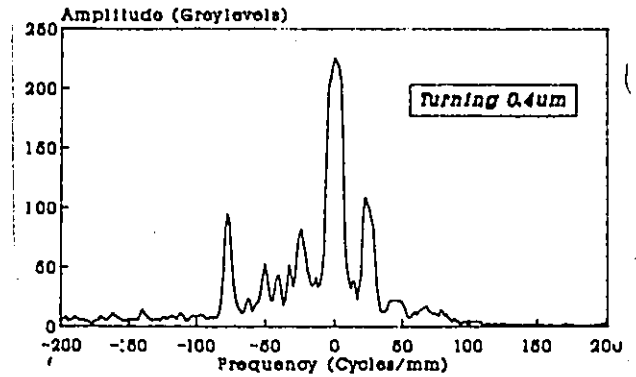
(b)



(c)



(d)



(e)

Figure 4.14 Typical characteristics of turning sample ($R_a=0.4\mu\text{m}$)

- (a) Time domain signal
- (b) Photograph of the original surface
- (c) Photograph of the Fourier pattern
- (d) Frequency spectrum obtained from stylus
- (e) Frequency spectrum obtained from the optical method

shown in Figure 4.14. The frequency spectrum obtained for the turned sample is similar, though not identical, to that obtained for the horizontal milling sample.

b) Correlation between optical Fourier transform and mechanical Fourier transform for different machining processes:

Table 4.3 shows the comparison of frequency spectra obtained by the optical and mechanical method for samples of different machining processes. The comparison was made by means of the coefficient of variation of frequency. It was observed that the deviation between the two frequency spectra was greater than 10% when surface roughness is greater than 0.4 μ m. Two typical samples from each category are used for illustration. More details about other samples can be found in Appendix D.

Figure 4.15 shows the correlation between the optical spectrum RMS and mechanical spectrum RMS for flat lapping samples. It can be seen, there is an inverse linear relationship between the two parameters similar to that obtained for the grinding samples(tool steel). Figure 4.16 shows a similar correlation between the normalized spectrum peak obtained by the optical and mechanical methods.

Table 4.3 Comparison of the frequency spectra obtained by the two methods for samples of different machining processes

Ra (μm)	Mechanical method		Optical method		Percent deviation %
	Mean (cycles/mm)	STD (cycles/mm)	Mean (cycles/mm)	STD (cycles/mm)	

Flat Lapping :

0.05	46.53	53.30	42.29	48.30	0.26
0.10	52.82	53.18	50.84	49.51	3.28

Grinding :

0.05	68.83	56.1	66.36	55.27	-2.08
0.20	66.82	50.98	68.67	51.29	2.28
0.812	62.49	53.40	89.50	59.90	21.66

Horizontal Milling :

0.40	53.53	52.6	54.27	54.93	-2.86
0.81	46.45	51.95	62.38	58.87	15.65

Reaming :

0.40	40.87	43.42	50.48	47.26	11.69
0.81	45.59	52.85	46.40	47.66	11.13

Turning :

0.40	35.80	38.05	42.3	47.94	-4.51
0.81	31.28	40.6	42.3	47.94	12.87

Vertical Milling :

0.40	53.22	50.93	58.20	50.22	9.9
------	-------	-------	-------	-------	-----

Spectrum RMS - Optical Vs Stylus

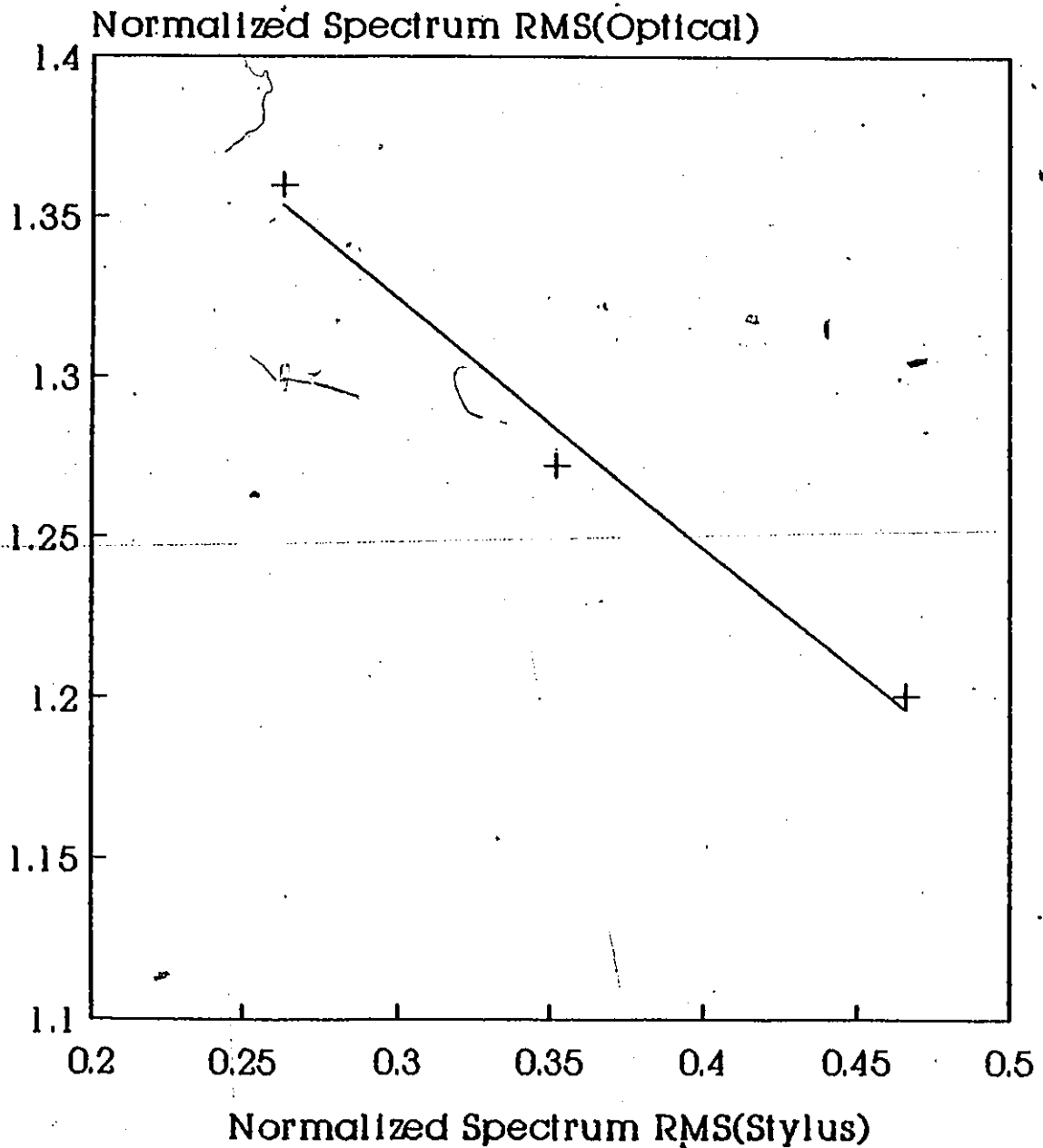


Figure 4.15 Correlation between the normalized spectrum RMS(optical) and normalized spectrum RMS(stylus) for flat lapping samples.

Spectrum Peak - Optical Vs Stylus

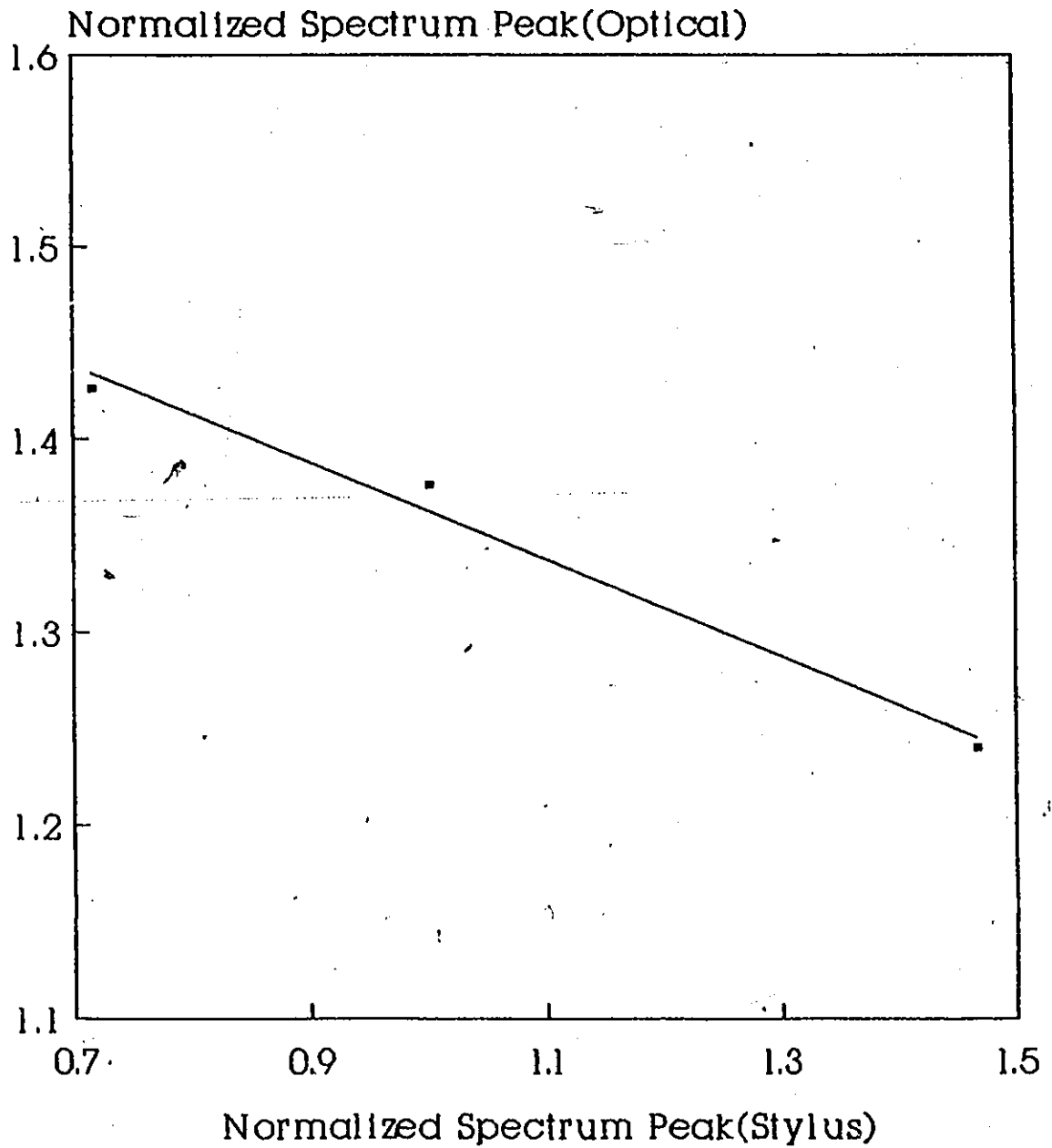


Figure 4.16 Correlation between the normalized spectrum Peak(optical) and normalized spectrum Peak(stylus) for flat lapping samples.

4.5 Characterization of surface roughness from the optical method:

Two parameters, normalized spectrum RMS and peak, were used for characterizing roughness from the optical method. These values were calculated in the bandwidth of 0 to 200 cycles/mm. Figure 4.17 shows the relationship between the surface roughness and the normalized spectrum RMS for tool steel samples. The abscissa in this graph represents the surface roughness R_a measured by the stylus profilometer, and the ordinate indicates the spectrum RMS values which were normalized using the standard calibrated sample with $R_a=0.5\mu\text{m}$. A similar plot for spectrum peak Vs R_a is shown in Figure 4.18.

A linear regression was employed for deriving the correlation equations for different materials. These equations and their correlation coefficients are listed in Table 4.4.

The following observations were also made from the results:

a) Materials

To test whether there is a general curve for optical RMS Vs R_a for all the materials in the grinding process, all the data points were plotted in Figure 4.19. There is a general trend for all the materials, i.e

Spectrum RMS(Optical) Vs Ra

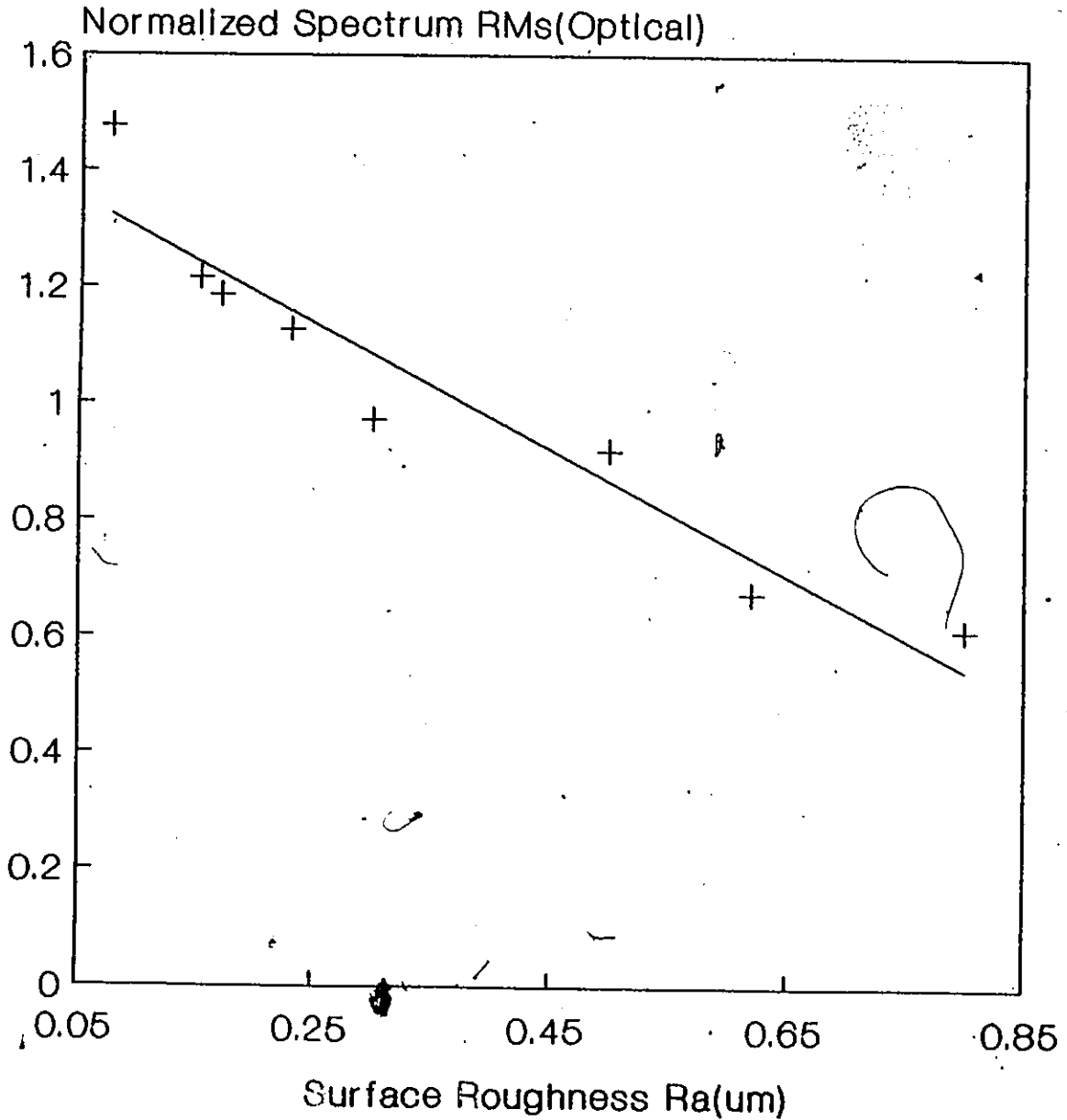


Figure 4.17 Correlation between the normalized spectrum RMS(optical) and surface roughness Ra for tool steel samples.

Spectrum Peak(Optical) Vs Ra

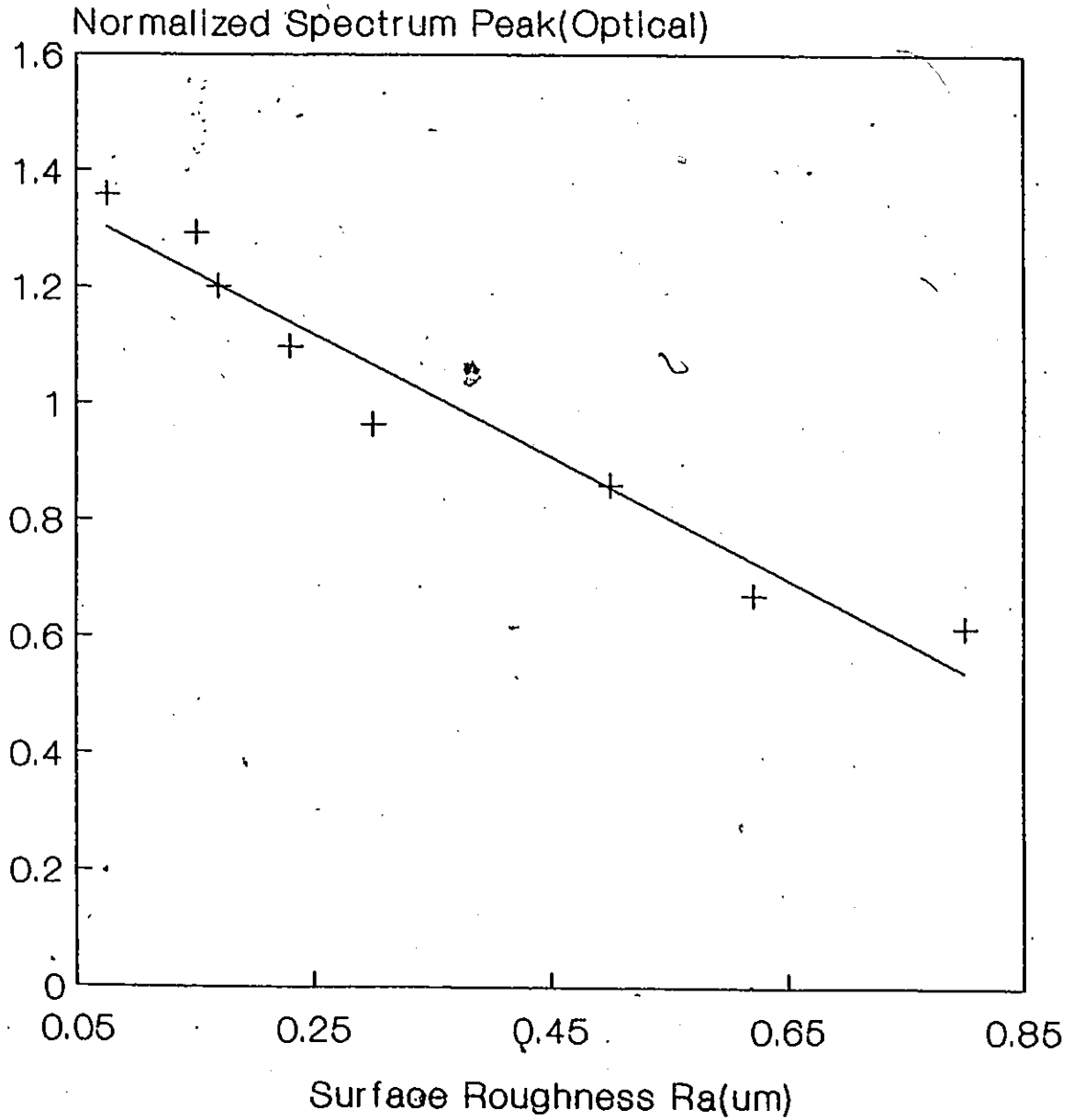


Figure 4.18 Correlation between the normalized spectrum Peak(optical) and surface roughness Ra for tool steel samples.

Table 4.4 Correlation equations for different materials

Material Type	Roughness Range	Correlation Equations	Correlation Coefficient
Aluminum	0.07 - 1.52 μ m	(RMS) _o = 1.38 - 0.9*Ra + 0.28*Ra ²	0.98
		(Peak) _o = 1.36 - 1.01*Ra + 0.36*Ra ²	0.992
Brass	0.07 - 1.3 μ m	(RMS) _o = 1.364 - 0.657*Ra	0.982
		(Peak) _o = 1.352 - 0.685*Ra	0.991
Copper	0.07 - 0.85 μ m	(RMS) _o = 1.516 - 0.354*Ra	0.977
		(Peak) _o = 1.453 - 1.175*Ra	0.985
Stainless Steel	0.05 - 0.82 μ m	(RMS) _o = 1.65 - 2.57*Ra + 1.72*Ra ²	0.994
		(Peak) _o = 1.39 - 1.92*Ra + 1.33*Ra ²	0.980
Tool Steel	0.075 - 0.8 μ m	(RMS) _o = 1.364 - 1.0*Ra	0.974
		(Peak) _o = 1.382 - 1.653*Ra	0.972

Correlation curve

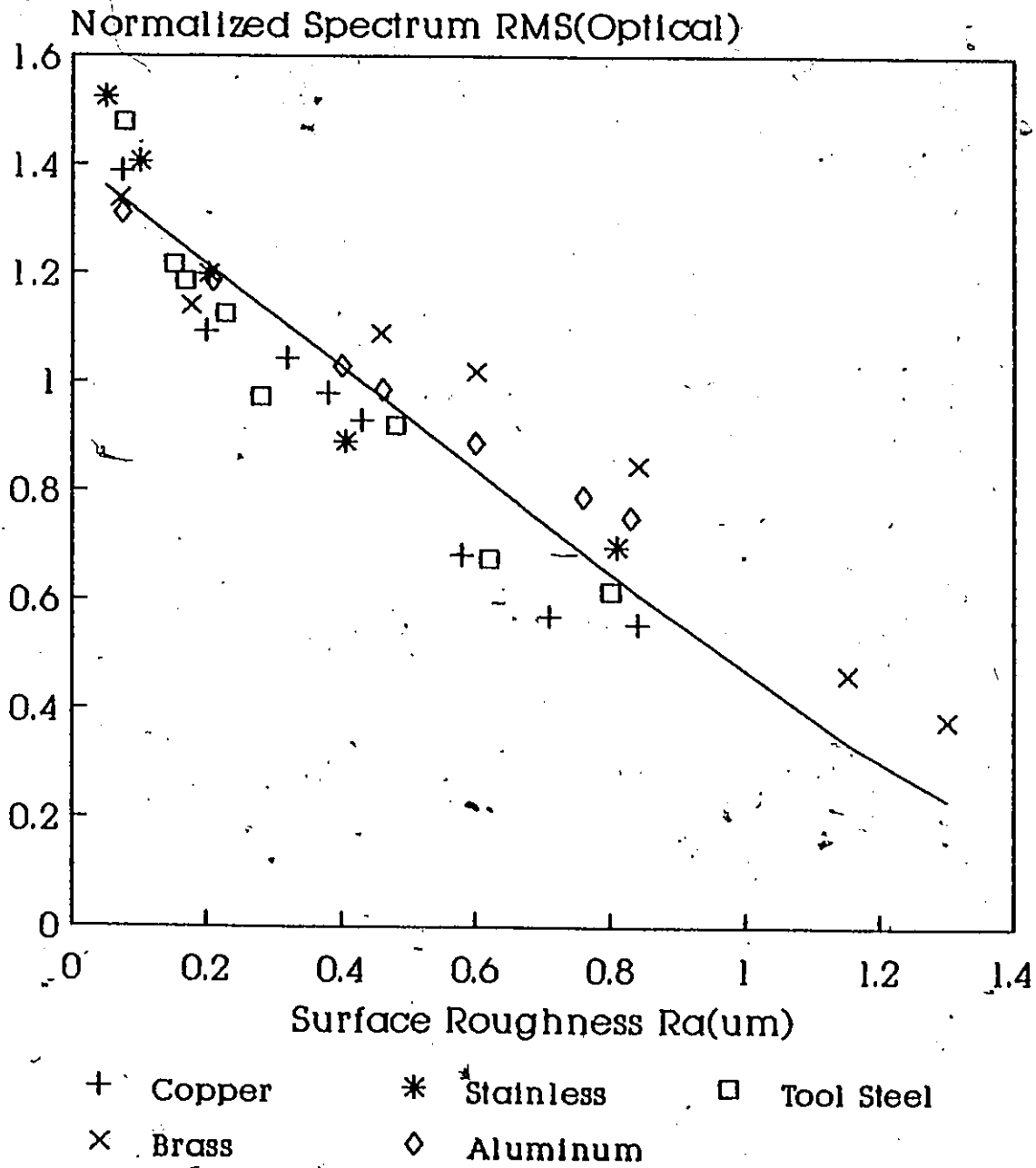


Figure 4.19 Correlation between spectrum RMS (optical) and surface roughness Ra for ground surfaces of five different materials

Correlation Curve

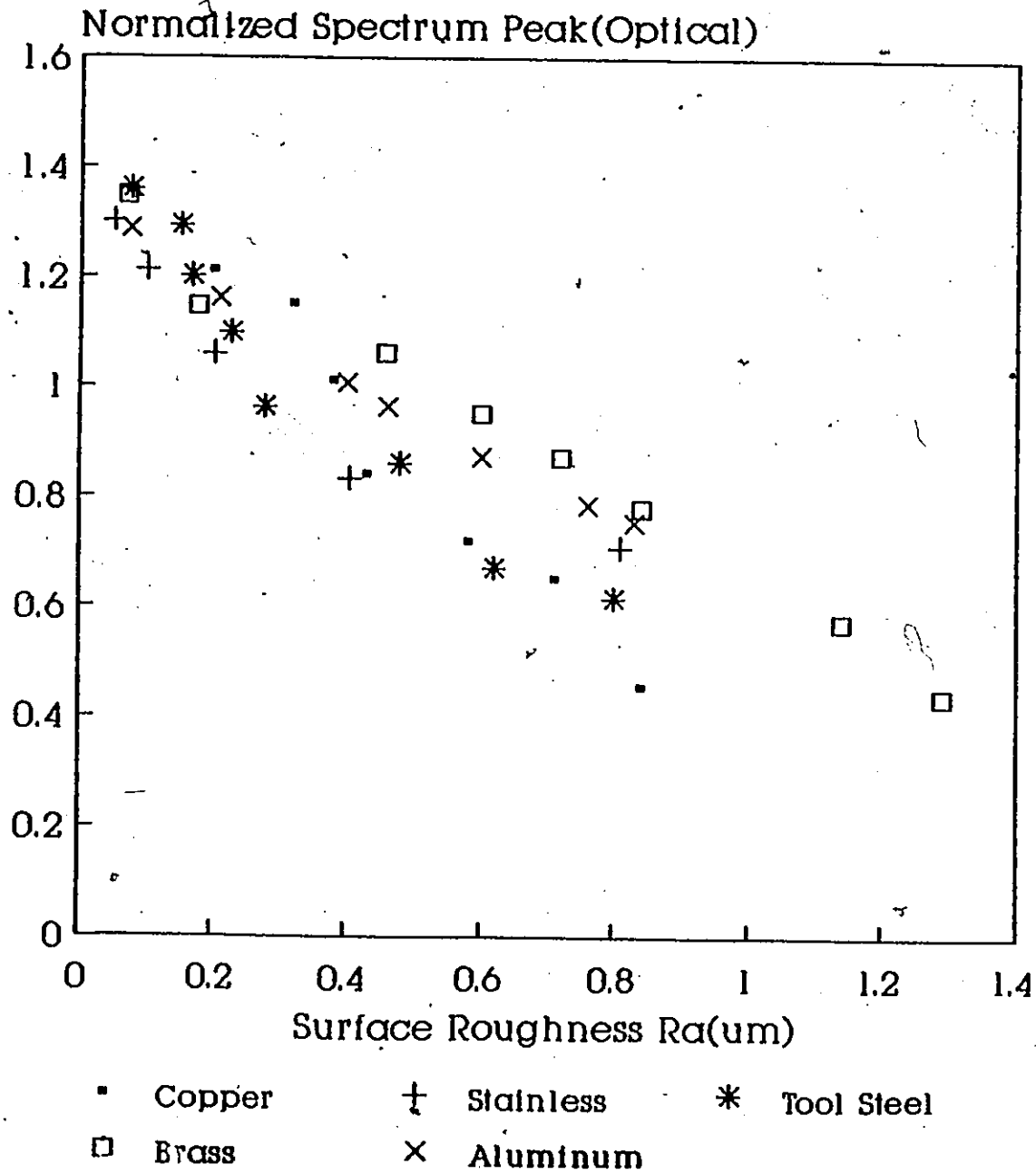


Figure 4.20 Correlation between the normalized spectrum Peak(optical) and surface roughness Ra for five different materials

optical spectrum RMS value decreases as the surface roughness Ra increases. However the scatter is large. A similar observation was made for optical peak Vs Ra plot (see Figure 4.20). Thus each material may have a unique calibration curve. These curves can be grouped into two types: Linear and quadratic.

i) The normalized spectrum RMS and peak were correlated to the average surface roughness for grinding samples of brass, copper and tool steel by a linear equation of the form :

$$R = c - m * Ra \quad \text{-----}(4.1)$$

where R is the spectrum RMS or Peak.

c, m are constants

and Ra is the surface roughness measured by the profilometer

ii) For aluminum and stainless steel the equation is given as

$$R = c - m * Ra + n * Ra^2 \quad \text{-----}(4.2)$$

where c, m, n are constants

Good correlation was obtained for all the materials as the correlation coefficient was greater than 0.97 (see Table 4.4)

b) Processes

A plot of optical RMS Vs Ra for different machining

Different Machining process

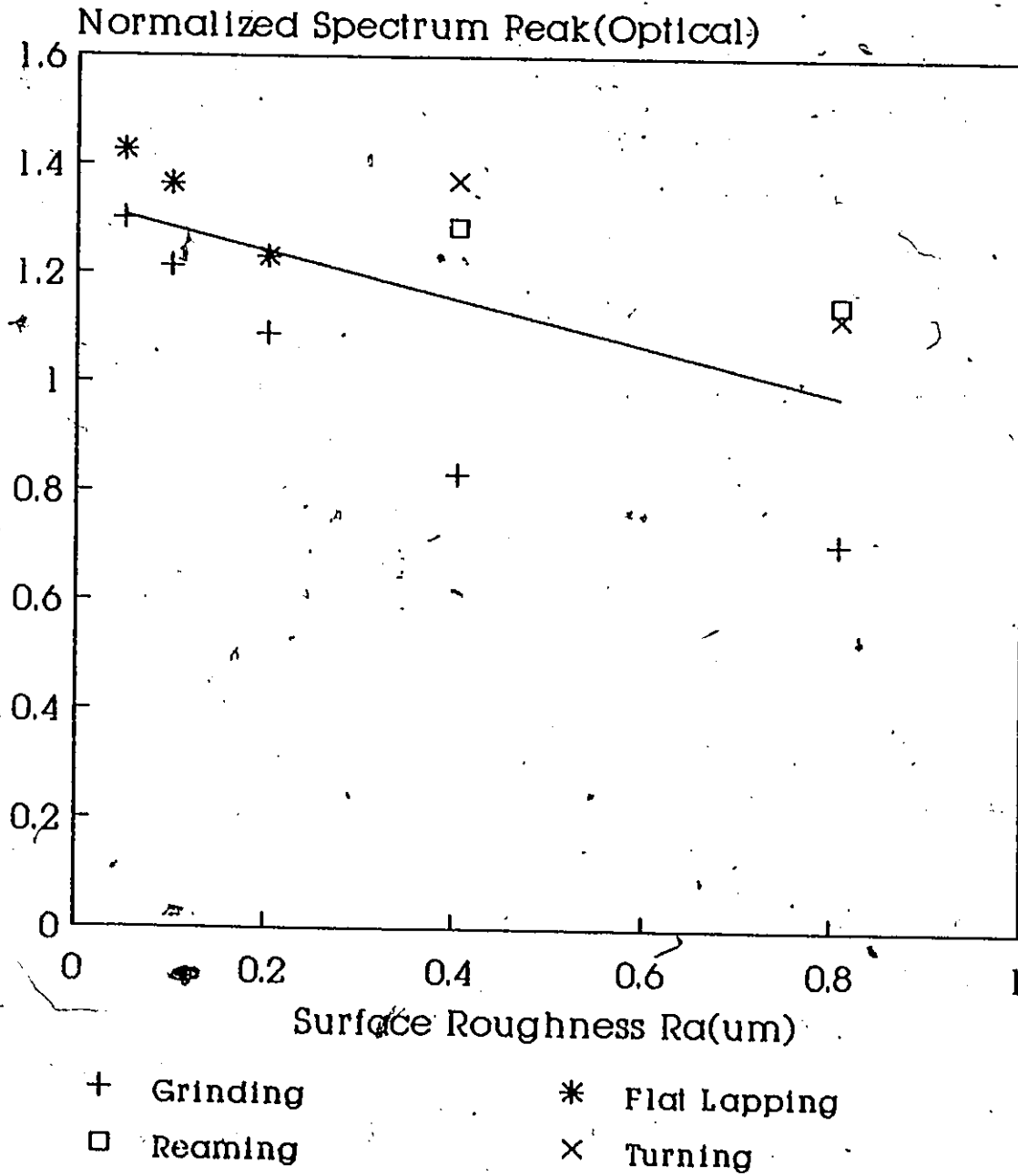


Figure 4.22 Correlation between spectrum peak (optical) and surface roughness Ra for four different machining processes

processes is shown in Figures 4.21. There is a general trend, however the scatter is very large, especially at lower Ra value. Thus there may not be a unique curve for all processes. Similar remarks can be made with peak Vs Ra, see Figure 4.22.

4.5.1 Experimental Uncertainty :

To estimate the uncertainty in the measurement, a technique proposed by Kline and McClintock was used. The measurement uncertainty was found to be $\pm 9.6\%$ of the full scale output of the frequency spectrum. For details of calculation, see Appendix F.

4.5.2 Measurement Precision:

The precision of the proposed optical method and the traditional stylus method was compared by taking nine readings on different locations of a surface ground Copper sample ($0.8\mu\text{m}$) and the results are shown in Tables 4.5 and 4.6. The results of mean frequency, normalized spectrum RMS and peak values which were used for comparing the frequency spectra obtained by the two methods are shown in tables. The comparatively smaller deviation from the mean values of all these parameters leads us to conclude the precision of optical method is superior to the stylus method. This could be attributed to the better averaging effect of the optical method,

Table 4.5 Measurement precision of stylus method for copper samples

Reading	Ra (μm)	Rms	Mean (Cycles/mm)	Peak
1	0.15	0.99	48.15	1.17
2	0.19	0.96	39.76	1.14
3	0.23	1.08	47.66	1.27
4	0.18	0.91	53.34	1.16
5	0.20	0.94	55.12	1.30
6	0.18	0.92	38.19	1.16
7	0.15	0.90	46.29	1.25
8	0.16	0.95	50.09	1.14
9	0.22	0.92	49.44	1.25
Mean	0.186	0.957	47.562	1.207
Standard Deviation	0.0271	0.0538	5.2831	0.0569
Std/Mean	14.59%	5.62%	11.11%	4.7%
Maximum Value	0.23	1.088	55.122	1.307
Minimum Value	0.15	0.902	38.192	1.143
Range	0.08	0.186	16.93	0.164
Percent variation from mean	+ 23.65 - 19.35	13.68 5.74	15.89 19.7	8.28 5.3

Table 4.6 Measurement precision of optical method for Copper samples

Reading	Rms	Mean (Cycles/mm)	Peak	Ra (μm) (from Rms)	Ra (μm) (from Peak)
1	1.16	49.67	1.24	0.21	0.18
2	1.17	47.65	1.25	0.20	0.17
3	1.16	42.21	1.20	0.24	0.20
4	1.19	50.39	1.23	0.18	0.18
5	1.18	45.66	1.19	0.19	0.21
6	1.18	40.09	1.24	0.18	0.17
7	1.19	46.68	1.21	0.17	0.2
8	1.17	48.02	1.25	0.19	0.17
9	1.18	49.98	1.22	0.18	0.19
Mean	1.176	46.7093	1.229	0.197	0.189
Standard Deviation	0.0191	3.3453	0.0194	0.0177	0.0165
Std/Mean	1.62%	7.162%	1.57%	8.90%	8.69%
Maximum Value	1.196	50.394	1.253	0.218	0.21
Minimum Value	1.130	40.0987	1.194	0.179	0.17
Range	0.066	9.407	0.059	0.061	0.05
Percent variation from mean	+ 1.7 - 3.9	7.88 14.15	1.9 2.8	10.65 9.1	11.11 10.05

which scans an area as compared to a stylus which traverses a line.

The optical roughness parameters can be transformed to the average roughness value R_a by using the calibration curves in Figures 4.19 and 4.20 and these are shown in Table 4.6. Thus for this copper sample,

the Stylus method gives

$$R_a = 0.186 \mu\text{m} \pm 0.027$$

and the Optical method gives

$$\text{from Peak : } R_a = 0.189 \mu\text{m} \pm 0.019$$

$$\text{from RMS : } R_a = 0.197 \mu\text{m} \pm 0.019$$

which shows a better precision for the optical method.

4.6 Measurement of Surface roughness along the direction of Lay:

The optical Fourier transform presents the surface roughness information in the two dimensional form. This property is used for quantifying roughness along the lay direction. Figures 4.23 and 4.24 show the plots for surface ground tool steel samples. The abscissa in these graphs represents the surface roughness measured perpendicular to the lay direction, and the ordinate indicates the normalized spectrum RMS and peak measured along the lay direction. It was observed that the

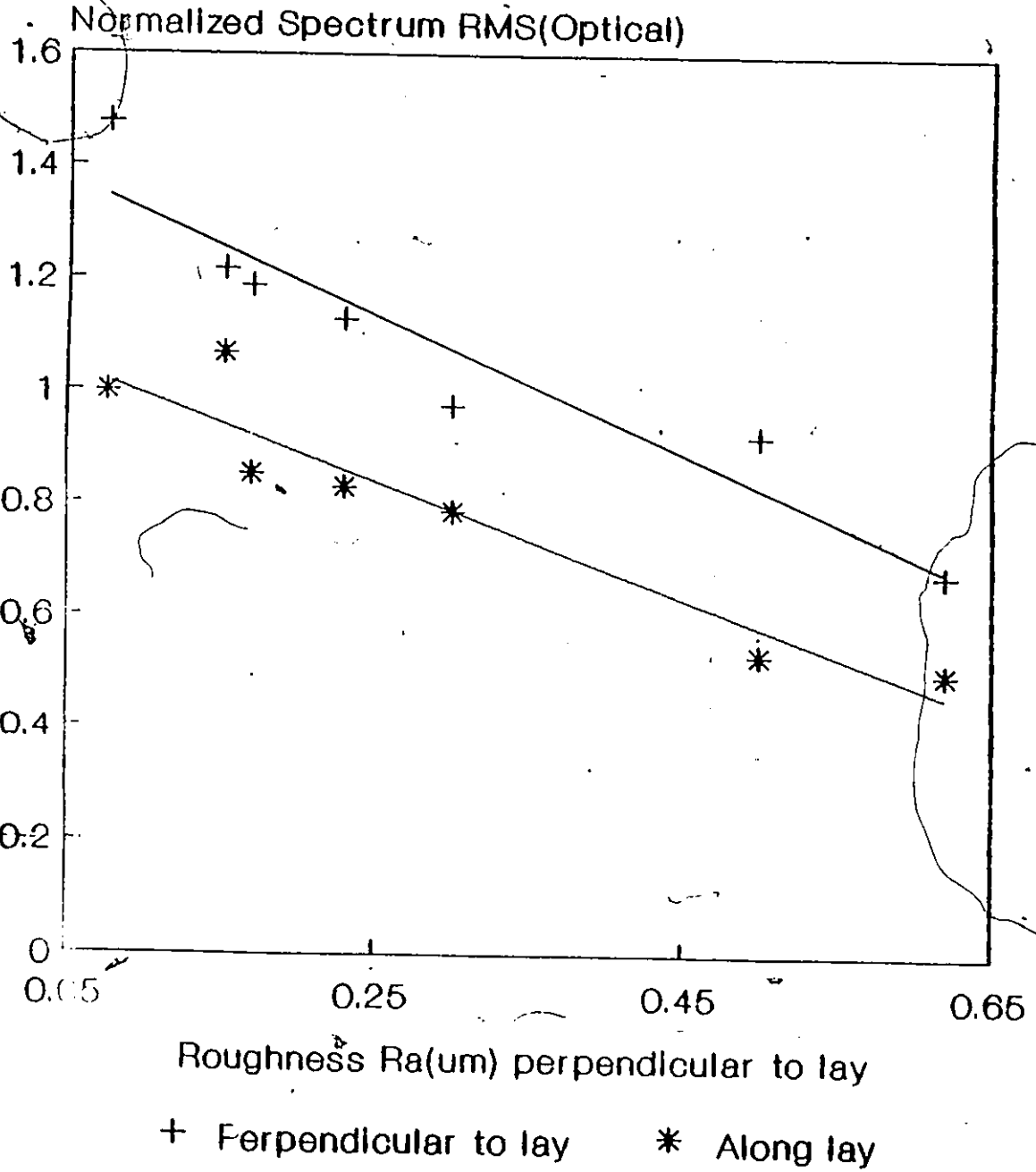


Figure 4.23 Correlation between the normalized spectrum RMS(optical) along lay and surface roughness Ra for tool steel samples.

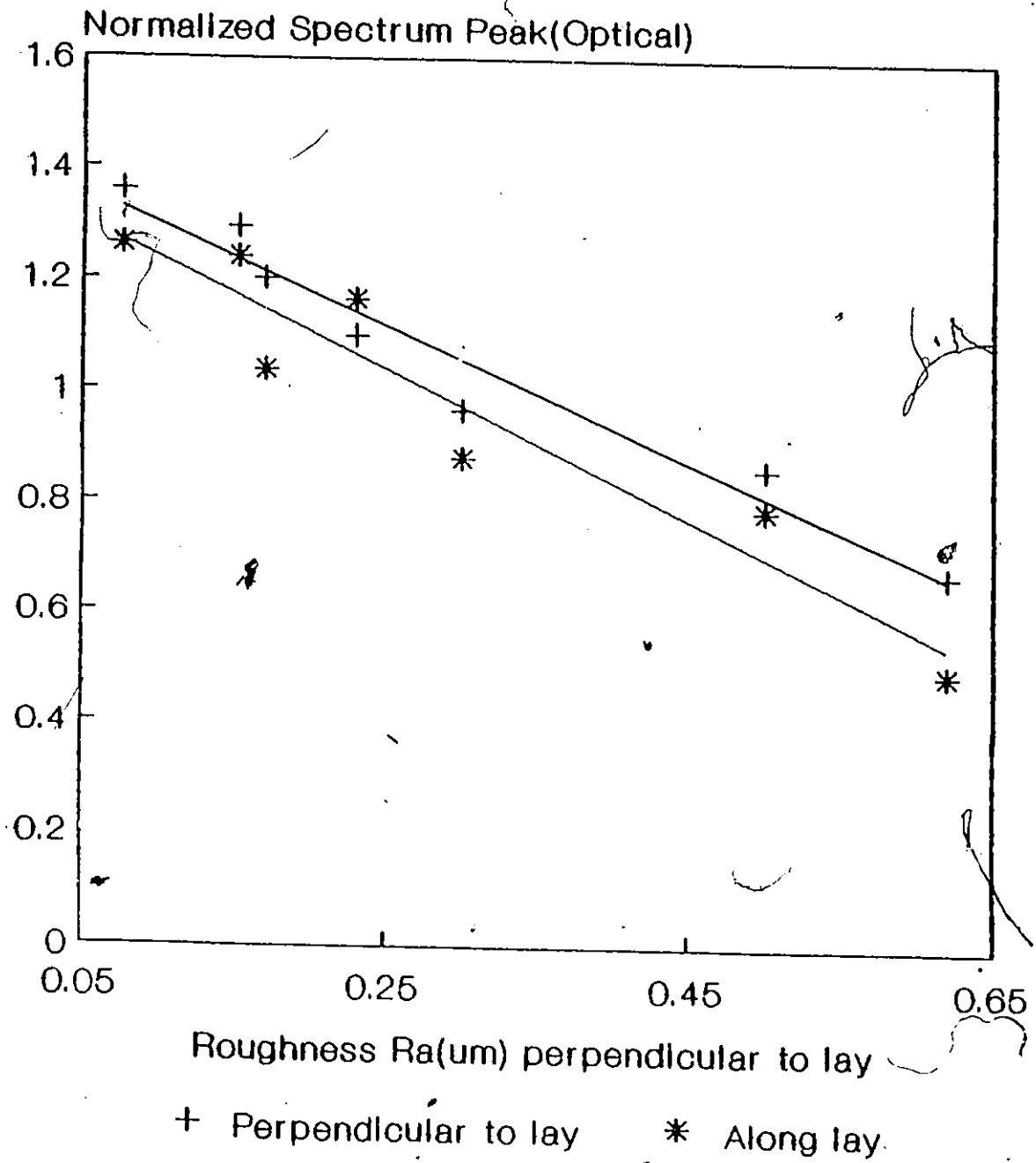


Figure 4.24 Correlation between the normalized spectrum Peak(optical) along lay and surface roughness Ra for tool steel samples.

spectrum RMS and Peak curves for perpendicular and parallel directions to lay, have a similar trend, they decrease as Ra increases. It was also observed that the spectrum RMS and peak values along the lay direction decrease in proportion to those values obtained in the perpendicular direction. The data were replotted in Figures 4.25 and 4.26 to show this trend. A linear equation can be fitted to the data as shown in Table 4.7.

4.7 Measurement in oil:

In production environment oil often exists on work surface, as a residue of cutting and other manufacturing processes. This serves either for corrosion resistance or for lubrication purposes. For roughness measurement, parts need to be cleaned (oil free) and after measurement re-oiled. To check whether the measurement method is applicable for specimens coated with oil, copper samples were coated with cutting oil (Cool Tool) and examined. The results of the analysis are presented in Figures 4.27 and 4.28. It can be observed that the values of spectrum RMS and peak decreased in comparison with those obtained for an oil free surface. This could be attributed to the fact that the oil coated on the surface reduces the amount of light scattered by filling up the machined grooves. The light coating of oil applied on the samples was retained in a surface with small grooves as compared

Optical method

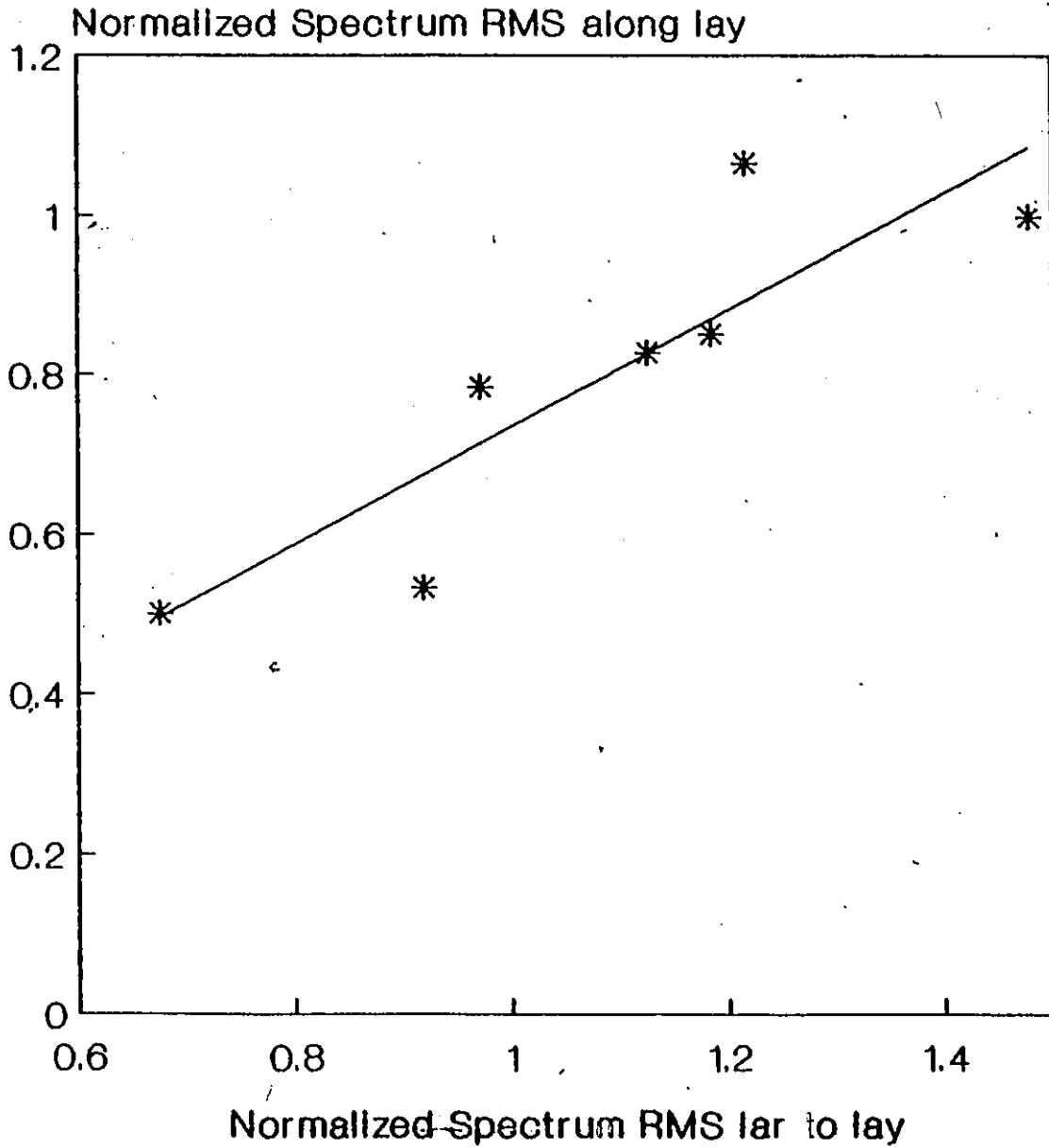


Figure 4.25 Correlation between the normalized spectrum RMS(optical) along lay and normalized spectrum RMS perpendicular for surface ground tool steel samples.

Optical method

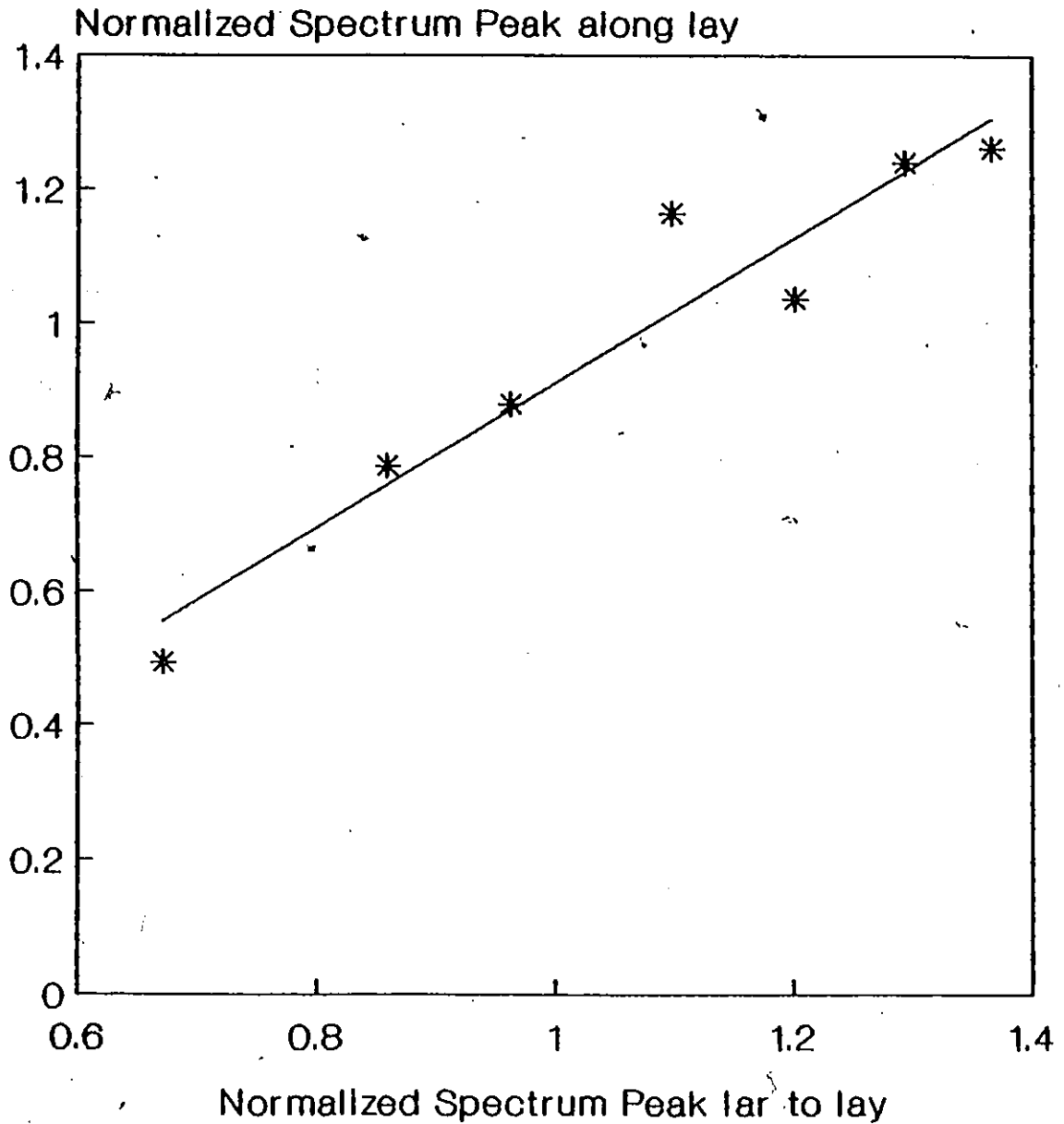


Figure 4.26 Correlation between the normalized spectrum Peak(optical) along lay and normalized spectrum Peak to lay perpendicular for surface ground tool steel samples.

Table 4.7 Correlation equations for tool steel samples relating roughness parameters in both the machining directions

	Roughness Range	Correlation Equation	Correlation Coefficient
Normalized Spectrum RMS:	0.07 - 0.65 μ m	$RMS_1 = 0.734 * RMS_2$	0.9432
Normalized Spectrum Peak:	0.07 - 0.65 μ m	$Peak_1 = 1.08 * Peak_2 + 0.17$	0.956

Subscript: (1): Along Lay
(2): Perpendicular to Lay

Oil Effect

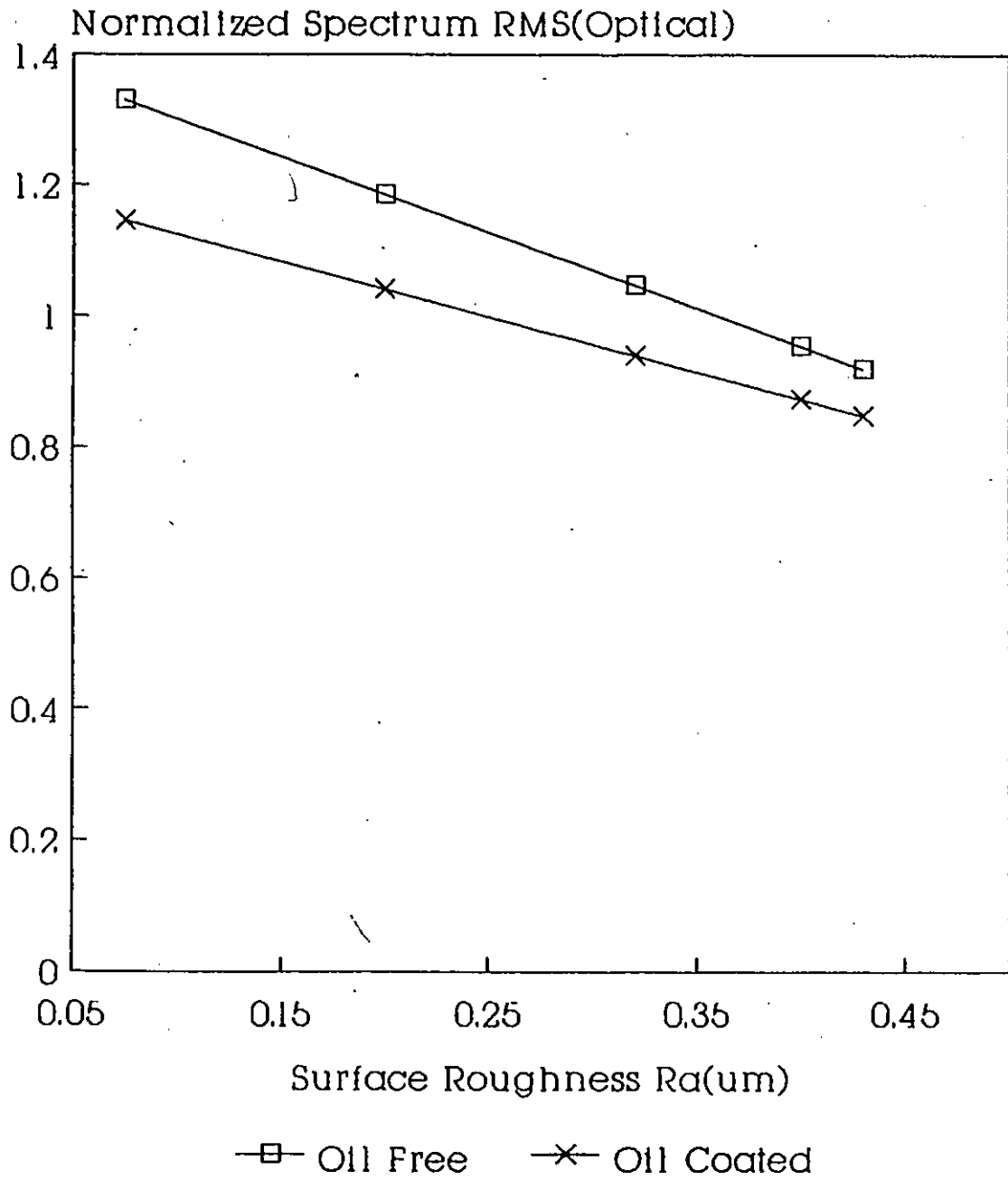


Figure 4.27 Correlation between the spectrum RMS(optical) and surface roughness Ra for oiled oil-free ground copper samples

Oil Effect

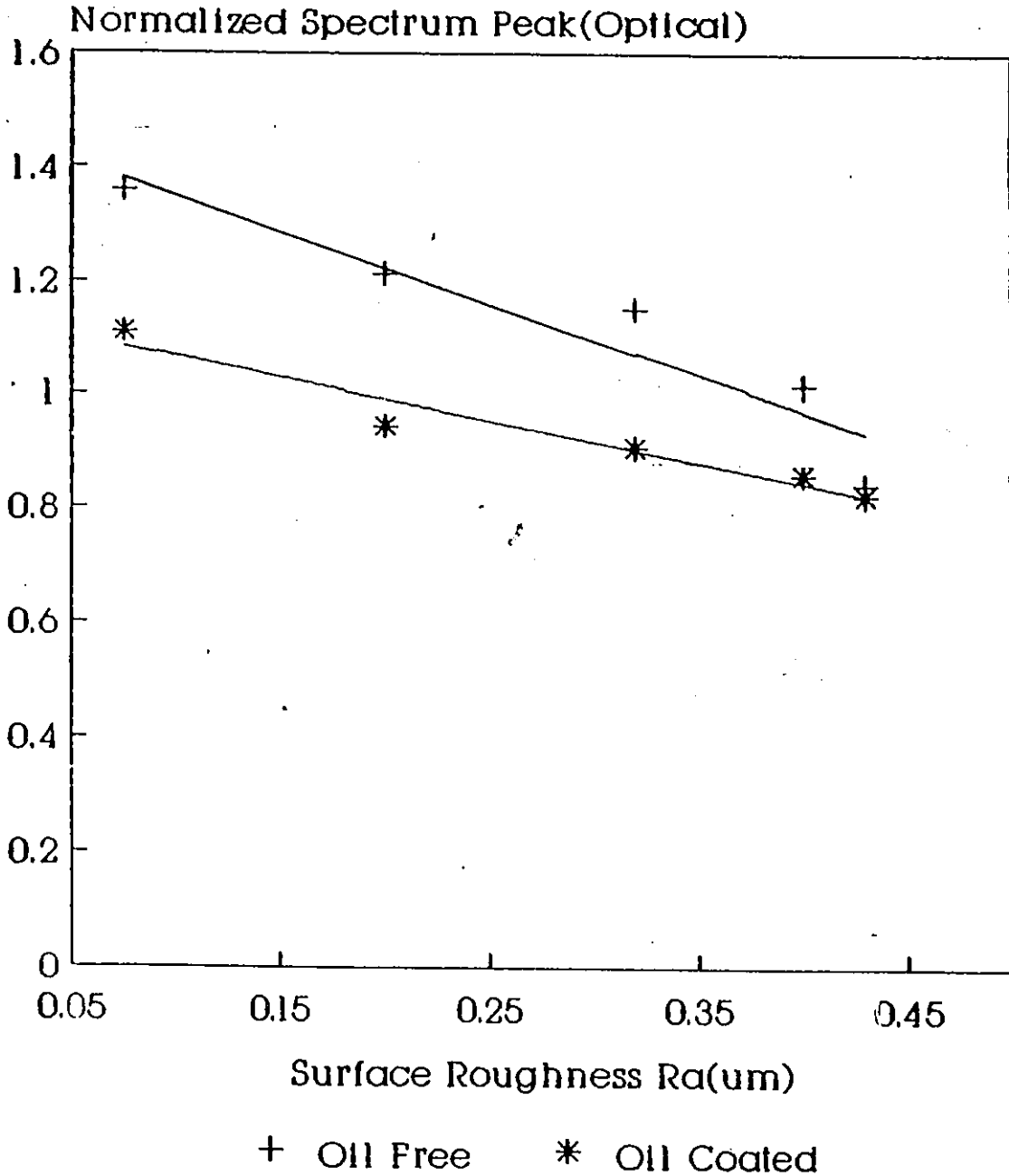
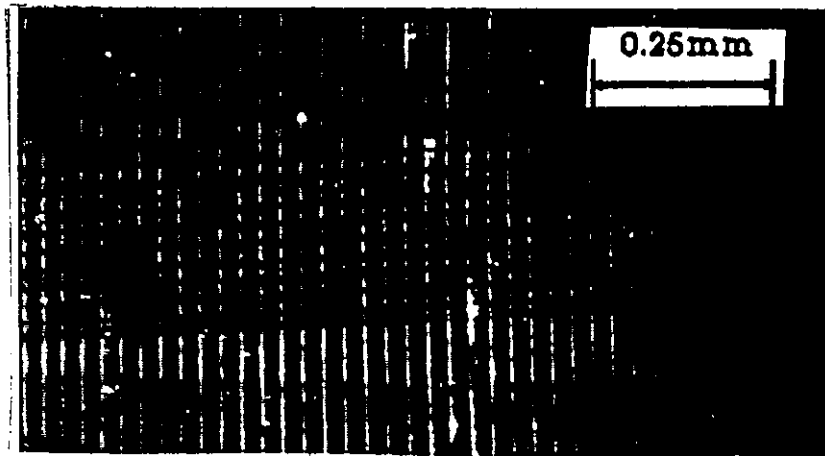


Figure 4.28 Correlation between the spectrum peak and roughness Ra for oiled & oil-free copper samples

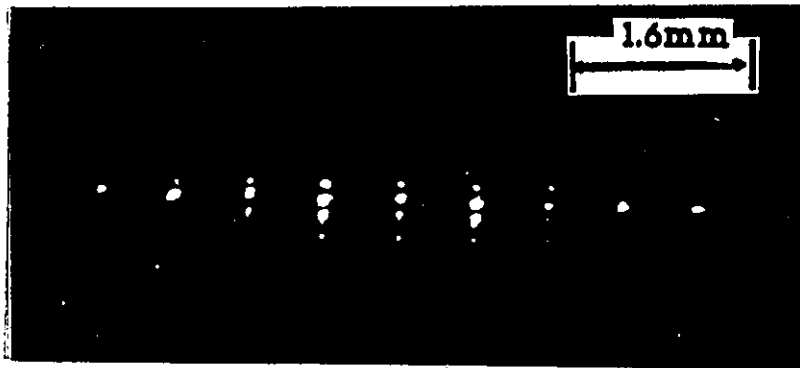
to a surface with large grooves. This would have contributed to the large reduction of RMS value, for example, at low Ra. It was also observed that the sensitivity of the measurement did not decrease appreciably in comparison with the oil free condition.

4.8 Identification of surface defects:

One of the major disadvantages of the stylus instrument is the inherent deformation or damage to the surface because of the excessive pressure from the tip of the stylus. This problem is apparent with hard materials and is worst with soft materials because the stylus pressure may approach 222 Kpa. To assess this problem a few samples with the scratches were considered. The optical Fourier method can be easily used to identify these scratches, which combined with the machining marks form a mesh. Figure 4.29 (a) and (b) show photographs of the original surface and its Fourier pattern. As can be seen from the Figure 4.29 (b), there is a significant difference in optical Fourier pattern in the lay direction when compared with the same surface without scratches (see Figure 4.2). The severity of scratches can be quantified by using the frequency spectrum (along lay) which is shown in Figure 4.30. In this Figure, the frequency spectrum of same direction but without scratch is also shown for comparison.

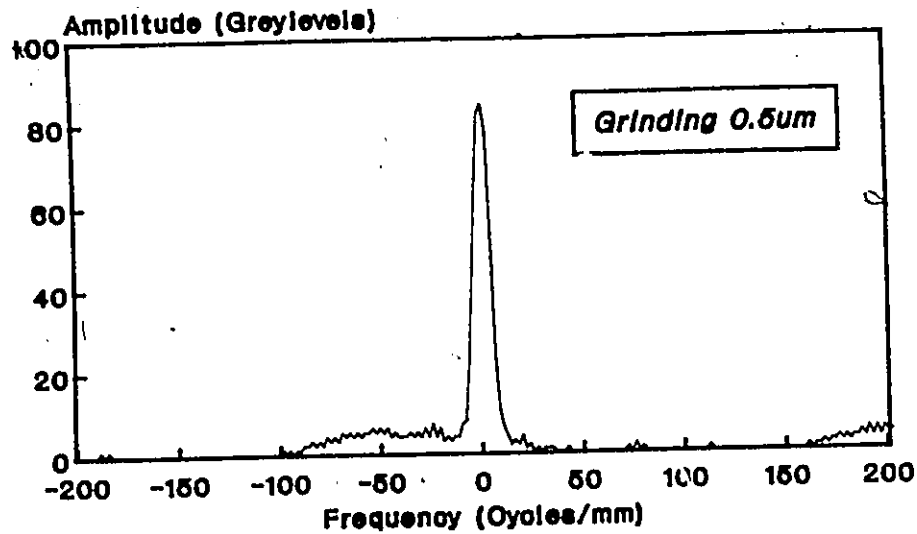


(a)

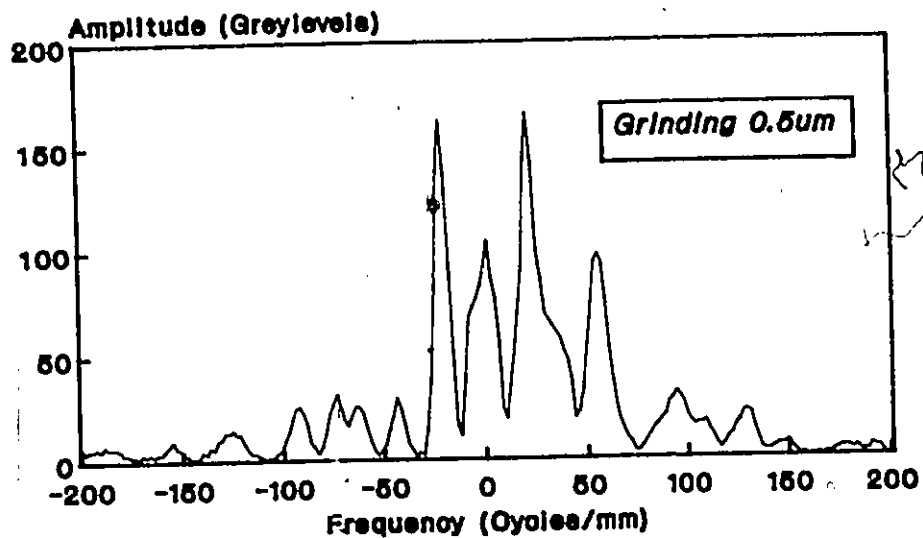


(b)

Figure 4.29 (a) The photograph of the standard calibrated sample ($R_a=0.5\mu\text{m}$) with scratches
(b) The Fourier pattern



(a)



(b)

Figure 4.30 (a) The frequency spectrum along lay for the standard calibrated sample ($R_a=0.5\mu\text{m}$) without scratches.
 (b) The frequency spectrum for the same surface without scratches.

CHAPTER V

CONCLUSIONS

A vision system based on the optical Fourier transform technique has been developed for analyzing surface texture of different types of machined surfaces. The measurement procedure utilizes the far field diffraction pattern (optical Fourier transform) formed at the image plane of the camera by a two lens system. The frequency spectra obtained from the optical method was then compared with that obtained from the stylus method. Five parameters derived from the frequency spectra were used in the study to facilitate the comparison. Samples of different machining processes were used, namely, Flat lapping, Grinding, Turning, Horizontal Milling, Vertical Milling and Reaming and different materials namely, Aluminum, Brass, Copper, Stainless steel and Tool steel.

Two important parameters derived from the optical Fourier spectrum were used to quantify the average roughness Ra. Good correlations were found for the two parameters. The precision of the optical method was found to be better than that obtained for the stylus method.

The two dimensional properties of the optical Fourier transform technique were found to be useful for

quantifying surface scratches produced by the stylus profilometer.

The study was also extended to a case where an oil film exists on the surfaces and reasonable correlation was found.

Based on the results of this work, the following conclusions are made :

1. The frequency spectra obtained by the optical method compares reasonably well with that obtained from the stylus method. The agreement between the two methods is within $\pm 10\%$ of each other for a roughness range of 0.05-0.5 μm . Beyond the roughness of 0.5 μm , there is increase in the difference which can be attributed to the drop in response of the stylus profilometer at frequencies above 70 cycles/mm.

2. Two parameters, normalized spectrum peak and RMS obtained from the optical Fourier spectrum, can be used to quantify surface roughness R_a .

a) The relationship between the spectrum RMS and the surface roughness can be expressed by an inverse linear function for the brass, copper and tool steel samples. The correlation equation is given by

$$R=c-m*R_a$$

where R is the normalized spectrum RMS

Ra is roughness value measured by the stylus profilometer

and c, m are constants

For aluminum and stainless steel the relationship is expressed by a second order polynomial. The equation is given by

$$R=c-m*Ra+n*Ra^2$$

where c, m, n are constants

b) A trend similar to spectrum RMS was observed for the spectrum Peak. The correlation equations for brass, copper and tool steel can be expressed in general form as

$$P=c-m*Ra$$

where P is normalized spectrum Peak

and Ra is roughness value measured by the stylus profilometer

c, m are constants

For aluminum and stainless steel the relationship is given by a quadratic relationship:

$$P=c-m*Ra-n*Ra^2$$

3. The precision of the optical system was found to be superior when compared to that of the stylus instrument. The precision of the optical system and the stylus instrument is given below:

Stylus instrument:

Precision : 15%

Optical method:

Spectrum Peak Precision: 8.7%

Spectrum RMS Precision: 8.9%

4. No universal calibration curve was found for different materials and different machining processes. Each calibration curve is unique.

5. The proposed method can be used in a situation where a thin film of oil exists on the surface of interest. Correlation was found in the roughness range of 0.07 to 0.45 μ m. The sensitivity of the optical method did not decrease appreciably.

6. The surface roughness parameters obtained for the lay direction can be correlated with that measured in the direction perpendicular to the lay. The trend was found to be similar for both directions.

7. The optical Fourier transform technique can be used to detect surface defects.

8. The biggest disadvantage with the proposed method is the low sensitivity.

CHAPTER VI

RECOMMENDATIONS

During the investigation there are some factors that we did not take into consideration. These factors may affect the obtained results. Thus further studies and in-depth investigation of these factors are needed.

1. A spatial filter (50 microns) was used in the study to eliminate the spatial noise. The effect of the filter aperture size on the optical parameters should be studied.

2. A He-Ne laser of wavelength $0.632\mu\text{m}$ was used in this study as a light source. The effect of the wavelength on the correlation curves and the roughness range should also be investigated.

3. The stylus profilometer was used as a standard for checking the frequency spectra obtained by the optical method. The stylus profilometer, however cannot measure high frequency components accurately because of the size of the stylus tip and the velocity of traverse. So a better method has to be found for measuring the surface profile.

Further investigation should be undertaken to extend the optical Fourier transform method for the

following applications.

1. Further measurements must be made with the optical Fourier transform method to obtain correlation curves for machining processes such as horizontal milling, vertical milling, reaming; as the number of samples used were not sufficient to draw any conclusion.

2. The present study could also be extended to non-metallic surfaces such as plastic, paper, wood finishes and other surfaces which cannot be contacted using a stylus instrument.

3. Studies should be conducted to establish a universal relationship between surface roughness measured in the direction perpendicular and parallel to the lay.

4. The two dimensional information provided by the optical Fourier transform should be used to derive a two dimensional Fourier spectrum. A parameter which describes the overall roughness of the surface can then be obtained from the spectrum.

REFERENCES

1. Michael Brock, "Fourier Analysis of Surface Roughness", Bruel & Kjaer Tech. Rev., n3, 1983, pp. 3-45.
2. "Surface Texture", American National Standards Institution, ANSI B46.1-1978, New York, 1978.
3. George H. Schaffer, "The many faces of surface texture", American Machinist & Automated Manufacturing, pp.61, June 1986.
4. Mitutoyo SurfTest III profilometer user's manual.
5. T.Asakura, "Speckle Metrology", ed.R.K.Erf (Academic Press, New York, 1978) Chapter 3.
6. H.Fujii, T.Asakura and Y.Shindo, "Measurement of surface roughness properties by using image speckle contrast", J. Opt. Soc. Amer. 66, pp. 1217 (1976).
7. H.Fujii and T.Asakura, "Development of laser speckle and its application to surface inspections", Appl. Opt. 16, pp.180 (1977).
8. R.F. Reason, "Modern Workshop Technology", (1976).
9. H. Sata, "Surface roughness measurement by Scanning Electron Microscope", Annals of CIRP. 30, 1982.
10. Russel D. Young, Theodore V Vorburger and E. Clayton Teague, "In-process and on-line measurement of surface finish", Annals of CIRP. 29, pp. 435 (1980).
11. "The fundamentals of signal analysis" < Application notes 243, Hewlett-Packard.
12. Eugene Hecht and Alfred Zajac, "Optics", Addison-Wesley Publishing Company, 1979
13. Allen Nussbaum and Richard A. Phillips, "Contemporary optics for scientists and engineers", Prentice-Hall, New Jersey, 1976, pp 214-302

14. B.J. Pernick, "Surface roughness measurements with an optical Fourier spectrum analyzer", Appl. Opt. 18, pp. 796 (1979).
15. E.G. Thwaite, "The direct measurement of the power spectrum of rough surfaces by optical Fourier transformation", Wear. 57, pp. 70-80 (1979).
16. E.G. Thwaite, "Power spectra of rough surfaces obtained by optical Fourier transformation", Annals of CIRP. 29, pp. 419-422 (1980).
17. E.G. Thwaite, "A quantitative comparison of the wavelength spectrum of a surface obtained by optical Fourier transformation with calculations from profile measurements", Wear. 83, pp. 181-187 (1982).
18. E.G. Thwaite, "The extension of optical angular scattering techniques to the measurement of intermediate scale roughness", Annals of CIRP. 31, pp. 463-465 (1982).
19. T. Sata, "Analysis of surface roughness generation in turning operation and its applications", Annals of CIRP. 34, pp. 473 (1985).
20. D. Shetty and C. Imbert, "Evaluation of engineering surfaces by diffraction pattern analysis", Jou. of Engg. Mat and Tech. 106, pp. 216-218 (1984).
21. R. Brodmann, "Roughness measurement of ground, turned and shot-peened surfaces by the light scattering method", Wear. 109, pp. 1-13 (1986).
22. J.W. Goodman, "Introduction to Fourier optics", McGraw-Hill, Inc., 1968.
23. J.C. Stover, "Roughness characterization of smooth machined surfaces by light scattering", Appl. Opt. 14, pp. 17961 (1975).
24. H.S. Corey, "Surface finish from reflected laser light", SPIE. 153, Advances in optical metrology, pp. 27 (1978).
25. F.Luk, Master's Thesis, University of Windsor, Windsor, Canada, 1987.

APPENDIX A.

Equipment Specifications

Table A.1 Specifications of He-Ne laser

Wavelength	:	0.6328 μ m
Output power	:	2mW
Operating temp	:	-20 to 50 $^{\circ}$ c
Power drift over 8 hr period	:	\leq + or - 5
Beam diameter	:	0.75mm @ $1/e^2$
Beam divergence	:	\leq 1.2 mrad
Beam amplitude noise	:	1% (30Hz to 1MHz)

Table A.2 Specifications of RCA CCD camera

CCD Imager	:	Model SID 504
Image cell size	:	16 μ m X 20 μ m
Picture elements	:	512 X 403
Image size	:	4.84mm X 6.45mm
Horizontal limiting resolution	:	302 TVL/PH
Vertical limiting resolution	:	480 TVL/PH
Signal system	:	EIA standards Rs-170
Signal to noise ratio	:	60dB
Shock resistance	:	50G
Vibration resistance	:	3g swept sine wave, 15Hz to 2000Hz
Size (H/W/L)	:	75 X 114 X 235mm
Weight	:	1.5Kg

Table A.3 Specifications of the PIP-1024 digitizer board (Matrox Corp.)

Frame grabber :

Resolution : 512 X 512
Bits/pixel : 8
Input Lookup table : 8 bits in / 8 bits out
8 software selectable maps
Video : Supports Rs-170 & Rs-330

Frame buffer :

Image store : One 1024 X 1024 buffer
or four 512 X 512 buffers

Display unit :

D/A converters : Three 8 bit D/A converters for RGB input
Output : 8 bits in / 24 bits out
Colour lookup table : 256 colours or intensities from a palette of 16.7 million colours

Dimensions :

Length : 335.3mm
Width : 106.77mm
Height : 32.7mm

Table A.4 Specifications of FFT analyzer

Inputs :

Impedance : 100k
A/D converter : 12 bits
Sampling rate : 2.56 X full scale
frequency scale
selected on internal
sampling control

Analysis :

Resolution : Time domain - 1024 pts
frequency domain -
400 lines
frequency accuracy: + or - 0.0025% of full
scale
Weighting : Hanning, Kaiser-Bessel,
Spel or rectangular

Display :

Type : Built in TV raster
scan display
Format : Single or dual channel

APRENDIX B.

Computer program listing

```

$INCLUDE: 'FORINTF.H'
C *****
C          DECLARATION STATEMENTS
C *****
IMPLICIT INTEGER*2(X,Y)
INTEGER*2 STATE,CHANNO,STABLE,UTABLE
INTEGER*2 QUAD,MODE,RETV,INDEX,VAL
INTEGER*2 BSIZE
INTEGER*2 VTYPE,RET
INTEGER*2 LEFT,RIGHT,UPPER,LOWER
INTEGER*2 QUAD1,QUAD2,QUAD3,AVG(512)
INTEGER*4 SUM
CHARACTER DUM,SER
CHARACTER*20 FILENAME,NAME,WORKBUFFER(256)
C *****
C          INITIALIZING THE PIP BOARD
C *****

RETV=INIT(620)
CHANNO=2
CALL CHAN(CHANNO)
VTYPE=0
CALL VIDEO(VTYPE)
STATE=1
CALL QUADM(STATE)
STABLE=0
UTABLE=7
CALL CLEAR(STABLE,UTABLE)
3 WRITE(*,4)
4 FORMAT(/,T20,' MAIN MENU ',/,T20,
*      ', ***** ')
5 WRITE(*,10)
10 FORMAT(/,T15,'ENTER YOUR CHOICE ')
29 WRITE(*,29)
*   FORMAT(/,T15,'1. GRAB PICTURE',
*         /,T15,'2. AVERAGE FRAMES',
*         /,T15,'3. SUBTRACT FRAMES',
*         /,T15,'4. CLEAR SCREEN',
*         /,T15,'5. SAVE PICTURE IN A FILE',
*         /,T15,'6. LOAD PICTURE FROM A FILE',
*         /,T15,'7. SHOW FREQUENCY SPECTRUM',
*         /,T15,'8. CHANGE QUADRANT',
*         /,t15,'9. SET GAIN',
*         /,T15,'10. SET OFFSET',
*         /,T15,'11. EXIT',
*         /,T15,'INPUT=  '$)
READ(*,*) NUM

C *****
C          * GRAB PICTURE *
C *****
IF (NUM.EQ.1) THEN
MODE=1

```



```

CALL SYNC(MODE)
STATE=1
CALL CGRAB(STATE)
WRITE(*,30)
30  FORMAT(/,T15,'TO GRAB PICTURE - HIT RETURN'\)
    READ(*,'(A1)') DUM
    STATE=0
    CALL CGRAB(STATE)
    STATE=1
    call setind(255)
    CALL KEY(STATE)
    CALL MOVETO(0,270)
    CALL LDRAW(512)
    CALL MOVETO(256,0)
    CALL LINETO(256,512)
    STATE=0
    CALL KEY(STATE)

C *****
C *           AVERAGING FRAMES           *
C *****
ELSEIF (NUM.EQ.2) THEN
17  WRITE(*,17)
    *  FORMAT(/,T15,'AVERAGE FRAMES',
        /,T15,'*****')
18  WRITE(*,18)
    FORMAT(/,T15,'ENTER QUADRANTS TO BE ADDED: '$)
    READ(*,*) QUAD1
    READ(*,*) QUAD2
    WRITE(*,19)
19  FORMAT(/,T15,'ENTER THE DESIRED QUADRANT: '$)
    READ(*,*) QUAD3
    CALL ADDTWO(QUAD1,QUAD2,QUAD3)

C *****
C *           SUBTRACT FRAMES           *
C *****
ELSEIF (NUM.EQ.3) THEN
31  WRITE(*,31)
    *  FORMAT(/,T15,'SUBTRACT FRAMES',
        /,T15,'*****')
32  WRITE(*,32)
    FORMAT(/,T15,'ENTER QUADRANTS TO BE SUBTRACTED: '$)
    READ(*,*) QUAD1
    READ(*,*) QUAD2
    WRITE(*,33)
33  FORMAT(/,T15,'ENTER THE DESIRED QUADRANT: '$)
    READ(*,*) QUAD3
    CALL SUBTWO(QUAD1,QUAD2,QUAD3)

C *****
C *           CLEAR SCREEN           *
C *****
ELSEIF (NUM.EQ.4) THEN
WRITE(*,40)

```

```

40      *      FORMAT(/,T15,'CLEAR SCREEN',/,T15,
          *      '*****')
          STABLE=0
          UTABLE=7
          CALL CLEAR(STABLE,UTABLE)

C      *      *****
C      *      *      SAVE PICTURE IN A FILE      *
C      *      *****
          ELSEIF (NUM.EQ.5) THEN
42      *      WRITE(*,42)
          FORMAT(/,T15,'SAVE PICTURE IN A FILE',/,T15,
          *      '*****')

          BSIZE=1024
          WRITE(*,50)
50      *      FORMAT(/,T15,'ENTER THE QUADRANT: '$)
          READ(*,'(I1)') QUAD
          WRITE(*,60)
60      *      FORMAT(/,T15,'ENTER THE FILENAME: '$)
          READ(*,'(A20)') FILENAME
          RET=ITODSK(BSIZE,QUAD,FILENAME,WORKBUFFER)
          IF (RET.EQ.1) THEN
70      *      WRITE(*,70)
          FORMAT(/,T15,'TRANSFER COMPLETED')
          ELSEIF (RET.EQ.0) THEN
          WRITE(*,80)
80      *      FORMAT(/,T15,'COULD NOT OPEN FILE')
          ELSEIF (RET.EQ.-1) THEN
          WRITE(*,90)
90      *      FORMAT(/,T15,'TRANSFER TERMINATED PREMATURELY')
          ENDIF

C      *      *****
C      *      *      LOAD PICTURE FROM A FILE      *
C      *      *****
          ELSEIF (NUM.EQ.6) THEN
91      *      WRITE(*,91)
          FORMAT(/,T15,'LOAD PICTURE FROM A FILE',/,T15,
          *      '*****')

          WRITE(*,92)
92      *      FORMAT(/,T15,'ENTER MODE: '$)
          READ(*,'(I1)') MODE
          CALL SYNC(MODE)
          BSIZE=1024
          WRITE(*,50)
          READ(*,'(I1)') QUAD
          WRITE(*,60)
          READ(*,'(A20)') FILENAME
          I1=IFRDSK(BSIZE,QUAD,FILENAME,WORKBUFFER)

C      *      *****
C      *      *      SHOW FREQUENCY SPECTRUM      *
C      *      *****
          ELSEIF (NUM.EQ.7) THEN
          WRITE(*,94)

```

```

94      *      FORMAT(/,T15,'FREQUENCY SPECTRUM ',/T15,
          *      '*****')
          CALL SELEC(LEFT,RIGHT,UPPER,LOWER)
          left=left-2 *
          right=right-4
          upper=upper-4
          lower=lower-4
95      *      WRITE(*,95) LEFT,RIGHT,UPPER,LOWER
          *      FORMAT(/,T15,'LEFT BOUNDARY IS LOCATED AT ',I3,'PIXELS',
          *      /,T15,'RIGHT BOUNDARY IS LOCATED AT ',I3,'PIXELS',
          *      /,T15,'UPPER BOUNDARY IS LOCATED AT ',I3,'PIXELS',
          *      /,T15,'LOWER BOUNDARY IS LOCATED AT ',I3,'PIXELS',/)
          CALL INPROF(QUAD,LEFT,RIGHT,UPPER,LOWER)

C      *      *****
C      *      CHANGE QUADRANT
C      *      *****
          ELSEIF (NUM.EQ.8) THEN
          WRITE(*,150)
          FORMAT(/,T15,'ENTER DESIRED QUADRANT: ', $)
          READ(*,*) QUAD
          CALL DQUAD(QUAD)
C      *      *****
C      *      GAIN
C      *      *****
          ELSEIF (NUM.EQ.9) THEN
          WRITE(*,888)
          FORMAT(/,T15,'ENTER THE GAIN :', $)
          READ(*,'(I3)') VAL
          CALL GAIN(VAL)

C      *      *****
C      *      OFFSET
C      *      *****
          ELSEIF (NUM.EQ.10) THEN
          WRITE(*,889)
          FORMAT(/,T15,'ENTER THE OFFSET :', $)
          READ(*,'(I3)') VAL
          CALL OFFSET(VAL)

C      *      *****
C      *      EXIT
C      *      *****
          ELSEIF (NUM.EQ.11) THEN
          CALL PEXIT
          GOTO 170
          ENDIF
          GOTO 3
          STOP
170     END

```

\$INCLUDE: 'FORINTF.H'

```

SUBROUTINE INPROF(QUAD,LEFT,RIGHT,UPPER,LOWER)
IMPLICIT INTEGER*2 (X,Y)
EXTERNAL IPIXR
EXTERNAL RECTF
* INTEGER*2 OFFSET,CNANNO,STABLE,UTABLE
INTEGER*2 STATE,BSIZE,WIDTH,BUFFER(512)
INTEGER*2 LEFT,RIGHT,UPPER,LOWER
INTEGER*2 QUAD,Y1,Y2,X1,X2,G,GG
INTEGER*2 AVG(512),ISUM(512),Z,B
INTEGER*4 SUM(512)
CHARACTER*2 SER,WORKBUFFER(256)
CHARACTER*20 FILENAME
REAL MMAX
REAL*4 COUNTER,M,RMS
REAL*4 S,F,MM,MEAN,GGG,SSS
MMAX=0
DO 499 I=1,512
SUM(I)=0
499 CONTINUE
WRITE(*,52)
52 FORMAT(/,T5,'ENTER B: 'I3)
READ(*,*)B
write(*,51)
51 FORMAT(/,T15,'SELECT YOUR OPTIC AXIS',/,T15,
*      '*****',/,T15,
*      '1. VERTICAL AXIS (INTENSITY AVERAGED ALONG Y)',/,T15,
*      '2. HORIZONTAL AXIS (INTENSITY AVERAGED ALONG X)',/,T15,
*      '3. EXIT ',/,T15,
*      'INPUT= '$)
READ(*,*) NUM
IF (NUM.EQ.1) THEN
WIDTH=LOWER-UPPER
DO 510 X=LEFT,RIGHT,1
DO 510 Y=UPPER,LOWER,1
Z=IPIXR(X,Y)
SUM(X)=SUM(X)+Z
510 CONTINUE
DO 500 X=LEFT,RIGHT,1
SUM(X)=SUM(X)/WIDTH
AVG(X)=SUM(X)+0.5-B
IF (AVG(X).GT.MMAX) MMAX=AVG(X)
500 CONTINUE
503 WRITE(*,504)
504 FORMAT(/,T5,'SAVE GREYLEVEL DATA (Y/N)? ')
READ(*,'(A1)') SER
IF (SER.EQ.'Y'.OR.SER.EQ.'y') THEN
WRITE(*,1100)
1100 FORMAT(/,T5,'PROCESSING LEFT OR RIGHT SIDE OF SPECTRUM (L/R)? ')
READ(*,'(A1)') SER
IF (SER.EQ.'R'.OR.SER.EQ.'r') THEN
WRITE(*,507)
```

507

```
FORMAT(/,T5,'ENTER FILENAME: ')
READ(*,'(A20)') FILENAME
OPEN(UNIT=3,FILE=FILENAME,STATUS='NEW')
```

511

```
DO 506 X=LEFT+2,RIGHT,1
S=(X-LEFT)
S=S-2.0
```

506

```
F=S*1.48685
WRITE(3,511) F,AVG(X)
FORMAT(F7.3,I5)
CONTINUE
CLOSE(UNIT=3,STATUS='KEEP')
```

```
M=0.0
MM=0.0
MMM=0.0
G=LEFT+2
GG=G+135
DO 515 X=G,GG,1
```

515

```
GGG=(X-LEFT)
GGG=GGG-2.0
F=GGG*1.48685
M=M+AVG(X)
MMM=MMM+(AVG(X)*AVG(X))
MM=MM+(AVG(X)*F)
CONTINUE
```

```
MEAN=MM/M
RMS=((MMM)/135)**0.5
SSS=0
DO 516 X=G,GG,1
GGG=(X-LEFT)
GGG=GGG-2.0
F=GGG*1.48685
SSS=SSS+(AVG(X)*(F-MEAN)**2)
```

516

```
CONTINUE
STD=SSS/M
STD=(STD**0.5)
```

519

```
WRITE(*,519) MEAN
FORMAT(/,T5,'1. MEAN VALUE IS : 'F7.3)
WRITE(*,556) RMS
```

556

```
FORMAT(/,T5,'2. ROOT MEAN SQUARE IS : 'F7.3)
WRITE(*,517) STD
```

517

```
FORMAT(/,T5,'3. STANDARD DEVIATION IS : 'F7.3)
ELSEIF (SER.EQ.'L'.OR.SER.EQ.'1') THEN
```

1507

```
COUNTER=-200.725
WRITE(*,1507)
FORMAT(/,T5,'ENTER FILENAME: ')
READ(*,'(A20)') FILENAME
OPEN(UNIT=3,FILE=FILENAME,STATUS='NEW')
DO 1125 X=LEFT+2,RIGHT,1
S=(X-LEFT)
S=S-2.0
```

1111

```
WRITE(3,1111) COUNTER,AVG(X)
FORMAT(F8.3,I5)
COUNTER=COUNTER+1.48685
```

1125

```
CONTINUE
CLOSE(UNIT=3,STATUS='KEEP')
```

```

M=0.0
MM=0.0
G=LEFT+2
GG=G+135
COUNTER=-200.725
DO 1515 X=G,GG,1
GGG=(X-LEFT)
GGG=GGG-2.0
M=M+AVG(X)
MMM=MMM+(AVG(X)*AVG(X))
MM=MM+(AVG(X)*COUNTER)
COUNTER=COUNTER+1.48685
1515 CONTINUE
MEAN=MM/M
RMS=((MMM)/135)
RMS=(RMS**0.5)
SSS=0
COUNTER=-200.725
DO 1516 X=G,GG,1
GGG=(X-LEFT)
GGG=GGG-2.0
SSS=SSS+(AVG(X)*(COUNTER-MEAN)**2)
COUNTER=COUNTER+1.48685
1516 CONTINUE
STD=SSS/M
STD=(STD**0.5)
WRITE(*,1519) MEAN
1519 FORMAT(/,T5,'1. MEAN VALUE IS : 'F8.3)
WRITE(*,1522) RMS
1522 FORMAT(/,T5,'2. ROOT MEAN SQUARE IS : 'F8.3)
WRITE(*,1517) STD
1517 FORMAT(/,T5,'3. STANDARD DEVIATION IS : 'F8.3)
ENDIF
ENDIF
520 write(*,521)
521 FORMAT(/,T5,'INPUT DRAWING LOCATION Y1 & Y2: ')
READ(*,*) Y1,Y2
SCALE=Y2-Y1
DO 530 X=LEFT,RIGHT,1
ISUM(X)=AVG(X)*SCALE/MMAX +0.5
530 CONTINUE
CALL SETIND(255)
IF (QUAD.EQ.0) THEN
CALL RECTF(LEFT,Y1,RIGHT,Y2)
CALL SETIND(30)
CALL MOVETO(LEFT,Y2)
DO 540 X=LEFT,RIGHT,1
J=X+1
Y=Y2-ISUM(J)
CALL LINETO(X,Y)
CALL MOVETO(J,Y2)
540 CONTINUE
CALL MOVETO(LEFT,UPPER)
CALL LDRAW(RIGHT)
CALL MOVETO(LEFT,LOWER)

```

```

CALL LDRAW(RIGHT)
ELSEIF (QUAD.EQ.1) THEN
Y1=Y1+512
Y2=Y2+512
CALL RECTF(LEFT,Y1,RIGHT,Y2)
CALL SETIND(30)
CALL MOVETO(LEFT,Y2)
DO 550 X=LEFT,RIGHT,1
J=X+1
Y=Y2-ISUM(J)
CALL LINETO(X,Y)
CALL MOVETO(J,Y2)
550 CONTINUE
CALL MOVETO(LEFT,UPPER)
CALL LDRAW(RIGHT)
CALL MOVETO(LEFT,LOWER)
CALL LDRAW(RIGHT)
ELSEIF (QUAD.EQ.2) THEN
CALL RECTF(LEFT,Y1,RIGHT,Y2)
CALL SETIND(30)
CALL MOVETO(LEFT,Y2)
DO 560 X=LEFT,RIGHT,1
J=X+1
Y=Y2-ISUM(J)
CALL LINETO(X,Y)
CALL MOVETO(J,Y2)
560 CONTINUE
CALL MOVETO(LEFT,UPPER)
CALL LDRAW(RIGHT)
CALL MOVETO(LEFT,LOWER)
CALL LDRAW(RIGHT)
ELSEIF (QUAD.EQ.3) THEN
Y1=Y1+512
Y2=Y2+512
CALL RECTF(LEFT,Y1,RIGHT,Y2)
CALL SETIND(30)
CALL MOVETO(LEFT,Y2)
DO 570 X=LEFT,RIGHT,1
J=X+1
Y=Y2-ISUM(J)
CALL LINETO(X,Y)
CALL MOVETO(J,Y2)
570 CONTINUE
CALL MOVETO(LEFT,UPPER)
CALL LDRAW(RIGHT)
CALL MOVETO(LEFT,LOWER)
CALL LDRAW(RIGHT)
ENDIF
ELSEIF (NUM.EQ.2) THEN
WIDTH=RIGHT-LEFT
DO 65 Y=UPPER,LOWER,1
DO 65 X=LEFT,RIGHT,1
Z=IPIXR(X,Y)
SUM(Y)=SUM(Y)+Z
65 CONTINUE

```

```

DO 66 Y=UPPER,LOWER,1
SUM(Y)=SUM(Y)/WIDTH
AVG(Y)=SUM(Y)+0.5
IF(AVG(Y).GT.MMAX) MMAX=AVG(Y)
66 CONTINUE
178 WRITE(*,179)
179 FORMAT(/,T5,'SAVE GREYLEVEL DATA(Y/N) ')
READ(*,'(A1)') SER
IF(SER.EQ.'Y'.OR.SER.EQ.'y') THEN
WRITE(*,181)
181 FORMAT(/,T5,'ENTER FILENAME: ')
READ(*,'(A20)') FILENAME
OPEN(UNIT=3,FILE=FILENAME,STATUS='NEW')
DO 183 Y=UPPER+2,LOWER,1
S=Y-UPPER
S=S-2.0
F=S*1.8585
WRITE(3,185) F,AVG(Y)
185 FORMAT(F7.3,I5)
183 CONTINUE
CLOSE(UNIT=3,STATUS='KEEP')
ENDIF
WRITE(*,189)
189 FORMAT(/,T5,'INPUT DRAWING LOCATIONS X1,X2: ')
READ(*,*) X1,X2
SCALE=X2-X1
DO 191 Y=UPPER,LOWER,1
ISUM(Y)=AVG(Y)*SCALE/MMAX +0.5
191 CONTINUE
CALL SETIND(255)
IF(QUAD.EQ.0) THEN
CALL RECTF(x1,UPPER,x2,LOWER)
CALL SETIND(30)
CALL MOVETO(x2,UPPER)
DO 193 Y=UPPER,LOWER,1
J=Y+1
X=X2-ISUM(J)
CALL LINETO(X,Y)
CALL MOVETO(X2,J)
193 CONTINUE
CALL MOVETO(LEFT,UPPER)
CALL LDRAW(RIGHT)
CALL MOVETO(LEFT,LOWER)
CALL LDRAW(RIGHT)
ELSEIF (QUAD.EQ.1) THEN
CALL RECTF(X1,UPPER,X2,LOWER)
CALL SETIND(30)
CALL MOVETO(X2,UPPER)
DO 195 Y=UPPER,LOWER,1
J=Y+1
X=X2-ISUM(J)
CALL LINETO(X,Y)
CALL MOVETO(X2,J)
195 CONTINUE
CALL MOVETO(LEFT,UPPER)

```



```

CALL LDRAW(RIGHT)
CALL MOVETO(LEFT,LOWER)
CALL LDRAW(RIGHT)
ELSEIF(QUAD.EQ.2) THEN
CALL RECTF(X1,UPPER,X2,LOWER)
CALL SETIND(30)
CALL MOVETO(X2,UPPER)
DO 196 Y=UPPER,LOWER,1
J=Y+1
X=X2-ISUM(J)
CALL LINETO(X,Y)
CALL MOVETO(X2,J)
196 CONTINUE
CALL MOVETO(LEFT,UPPER)
CALL LDRAW(RIGHT)
CALL MOVETO(LEFT,LOWER)
CALL LDRAW(RIGHT)
ELSEIF (QUAD.EQ.3) THEN
CALL RECTF(X1,UPPER,X2,LOWER)
CALL SETIND(30)
CALL MOVETO(X2,UPPER)
DO 197 Y=UPPER,LOWER,1
J=Y+1
X=X2-ISUM(J)
CALL LINETO(X,Y)
CALL MOVETO(X2,J)
197 CONTINUE
CALL MOVETO(LEFT,UPPER)
CALL LDRAW(RIGHT)
CALL MOVETO(LEFT,LOWER)
CALL LDRAW(RIGHT)
ENDIF
ELSEIF (NUM.EQ.3) THEN
ENDIF
900 CALL SETIND(255)
RETURN
END

```

```

$INCLUDE: 'FORINTF.H'
SUBROUTINE SELEC(LEFT,RIGHT,UPPER,LOWER)
INTEGER*2 LEFT,RIGHT,UPPER,LOWER
INTEGER*2 X1,Y,INDEX,BOUND
INTEGER*2 BSIZE,QUAD,IND(512)
INTEGER*4 SUM
CHARACTER*20 FILENAME,NAME
CHARACTER*2 DUM,WORKBUFFER(256)
WRITE(*,200)
200 FORMAT(/,T15,'ENTER WORKING QUAD: '$)
READ(*,*) QUAD
C *****
C QUADRANT 0
C *****

IF (QUAD.EQ.0) THEN
J1=0
J2=511.
J3=0
J4=511
C *****
C QUADRANT 1
C *****
ELSEIF (QUAD.EQ.1) THEN
J1=515
J2=1023
J3=0
J4=511
C *****
C QUADRANT 2
C *****
ELSEIF (QUAD.EQ.2) THEN
J1=0
J2=511
J3=515
J4=1023
C *****
C QUADRANT 3
C *****
ELSEIF (QUAD.EQ.3) THEN
J1=515
J2=1023
J3=515
J4=1023
ENDIF
WRITE(*,210)
210 FORMAT(/,T15,' ENTER DRAWING INDEX: '$)
READ(*,*) INDEX
CALL SETIND(INDEX)
C *****
C LEFT BOUNDARY
C *****
X1=J3

```

```

WRITE(*,220)
220  FORMAT(/,T15,'LEFT BOUNDARY ',/,T15,
*      '***** ',/,T15,
*      'PRESS RETURN TO MOVE LINE',/,T15,
*      'PRESS T TO TERMINATE THE PROGRAM',/,T15,
*      'L & RETURN TO STOP '\)
221  CONTINUE
      DO 230 I=J1,J2,1
      IF (I.GT.512) THEN
      IN=I-512
      ELSE
      IN=I
      ENDIF
      IND(IN)=IPIXR(X1,I)
230  CONTINUE
      CALL MOVETO(X1,J1)
      CALL LINETO(X1,J2)
      X1=X1+2
      READ(*,'(A1)') DUM
      IF ((DUM.EQ.'T').OR.(DUM.EQ.'t')) GOTO 371
      IF ((DUM.EQ.'L').OR.(DUM.EQ.'l')) GOTO 243.
      IF ((DUM.EQ.'S').OR.(DUM.EQ.'s')) THEN
      BOUND=X1
234  WRITE(*,234) BOUND
      FORMAT(/,T5,I3)
      ELSE
      ENDIF
      Y=X1-2
      DO 240 I=J1,J2,1
      IF (I.GT.512) THEN
      IN=I-512
      ELSE
      IN=I
      ENDIF
      CALL PIXW(Y,I,IND(IN))
240  CONTINUE
      GOTO 221
243  CONTINUE
      LEFT=X1
      WRITE(*,250)LEFT
250  FORMAT(/,T5,'LEFT BOUNDARY IS LOCATED AT: ',I3,
*      ' PIXELS FROM THE RIGHT EDGE')
C      *****
C      RIGHT BOUNDARY
C      *****
      WRITE(*,260)
260  FORMAT(/,T15,'RIGHT BOUNDARY ',/,T15,
*      '***** ',/,T15,
*      'PRESS RETURN TO MOVE LINE',/,T15,
*      'PRESS T TO TERMINATE THE PROGRAM',/,T15,
*      'R. & RETURN TO STOP '\)
263  CONTINUE
      DO 270 I=J1,J2,1
      IF (I.GT.512) THEN
      IN=I-512

```

```

ELSE
IN=I
ENDIF
270 IND(IN)=IPIXR(X1,I)
CONTINUE
CALL MOVETO(X1,J1)
CALL LINETO(X1,J2)
X1=X1+4
READ(*,'(A1)') DUM
IF ((DUM.EQ.'T').OR.(DUM.EQ.'t')) GOTO 371
IF ((DUM.EQ.'R').OR.(DUM.EQ.'r')) GOTO 283
IF ((DUM.EQ.'S').OR.(DUM.EQ.'s')) THEN
BOUND=X1
271 WRITE(*,271) BOUND
FORMAT(/,T5,I3)
ELSE
ENDIF
Y=X1-4
DO 280 I=J1,J2,1
IF (I.GT.512) THEN
IN=I-512
ELSE
IN=I
ENDIF
CALL PIXW(Y,I,IND(IN))
280 CONTINUE
GOTO 263
283 CONTINUE
RIGHT=X1
WRITE(*,290) RIGHT
290 FORMAT(/,T5,'RIGHT BOUNDARY IS LOCATED AT: ',I3,
* ' PIXELS FROM THE RIGHT EDGE')
C *****
C UPPER BOUNDARY
C *****
X1=J1
WRITE(*,300)
300 FORMAT(/,T15,'UPPER BOUNDARY ',/,T15,
* '***** ',/,T15,
* 'PRESS RETURN TO MOVE LINE',/,T15,
* 'PRESS T TO TERMINATE THE PROGRAM',/,T15,
* 'U & RETURN TO STOP'\)
303 CONTINUE
DO 310 I=J3,J4,1
IF (I.GT.512) THEN
IN=I-512
ELSE
IN=I
ENDIF
310 IND(IN)=IPIXR(I,X1)
CONTINUE
CALL MOVETO(J3,X1)
CALL LINETO(J4,X1)
X1=X1+4
READ(*,'(A1)') DUM

```

```

IF ((DUM.EQ.'T').OR.(DUM.EQ.'t')) GOTO 371
IF ((DUM.EQ.'U').OR.(DUM.EQ.'u')) GOTO 323
IF ((DUM.EQ.'S').OR.(DUM.EQ.'s')) THEN
BOUND=X1
WRITE(*,234) BOUND
ELSE
ENDIF
Y=X1-4
DO 320 I=J3,J4,1
IF (I.GT.512) THEN
IN=I-512
ELSE
IN=I
ENDIF
CALL PIXW(I,Y,IND(IN))
320 CONTINUE
GOTO 303
323 CONTINUE
UPPER=X1
WRITE(*,330) UPPER
330 FORMAT(/,T5,'UPPER BOUNDARY IS LOCATED AT: ',I3,
* ' PIXELS FROM THE UPPER EDGE')
C *****
C LOWER BOUNDARY
C *****
340 WRITE(*,340)
FORMAT(/,T15,'LOWER BOUNDARY ',/,T15,
* '*****',/,T15,
* 'PRESS RETURN TO MOVE LINE',/,T15,
* 'L & RETURN TO STOP'\)
343 CONTINUE
DO 350 I=J3,J4,1
IF (I.GT.512) THEN
IN=I-512
ELSE
IN=I
ENDIF
IND(IN)=IPIXR(I,X1)
350 CONTINUE
CALL MOVETO(J3,X1)
CALL LINETO(J4,X1)
X1=X1+4
READ(*,'(A1)') DUM
IF ((DUM.EQ.'L').OR.(DUM.EQ.'l')) GOTO 363
IF ((DUM.EQ.'S').OR.(DUM.EQ.'s')) THEN
BOUND=X1
WRITE(*,234) BOUND
ELSE
ENDIF
Y=X1-4
DO 360 I=J3,J4,1
IF (I3.GT.512) THEN
IN=I-512
ELSE
IN=I

```

```
ENDIF
CALL PIXW(I,Y,IND(IN))
360 CONTINUE
GOTO 343
363 CONTINUE
LOWER=X1
WRITE(*,370) LOWER
370 * FORMAT(/,T5,'LOWER BOUNDARY IS LOCATED AT: ',I3,
        ' PIXELS FROM UPPER EDGE')
RETURN
371 . END
```

APPENDIX C.
Chemical Composition and Mechanical Properties
of
Test Samples [25]

ALUMINUM 2024-T4

Chemical Composition:

Copper	4.5%
Manganese	0.6%
Magnesium	1.5%
Aluminum	Balance

Mechanical Properties:

Tensile Strength,psi	68,000
Yield Strength,psi	47,000
Elongation,% in 2"	19
Shear Strength,psi	37,000
Brinell Hardness 10/500	120

BRASS

Chemical Composition:

Copper	61.5%
Zinc	35.5%
Lead	3.0%

Mechanical Properties:

Tensile Strength,psi	58,000
Yield Strength,psi	45,000
Elongation,% in 2"	25
Shear Strength,psi	34,000
Rockwell Hardness,B scale	78

COPPER

Chemical Composition:

Copper	99.9%
--------	-------

Mechanical Properties:

Tensile Strength,psi	48,000
Yield Strength,psi	44,000
Elongation,% in 2"	16
Shear Strength,psi	27,000
Rockwell Hardness, F scale	87

TOOL STEEL

K.E.672/Newhall oil hardening alloy tool steel
A.I.S.I. type 01: BS 4659 B01
Werkstoff 1.2510

Chemical Composition:

Carbon	0.95%
Manganese	1.20%
Chromium	0.55%
Tungsten	0.55%
Vanadium	0.2%

Mechanical Property (as hardened):

Rockwell Hardness, C scale 63/64

APPENDIX D.
Data for Grinding samples ●

Table D.1 Frequency data obtained by the optical & mechanical methods for surface ground Copper samples.

Ra (μ m)	Mechanical method		Optical method		Percent deviation %
	Mean frequency (cycles/mm)	STD frequency (cycles/mm)	Mean frequency (cycles/mm)	STD frequency (cycles/mm)	
0.07	40.67	46.467	38.921	45.988	-3.4
0.2	40.79	43.92	49.67	50.33	5.9
0.32	35.15	32.69	56.07	51.45	1.2
0.38	48.76	42.91	58.67	47.46	7.54
0.43	53.79	43.14	74.86	57.34	5.59
0.58	33.52	26.571	80.35	59.66	6.9
0.71	29.24	26.73	79.42	58.29	19.27
0.84	32.99	30.57	71.48	50.82	23.95

Table D.2 Frequency data obtained by the optical & mechanical methods for surface ground Aluminum samples.

Mechanical method			Optical method		
Ra (μm)	Mean frequency (cycles/mm)	STD frequency (cycles/mm)	Mean frequency (cycles/mm)	STD frequency (cycles/mm)	Percent deviation %
0.07	28.14	42.31	25.71	39.16	-1.3
0.21	46.37	40.66	71.17	60.67	2.8
0.4	47.15	39.84	67.01	55.66	1.77
0.46	50.71	42.29	73.01	60.23	1.2
0.6	42.275	36.72	75.85	61.44	5.7
0.76	44.85	38.03	76.65	57.26	11.8
0.83	28.83	29.73	78.2	62.09	22.9

Table D.3 Frequency data obtained by the optical & mechanical methods for surface ground Brass samples.

Ra (μm)	Mechanical method		Optical method		Percent deviation %
	Mean frequency (cycles/mm)	STD frequency (cycles/mm)	Mean frequency (cycles/mm)	STD frequency (cycles/mm)	
0.07	47.53	48.37	52.03	50.882	3.3
0.17	43.67	42.06	53.34	49.24	4.1
0.45	39.22	37.45	64.22	56.18	7.8
0.6	42.24	38.41	78.58	62.39	12.65
0.72	44.48	39.51	80.50	63.46	11.23
0.84	29.38	31.96	68.427	60.47	18.7
1.14	28.62	30.32	72.86	61.95	19.73
1.29	37.62	38.18	80.14	62.789	22.78

Table D.4 Frequency data obtained by the optical & mechanical methods for surface ground Stainless Steel samples.

Ra (μ m)	Mechanical method		Optical method		
	Mean frequency (cycles/mm)	STD frequency (cycles/mm)	Mean frequency (cycles/mm)	STD frequency (cycles/mm)	Percent deviation %
0.05	68.83	56.1	66.36	55.27	-2.08
0.1	68.22	54.33	71.02	56.09	-0.8
0.2	66.82	50.98	68.67	51.29	2.28
0.4	68.41	50.02	86.89	61.73	2.89
0.8	62.49	53.40	89.5	59.9	21.66

Table D.5 Normalized spectrum RMS and Peak values obtained by the optical & mechanical methods for surface ground Tool Steel samples

Roughness	Mechanical method		Optical method	
	RMS	Peak	RMS	Peak
Ra (μm)				
0.07	0.27	0.37	1.47	1.36
0.15	0.31	0.40	1.21	1.29
0.17	0.45	0.55	1.18	1.20
0.23	0.75	1.13	1.12	1.09
0.3	0.80	1.35	0.97	0.96
0.5	1.26	1.57	0.91	0.86
0.62	1.59	2.02	0.67	0.67
0.8	1.95	2.17	0.61	0.61

Table D.6 Normalized spectrum RMS and Peak values
 obtained by the optical & mechanical methods
 for surface ground Stainless Steel samples

Roughness Ra (μm)	Mechanical method		Optical method	
	RMS	Peak	RMS	Peak
0.05	0.53	0.73	1.56	1.36
0.1	0.82	1.07	1.37	1.17
0.2	1.32	1.64	1.15	1.01
0.4	2.55	3.54	0.92	0.87
0.8	3.81	6.33	0.69	0.7

Table D.7 Normalized spectrum RMS and Peak values obtained by the optical & mechanical methods for surface ground Brass samples

Roughness Ra (μm)	Mechanical method		Optical method	
	RMS	Peak	RMS	Peak
0.07	0.4	0.6	1.33	1.34
0.17	0.55	0.68	1.14	1.14
0.45	1.22	1.20	1.08	1.06
0.6	1.41	1.35	1.01	0.95
0.72	1.7	1.6	0.93	0.87
0.84	2.86	4.13	0.84	0.78
1.14	3.35	4.4	0.56	0.57
1.29	4.0	7.05	0.48	0.43

Table D.8 Normalized spectrum RMS and Peak values obtained by the optical & mechanical methods for surface ground Copper samples

Roughness	Mechanical method		Optical method	
	RMS	Peak	RMS	Peak
Ra (µm)				
0.07	0.51	0.97	1.38	1.36
0.2	0.99	1.40	1.09	1.21
0.32	1.27	1.46	1.04	1.15
0.38	1.41	1.6	0.97	1.01
0.43	1.94	1.98	0.93	0.84
0.58	2.4	2.83	0.68	0.72
0.71	2.52	3.02	0.57	0.65
0.84	2.69	3.17	0.55	0.45

Table D.9 Normalized spectrum RMS and Peak values obtained by the optical & mechanical methods for surface ground Aluminum samples

Roughness (Ra (μm)	Mechanical method		Optical method	
	RMS	Peak	RMS	Peak
0.07	0.24	0.44	1.33	1.26
0.21	0.69	0.68	1.12	1.14
0.4	0.73	0.91	1.06	1.05
0.46	0.9	1.18	0.99	0.98
0.6	1.09	1.51	0.90	0.88
0.78	1.88	2.47	0.85	0.77
0.83	2.63	3.75	0.66	0.71

APPENDIX E.

Data for samples from different machining
processes



Table E.1. Comparison of the frequency spectra obtained by the two methods for samples of different machining processes

Ra (μm)	Mechanical method		Optical method		
	Mean (cycles/mm)	STD (cycles/mm)	Mean (cycles/mm)	STD (cycles/mm)	Percent deviation %
<u>Flat Lapping :</u>					
0.05	46.53	53.30	42.29	48.30	0.26
0.1	52.8	53.18	50.84	49.51	3.28
0.2	52.52	53.18	54.97	53.20	1.52
<u>Grinding :</u>					
0.05	68.834	56.1	66.36	55.271	-2.08
0.1	68.22	54.33	71.02	56.09	-0.8
0.2	66.82	50.984	68.67	51.294	2.28
0.4	68.41	50.02	86.89	61.73	2.89
0.8	62.49	53.40	89.50	59.90	21.66
<u>Horizontal Milling :</u>					
0.406	53.530	52.62	54.2769	54.9352	-2.86
0.812	46.457	51.954	62.385	58.877	15.65
<u>Reaming :</u>					
0.4	40.87	43.42	50.48	47.26	11.69
0.8	45.59	52.85	46.40	47.66	11.13
<u>Turning :</u>					
0.4	35.80	38.05	42.3	47.94	-4.51

0.8	31.28	40.6	42.3	47.94	12.87
1.6	23.68	36.95	25.92	41.32	-2.08
3.2	11.98	22.7	40.26	46.16	39.49

Vertical Milling :

0.406	53.225	50.938	58.207	50.221	9.9
-------	--------	--------	--------	--------	-----

APPENDIX F.
Uncertainty Analysis

$$F = \frac{(z * M)}{(\lambda * f)}$$

$$\frac{dF}{dz} = \frac{M}{\lambda f} ; \quad \frac{dF}{dM} = \frac{z}{\lambda f} ; \quad \frac{dF}{d\lambda} = \frac{zM}{\lambda^2 f} ;$$

$$\frac{dF}{df} = \frac{zM}{\lambda f^2}$$

$$w = \pm 2.248 \text{ mm} \quad w = \pm 0.000001 \mu\text{m}$$

$$w = \pm 1.1$$

$$\frac{w}{F} = \left[\left(\frac{dF}{dz} * \frac{w_z}{F} \right)^2 + \left(\frac{dF}{dM} * \frac{w_M}{F} \right)^2 + \left(\frac{dF}{d\lambda} * \frac{w_\lambda}{F} \right)^2 + \left(\frac{dF}{df} * \frac{w_f}{F} \right)^2 \right]^{0.5}$$

VITA AUCTORIS

- 1964 Born in Ottawa, Ont on December 16.
- 1980 Received secondary school diploma at B.V.K.Junior college, Vizag, India.
- 1984 Received the degree of Bachelor of Engineering from the department of Mechanical Engineering, Andhra University, Vizag, India.
- 1988 Currently a candidate for the degree of Master of Applied Science in Mechanical Engineering at the University of Windsor.
-